

AN APPROACH FOR SEISMIC DAMAGE ASSESSMENT OF RESIDENTIAL
BUILDINGS

A THESIS SUBMITTED TO
THE GRADUATE SCHOOL OF NATURAL AND APPLIED SCIENCES
OF
MIDDLE EAST TECHNICAL UNIVERSITY

BY

CEREN DEMİRCİ

IN PARTIAL FULFILLMENT OF THE REQUIREMENTS
FOR
THE DEGREE OF MASTER OF SCIENCE
IN
CIVIL ENGINEERING

MAY 2014

Approval of the thesis:

**AN APPROACH FOR SEISMIC DAMAGE ASSESSMENT OF
RESIDENTIAL BUILDINGS**

submitted by **CEREN DEMİRCİ** in partial fulfillment of the requirements for the degree of **Master of Science in Civil Engineering Department, Middle East Technical University** by,

Prof. Dr. Canan Özgen
Dean, Graduate School of **Natural and Applied Sciences**

Prof. Dr. Ahmet Cevdet Yalçiner
Head of Department, **Civil Engineering**

Assoc. Prof. Dr. Murat Altuğ Erberik
Supervisor, **Civil Engineering Dept., METU**

Assoc. Prof. Dr. Ayşegül Askan Gündoğan
Co-Supervisor, **Civil Engineering Dept., METU**

Examining Committee Members:

Prof. Dr Ahmet Yakut
Civil Engineering Dept., METU

Assoc. Prof. Dr. Murat Altuğ Erberik
Civil Engineering Dept., METU

Assoc. Prof. Dr. Ayşegül Askan Gündoğan
Civil Engineering Dept., METU

Assoc. Prof. Dr. Erdem Canbay
Civil Engineering Dept., METU

Volkan Aydoğan, M.Sc
Promer Consultancy Engineering Ltd. Co.

Date : 30 May 2014

I hereby declare that all information in this document has been obtained and presented in accordance with academic rules and ethical conduct. I also declare that, as required by these rules and conduct, I have fully cited and referenced all material and results that are not original to this work.

Name, Last name : Ceren DEMİRCİ

Signature :

ABSTRACT

AN APPROACH FOR SEISMIC DAMAGE ASSESSMENT OF RESIDENTIAL BUILDINGS

Demirci, Ceren

M.Sc., Department of Civil Engineering

Supervisor: Assoc. Prof. Dr. Murat Altuğ Erberik

Co-Supervisor: Assoc. Prof. Dr. Ayşegül Askan Gündoğan

May 2014, 131 pages

For developing countries in earthquake-prone regions, two main issues in seismic damage estimation are identification of seismic hazard in the region of interest and up-to-date information of the existing building stock. This study proposes an approach to handle these key issues and to obtain reliable measures for regional seismic damage estimation. The approach makes use of the basic structural information for different types of construction. This information can be readily available or may have been obtained after conducting a walk-down (street) survey in the region of interest. Then these parameters, which reflect the local characteristics of the building stock, are used to classify the residential buildings and to construct idealized SDOF models in order to provide an estimation of seismic damage of the buildings under consideration. After the formation of SDOF models, the seismic response of each building sub-classes are obtained through dynamic analyses. Within the scope of the proposed approach, scenario earthquakes are simulated due to scarcity of the real ground motion records recorded in the region during past earthquakes. The simulated records are obtained with regional seismic parameters regarding the source, path and site effects. The SDOF models are assumed to be subjected to these simulated records in order to obtain the seismic response. At the final step, the SDOF displacements obtained from dynamic analyses are compared

with pre-defined limit states for different building types and the corresponding damage states of the buildings are estimated. The final part of the study is devoted to the application of the proposed approach to one of the most earthquake-prone regions in Turkey and the world; the city of Erzincan. The results reveal that Erzincan city is under high risk, hence precautions should be taken immediately before an other major earthquake hits to the city.

Keywords: Seismic damage estimation, SDOF models, limit states, dynamic analysis.

ÖZ

KONUT TİPİ YAPILARIN SİSMİK HASAR DEĞERLENDİRMESİ İÇİN BİR YAKLAŞIM

Demirci, Ceren

Yüksek Lisans, İnşaat Mühendisliği Bölümü

Tez Yöneticisi: Doc. Dr. Murat Altuğ Erberik

Ortak Tez Yöneticisi : Doc. Dr. Ayşegül Askan Gündoğan

Mayıs 2014, 131 sayfa

Gelişmekte olan deprem bölgesi ülkeler için sismik hasar tahminindeki başlıca iki konu, bölgesel deprem tehlikesinin belirlenmesi ve bölgede yer alan bina stoğu ile ilgili güncel verilerin bir araya getirilmesidir. Bu çalışma, bu temel konuları ele almak ve bölgesel sismik hasar tahminini gerçekleştirmek için alternatif yaklaşım önermektedir. Bu yaklaşım, mevcutta hazır olan bina bilgilerini ya da sokak taraması sonucu elde edilmiş olan temel yapısal bilgileri kullanmayı amaçlamaktadır. Bina stoğunun yerel özelliklerini yansıtan bu özellikler, bir sonraki aşamada binaları sınıflandırmak ve binaların sismik hasar tahminlerini için tek dereceli system (TDS) modelleri oluşturmak amacıyla kullanılır. TDS modelleri oluşturduktan sonra, dinamik analiz sonucunda her bir bina alt sınıfı için sismik tepkiler elde edilir. Önerilen yöntem kapsamında, bölgede kaydedilmiş gerçek yer hareketi kayıtlarının azlığı nedeniyle senaryo depremleri simüle edilmektedir. Simüle edilen kayıtlar, kaynak, yol ve saha etkilerine ilişkin bölgesel sismik parametreleri ile elde edilir. TDS modellerinin sismik tepkileri, simüle edilen kayıtlar kullanılarak elde edilmektedir. Son adımda, dinamik analizler sonucu elde edilen TDS deplasmanları daha önceden tanımlanmış olan limit durumlarla karşılaştırılır ve bunun sonucu olarak tüm bina türleri için içinde buldukları hasar durumları tahmin edilir. Çalışmanın son bölümü önerilen yaklaşımın, Türkiye ve dünyada depreme en yakın

bölgelerden biri olan Erzincan şehrinde uygulanmasına ayrılmıştır. Elde edilen sonuçlar göstermektedir ki, Erzincan şehri deprem açısından yüksek risk taşımaktadır ve olası büyük bir deprem şehri vurmadan önce bu konuda bir an önce tedbirlerin alınması gerekmektedir.

Anahtar Sözcükler: Sismik hasar tahmini, TSD modeller, limit durumu, dinamik analiz

To my Dear Family,

ACKNOWLEDGMENTS

First of all, I would like to thank to my supervisor Assoc. Prof. Dr. Murat Altuğ Erberik and co-advisor Assoc. Prof. Dr. Ayşegül Askan Gündoğan for supports, motivation and guidance that they have provided me throughout the study.

Some of the works on this study have been carried out by TUJJB project under grant TUJJB-UDP-01-12. I want to thank my friends in the project for their help.

I would also thank to my friend, Shaghayegh Naghshineh, for her support and friendship during the study.

Tolga KINA deserves special thanks for his encouragement and support in the most difficult period of this study.

Finally, I would like to express my deepest appreciate to my parents Canan DEMİRCİ, Vahdettin DEMİRCİ and my sister Cansu DEMİRCİ for their support, patience and understanding throughout my whole life.

TABLE OF CONTENTS

ABSTRACT.....	v
ÖZ	vii
ACKNOWLEDGMENTS	x
TABLE OF CONTENTS	xi
LIST OF TABLES	xv
TABLES.....	xv
LIST OF FIGURES	xvii
FIGURES	xvii
LIST OF SYMBOLS AND ABBREVIATIONS	xxi
CHAPTERS	
1. INTRODUCTION	1
1.1 General	1
1.2 Literature Survey	2
1.3 Objective and Scope	7
2. IDEALIZED MODELS FOR BUILDING STRUCTURES	11
2.1 General	11
2.2 Previous Studies That Use Idealized Structural Models	11
2.3 Hysteresis Model Selection for the ESDOF System	16
3. EQUIVALENT SDOF PARAMETERS FOR MASONRY BUILDINGS	21
3.1 General	21
3.2 Generation of Structural Data for Masonry Buildings	21
3.3 Classification of Masonry Buildings	24
3.4 Major SDOF Parameters for Masonry Buildings.....	25

3.4.1 Fundamental Period	26
3.4.2 Strength Ratio and Ductility	34
3.4.3 Other SDOF Model Parameters	39
4. EQUIVALENT SDOF PARAMETERS FOR REINFORCED CONCRETE BUILDINDGS	41
4.1 General.....	41
4.2 Reinforced Concrete Frame Buildings	42
4.2.1 Available Studies Regarding Turkish RC Frame Buildings	42
4.2.2 Classification of RC Frame Buildings	48
4.2.3 Major SDOF Parameters for RC Frame Structures	55
4.3 Reinforced Concrete Tunnel-form Buildings	62
4.3.1. Available Studies Regarding RC Tunnel-form Buildings	63
4.3.2. Major SDOF Parameters for RC Tunnel-form Buildings.....	64
4.4 Reinforced Concrete Dual Buildings.....	68
4.4.1. Available Studies Regarding RC Dual Buildings.....	68
4.4.2. Major SDOF Parameters for RC Dual Buildings	72
5. A CASE STUDY FOR ESTIMATION OF DAMAGE RATES IN ERZINCAN	75
5.1 General.....	75
5.2 Synthetic Database: Simulated Ground Motions in Erzincan City Center.....	76
5.2.1 Methodology	76
5.2.2. Seismicity of the Area.....	77
5.2.3. Simulated Ground Motion Dataset	79
5.3 Equivalent SDOF Analyses to Estimate Seismic Damage in Selected Districts	88
5.3.1 General Characteristics of the Building Stock in the Selected Districts....	88

5.3.2 Dynamic Response Obtained from SDOF Analyses for the Selected Districts.....	90
5.4 Limit States Defined for the Building Sub-classes.....	93
5.5 Estimated Damage States for Existing Building Sub-classes in the Selected Districts	95
5.6 Comparison of Estimated and Observed Damage for the 1992 Erzincan Earthquake.....	99
6. SUMMARY AND CONCLUSIONS	101
6.1 Summary	101
6.2 Conclusions	103
REFERENCES.....	105
APPENDIX A	113
PLAN GEOMETRY OF GENERATED MASONRY BUILDING MODELS	113
A.1. R1-W1 MODEL	113
A.2. R1-W2 MODEL	114
A.3. R1-W3 MODEL	115
A.4. R2-W1 MODEL	116
A.5. R2-W2 MODEL	117
A.6. R2-W3 MODEL	118
APPENDIX B	119
CAPACITY CURVES OF MASONRY BUILDING MODELS	119

LIST OF TABLES

TABLES

Table 3.1 Story mass and mass moment of inertias of masonry building models	24
Table 3.2 Major SDOF parameters obtained from MAS program	28
Table 3.2 Continued	29
Table 3.3. Linear empirical equations for predicting fundamental periods of masonry buildings	30
Table 3.4. Comparison of empirical period formulation with the reference values obtained through eigenvalue analyses	32
Table 3.4. Continued	33
Table 3.5. Error estimations in the empirical formulations	34
Table 3.6 Base shear coefficient (V_b/W) as a function of seismic zone (A_0)	36
Table 3.7 Proposed SDOF parameters of masonry building subclasses	40
Table 4.1. General properties of the selected buildings in Düzce. (Ozun, 2007)	45
Table 4.2. General properties of the existing structures in Eskişehir (Karaca, 2013)	47
Table 4.3 The classification of all RC frame buildings used in this study	50
Table 4.3 Continued	51
Table 4.3 Continued	52
Table 4.3 Continued	53
Table 4.3 Continued	54
Table 4.4. Mean and standard deviation of low-rise, mid-rise and all buildings	55
Table 4.5. Mean and standard deviation of buildings	57
Table 4.6 Error estimations in the period formulations	60
Table 4.7 Major SDOF parameters for RC frame structures	61
Table 4.8 Error estimations in the period formulations	66

Table 4.9 Major SDOF parameters for RC tunnel-form structures.....	67
Table 4.10. General properties of the existing structures in Eskişehir (Karaca, 2013)	71
Table 4.11. The classification of all RC dual buildings used in this study	72
Table 4.12 Error estimations in the period formulations	74
Table 4.13 Major SDOF parameters for RC dual buildings	74
Table 5.1 Information regarding the scenario earthquakes	87
Table 5.2 SDOF displacement demand (in cm) for building sub-classes in Cumhuriyet district.....	90
Table 5.3 SDOF displacement demand (in cm) for building sub-classes in Fatih district.....	91
Table 5.4 SDOF displacement demand (in cm) for building sub-classes in Yavuz Sultan Selim district	92
Table 5.5 SDOF displacement demand (in cm) for building sub-classes in Yunus Emre district	92
Table 5.6 The abbreviations and definitions of damage states	95
Table 5.7 Limit states of building sub-classes in terms of SDOF displacement (cm)	95
Table 5.8 Estimated damage states for building sub-classes in Cumhuriyet district .	96
Table 5.9 Estimated damage states for for building sub-classes in Fatih district	96
Table 5.10 Estimated damage states for building sub-classes in Yavuz Sultan Selim district.....	97
Table 5.11 Estimated damage states for building sub-classes in Yunus Emre district	98
Table 5.12 Observed damage distribution in the selected districts during the 1992 Erzincan earthquake	99

LIST OF FIGURES

FIGURES

Figure 1.1 Data collection form used in the context of ATC-21 (FEMA-154) methodology.....	3
Figure 1.2 a) Data collection form of masonry buildings in the context of Istanbul Earthquake MasterPlan Project (front page)	8
Figure 1.2 b) Data collection form of masonry buildings in the context of Istanbul Earthquake MasterPlan Project (information page).....	9
Figure 1.3. Structure of the damage estimation	10
Figure 2.1 MDOF System Represented By a Single Mass System (ATC 40, 1996). 13	
Figure 2.2. Conversion of capacity curve to capacity spectrum (ATC-40, 1996)	14
Figure 2.3 Force-displacement relationship of the ESDOF system. (ATC-40, 1996)15	
Figure 2.4 Degrading stiffness model by Clough and Johnston (1966).....	17
Figure 2.5. Backbone curve of the stiffness and strength degrading Clough model .	18
Figure 2.6. Stiffness and strength degrading Clough hysteretic model	19
Figure 3.1. Experimental capacity curves of tested buildings (Costley and Abram, 1996)	34
Figure 3.1. Continued.....	35
Figure 3.2 Bilinear idealization of capacity curve (ATC-40, 1996)	37
Figure 3.3 Bilinear idealization of capacity curve. (Tomatevic, 1999)	38
Figure 4.1a) 3 story model, b) 5 story model, c) 7 story model (Ay, 2006)	43
Figure 4.2a) F2S2B, b)F5S4B, c)F5S2B, d)F8S3B, e)F3S2B, f)F5S7B (Kadas, 2006)	46
Figure 4.3 The relationship between period and number of storey a)Low-rise buildings. b) Mid-rise buildings. c)All buildings.....	56

Figure 4.4 The relationship between period and number of storey a) Level A, b) Level B	57
Figure 4.4 Continued c) Level C, d) All buildings.....	58
Figure 4.5 Comparison of fundamental periods in terms of building height	60
Figure 4.6 Idealization of pushover curve (Metin, 2006)	61
Figure 4.7 A typical tunnel form building (Yakut and Gulkan, 2003).....	62
Figure 4.8. Period versus number of the stories relationship in RC tunnel-form structures	64
Figure 4.9 Comparison of fundamental periods in terms of building height	66
Figure 4.10 Capacity curves for 2 stories and 5 story RC tunnel-form buildings (Balkaya and Kalkan, 2004).....	67
Figure 4.11 Plan view of the building with a) 0.5% shear wall ratio, b) 1.0% shear wall ratio, c) 1.5% shear wall ratio.....	69
Figure 4.11 Continued, d) 2.0% shear wall ratio (Günel, 2013).....	70
Figure 4.12 Variation of fundamental period with shear wall ratio for the generic building (Günel, 2013)	70
Figure 4.13. Period versus number of the stories relationship in RC dual structures	73
Figure 4.14 Comparison of fundamental periods in terms of building height	73
Figure 5.1. Source mechanism in stochastic finite fault method (adapted from Hisada, 2008)	77
Figure 5.2. The focal mechanisms and the related faults of the 1939 (red) and 1992 (blue) Erzincan earthquakes (Stars indicate the epicenters, triangles indicate the locations of the (three) strong motion stations that recorded the 1992 mainshock, shaded area is the Erzincan basin).....	78
Figure 5.3. The seismic activity in Erzincan region within the instrumental era (only mainshocks are presented in this figure)	79
Figure 5.4 The anticipated distribution of peak ground motion parameters for each scenario earthquake	80

Figure 5.4 Continued.....	81
Figure 5.4 Continued.....	82
Figure 5.4 Continued.....	83
Figure 5.4 Continued.....	84
Figure 5.4 Continued.....	85
Figure 5.4 Continued.....	86
Figure A.1. 1. Plan geometry of subclass R1W1 of masonry building model.....	113
Figure A.2. 1. Plan geometry of subclass R1W2 of masonry building model.....	114
Figure A.3. 1. Plan geometry of subclass R1W3 of masonry building model.....	115
Figure A.4. 1. Plan geometry of subclass R2W1 of masonry building model.....	116
Figure A.5. 1. Plan geometry of subclass R2W2 of masonry building model.....	117
Figure A.6. 1. Plan geometry of subclass R2W3 of masonry building model.....	118
Figure B.1 Capacity Curves of subclass R1W1 of masonry building model.....	119
Figure B.1 Continued	120
Figure B.1 Continued	121
Figure B.2 Capacity Curves of subclass R1W2 of masonry building model.....	121
Figure B.2 Continued	122
Figure B.2 Continued	123
Figure B.3 Capacity Curves of subclass R1W3 of masonry building model.....	123
Figure B.3 Continued	124
Figure B.3 Continued	125
Figure B.4 Capacity Curves of subclass R2W1 of masonry building model.....	125
Figure B.4 Continued	126
Figure B.4 Continued	127
Figure B.5 Capacity Curves of subclass R2W2 of masonry building model.....	127

Figure B.5 Continued	128
Figure B.5 Continued	129
Figure B.6 Capacity Curves of subclass R2W3 of masonry building model.....	129
Figure B.6 Continued	130
Figure B.6 Continued	131

LIST OF SYMBOLS AND ABBREVIATIONS

A	: Gross floor area
A_C	: Combined effective area
A_i	: Horizontal cross-sectional area
A_0	: Seismic zone coefficient
ATC	: Applied Technology Council
a, b, c, d	: Multivariable linear regression coefficients of masonry buildings
c_1, c_2, c_3	: Nonlinear regression coefficients of masonry buildings
D	: Dimension in the direction under consideration
D^*	: Displacement of the equivalent SDOF system
D_t	: Top displacement of the MDOF system
E_o	: Basic structural performance
E_S	: Reliability index
F^*	: Force of the equivalent SDOF system
f_y	: Yield strength
f_m	: Maximum strength
f_r	: Residual strength
G	: Linear limit of secant shear modulus
G'	: Ground index
H	: Height of the building
I	: Building importance factor
I_S	: Seismic performance index
I_{S0}	: Seismic judgement index
K^*	: Effective stiffness of SDOF system

k_y	: Initial elastic stiffness
k_u	: Post-yielding stiffness
k_r	: Post-capping stiffness
L_d	: Total length of masonry load-bearing walls
M^*	: Effective mass of SDOF system
N	: Number of stories
NW	: Total number of shear walls
$R_a(T)$: Seismic load reduction factor
$RMSE$: Root mean square error
$S(T)$: Spectrum coefficient
S_D	: Structural design of the building
T	: Period of the building
TEC	: Turkish Earthquake Code
V_b	: Design base shear force
W	: Weight of the building
w_{eff}	: Effective frequency of SDOF
Z	: Zone index
α_r	: Post-yielding stiffness ratio
α_u	: Post-capping stiffness ratio
β_a, β_b	: Strength degradation factor
β_0	: Stiffness degradation factor
λ	: Residual to yielding strength ratio
μ	: Ductility
η	: Strength ratio
δ_m	: Maximum displacement

δ_u : Ultimate displacement

δ_y : Yield displacement

CHAPTER 1

INTRODUCTION

1.1 General

Within the last three decades, Turkey has suffered from large earthquakes with severe damage potential such as Erzincan (1992), Kocaeli (1999), Düzce (1999), Bingol (2003), Elazig (2009) and Van (2011) events. These earthquakes resulted in significant damages, a significant number of deaths and injuries. Since majority of the urban regions in Turkey is on seismically active fault zones, it is not possible to avoid earthquakes but it is possible to reduce the structural, social and economic losses due to these natural disasters. A first step in seismic risk mitigation is the estimation of seismic damages and losses in potential earthquakes.

Two key components of seismic damage studies are the regional seismic hazard and vulnerability of the building stock of interest. Seismic hazard is mostly expressed in terms of (real or simulated) ground motions while building vulnerability can be assessed in a variety of ways ranging from damage parameters to detailed complex models of dynamic building response during earthquakes.

This study proposes an alternative approach to estimate seismic damage levels in residential structures based on the basic structural information which is obtained by a walk-down (street) survey. This structural information contains parameters which can be obtained in a very short period of time such as the construction type, number of stories, deficiencies in plan, etc. By a rapid visual screening, the local characteristics of the building stock can be obtained in order to construct idealized structural models. These models are assumed to be subjected to simulated records in order to obtain seismic vulnerability of building structures. At the final step, hazard, fragility and inventory components are used to estimate seismic damage given a certain scenario event.

As the case study area, Erzincan is selected since the city had experienced two major earthquakes within the last century in 1939 and 1992. The city center is located on a basin structure that amplifies the ground motions. In addition, due to the short distances from the nearest fault zone, large ground motion amplitudes are always anticipated in that area which makes it worthwhile to handle within such a study.

1.2 Literature Survey

Among the challenges involved with seismic damage estimation, handling a large population of buildings is one of the most difficult processes. Rapid visual screening is an important tool for evaluating such a large group of buildings because it is a rapid and easy identification of the building.

The pioneer works regarding rapid visual screening methodology were titled as ATC-21 (a.k.a FEMA-154) and ATC-21-1 (a.k.a FEMA-155). These reports, which date back to 1988, were developed by the Applied Technology Council (ATC) for the Federal Emergency Management Agency (FEMA). Then the methodology was modified in 2002 to yield more reliable results. The methodology is based on the idea of collecting structural information from the surveyed buildings in a short period of time without entering the building and then assigning performance scores to the surveyed buildings by employing the collected data. Data collection form used within the context of ATC-21 methodology is given in Figure 1.1. It is a simple form containing major information about the surveyed building, which can be filled in a short period of time. In score assignment stage, a base score is given to each building depending on the construction type and the seismic zone that the building resides. High base score means less vulnerable building to seismic action. Then some penalty scores are assigned to the buildings due to the existing structural properties and deficiencies (site condition, plan irregularity, vertical irregularity, compliance with the seismic code, etc.). The final score is the combination of the base score and the penalty scores. Based on the final score it becomes possible to rank buildings in a relative manner in terms of their predicted seismic damage and to give the decisions of evaluating the surveyed buildings in a more detailed manner or not. The methodology had been developed for the buildings in the United States, but due to its simplicity, it has been popular in many earthquake prone countries and used with

Some researchers adopted the FEMA procedure to their own research. For instance Karbassi and Nollet (2008) proposed a similar visual screening methodology to assess existing buildings in the Quebec province of Canada. In this study, original base and penalty scores of the FEMA procedure were modified in order to reflect the local characteristics of the building stock in Quebec.

The assessment of seismic performance of existing Japanese reinforced concrete buildings with less than 6 storeys has been carried out by using the Japanese Seismic Index Method (JBDPA 1990). In this method, the seismic performance of a building is assessed by employing a seismic performance index I_S in three screening levels with increasing reliability. The seismic performance index can be defined as a function of three parameters for basic structural performance (E_o), structural design of the building (S_D), and time-dependent deterioration of the building (T).

$$I_S = E_o S_D T \quad (1.1)$$

In the above equation, parameter E_o is related to the ultimate strength and ductility of the building with an emphasis on the failure mode and the total number of stories. Parameter S_D represents the effects of irregularity, stiffness and mass concentration in a building whereas the influence of cracking and deterioration is considered by the parameter T . After calculated, index I_S is compared with another index, I_{S0} , called as the seismic judgement index.

$$I_{S0} = E_S Z G' U \quad (1.2)$$

In Equation 1.2, parameter E_S is the reliability index based on the screening level, parameter Z represents the zone index to modify the on-site intensity of the ground motion, parameter G' denotes the ground index to quantify soil-structure interaction, amplification in the top layer of ground or topographical effects and finally parameter U is an importance factor for the occupancy type of the building. Depending on the comparative values of I_S and I_{S0} , there are three different cases: If $I_S > I_{S0}$, then vulnerability condition is low for all three screening levels. If $I_S \ll I_{S0}$, then the level of vulnerability is so high that it requires either retrofit or demolition of the building under consideration. And finally the case $I_S < I_{S0}$ refers to an uncertain condition. In this case, a more detailed assessment is required in the next screening level.

Different rapid visual screening methodologies have become popular also in Turkey within the last two decades. One of the well known assessment methods belong to Hassan and Sozen (1997), which is limited to low-rise reinforced concrete structures. These researchers developed an assessment parameter called “priority index”, which enables the quick decision of strengthening or removing the considered structure, is the summation of two other indices: the wall index and the column index. The wall index is the ratio of total wall area (structural walls plus filler walls with some weighing factors) to total floor area above base of the building whereas the column index is defined as the ratio of column cross sectional area to floor area. Hassan and Sozen used the damaged building database obtained after the 1992 Erzincan earthquake to calibrate their index. Overall, this is an early attempt to assess the relative vulnerability of a population of buildings by using basic structural information that can be obtained through field survey.

Ozcebe et al (2004) developed a preliminary evaluation methodology to assess seismic vulnerability of existing low-rise and mid-rise reinforced concrete buildings by using a statistical technique called as “discriminant analysis”. Their main goal was to address relatively vulnerable buildings in a large population. The structural parameters used to obtain the damage scores and to classify the buildings in low, moderate and high levels of seismic risk according to these scores were the number of stories, minimum normalized lateral stiffness index, minimum normalized lateral strength index, normalized redundancy score, soft story index and overhang ratio, details of which are provided in the reference.

Yakut (2004) proposed a comprehensive preliminary evaluation procedure for low-rise and mid-rise reinforced concrete buildings in Turkey. He defined a parameter called as “capacity index”, which considers the orientation, geometrical and material characteristics of the structural system together with the quality of workmanship and materials and architectural features such as short columns and plan irregularities. At the final stage, the capacity index values are compared with some limiting values in order to make the final decision regarding the seismic safety of the considered building.

Ozdemir et al. (2005) developed the Seismic Safety Screening Method (SSSM), that was inspired from the Japanese Seismic Index Method (JBDPA, 1990). The

application of the method was limited to reinforced concrete frame, shearwall and dual buildings up to 6 stories. The parameters in the proposed index were calibrated by making use of the data taken from existing Turkish buildings in Zeytinburnu district in Istanbul.

The screening procedure proposed by Sucuoğlu et al. (2007) was applicable to three- to six-story substandard concrete buildings in Turkey by employing the sidewalk survey approach in a population of buildings. The calibration of the methodology was conducted with the field data compiled after the 1999 Düzce earthquake. Their main goal was to accelerate the vulnerability assessment studies in large stocks of vulnerable buildings. The screening procedure was then applied to more than 15,000 buildings in a pilot region, Zeytinburnu district in Istanbul, in the context of Istanbul Earthquake MasterPlan (2003). Masonry buildings were also assessed in the same project by obtaining the basic structural parameters from the sidewalk survey (Figure 1.2) and using them to classify masonry buildings. In this way, 120 different sub-classes of buildings were generated. Then fragility curve sets were developed for each masonry building sub-class. Then the surveyed buildings were assigned to appropriate building sub-classes with a representative set of fragility curves. The vulnerability of each building was determined by using a performance index that uses the fragility information and the on-site value of seismic hazard parameter, which was selected as the peak ground acceleration for masonry buildings in the study. The details of the assesment procedure can be found elsewhere (Erberik 2010).

Considering all of the above studies in the literature, this study is different from the previous ones in the following aspects: First, most of the methods concentrate on one particular type of construction such as mid-rise reinforced concrete frame structures, etc. In this study, it is possible to consider all types of constructions required that the basic structural information to construct the idealized model is available. Second, most of the previous methods use techniques based on score assignment to evaluate seismic damage of building populations. In the proposed approach, actual nonlinear analyses are performed to obtain the seismic demand of building structures. It is possible to reflect the local structural characteristics explicitly depending on the robustness and complexity of the hysteresis model used in the idealized model. Another advantage is that when the idealized SDOF models are once developed, they

can be used for populations of buildings in different regions with similar structural characteristics without extra analyses. On the other hand, similar to the other preliminary assessment procedures, this method gives the general distribution of seismic damage and it is not accurate enough to estimate the vulnerability of individual buildings in a detailed manner.

1.3 Objective and Scope

This study aims to propose an approach for estimating potential seismic damage to populations of residential buildings with different construction types under certain intensities of seismic hazard. Such a study could be useful for rapid estimation of future seismic damage in any region of interest.

The proposed approach is illustrated in Figure 1.3. First steps of the procedure are the identification of seismic hazard in terms of scenario earthquakes and the development of idealized SDOF models to represent population of residential buildings of different construction types in terms of simple model parameters. In seismic hazard identification stage, scenario earthquakes should be generated if the available ground motion data is not sufficient to conduct such a damage estimation study. Then dynamic analyses are performed by using the ESDOF models and the generated scenario earthquakes. In the next step, displacement demands obtained from dynamic analyses of ESDOF models is converted into damage states through definitions of limit states. In this thesis, different construction types are considered to represent the residential building stock. These are reinforced concrete frame, reinforced concrete dual, reinforced concrete tunnel form and unreinforced masonry building types. In this study, the proposed approach is applied to Erzincan city. However if the local seismicity and building stock characteristics can be defined, it can be applied to any earthquake prone region in a similar way.

MINISTRY DISASTER EMERGENCY MANAGEMENT PRESIDENCY SURVEY FORM FOR SEISMIC SAFETY ASSESSMENT OF MASONRY BUILDINGS			
BUILDING ID INFO		Photo of the building	
BUILDING ID			
DATE OF SURVEY			
BUILDING ADDRESS			
GPS COORDINATES (E/N)			
CONSTRUCTION YEAR			
TECHNICAL PERSON			
CONSTRUCTION TYPE (See -1-)			
<input type="checkbox"/> UNREINFORCED	<input type="checkbox"/> UNCONFINED		
<input type="checkbox"/> REINFORCED	<input type="checkbox"/> HYBRID (URM + RC)		
OBSERVATIONS OUTSIDE THE BUILDING (See -2-)			
NUMBER OF STORIES (NUMBER)		
HIGH SLOPE ?	NO ()	YES ()	
BASEMENT FLOOR	NO ()	YES ()	N/A ()
PLAN GEOMETRY	REGULAR ()	IRREGULAR ()	
FAÇADE LENGTH (FRONT) Meters	CRITICAL STORY OPENING LENGTH (FRONT) Metre		
FAÇADE LENGTH (SIDE) Meters	CRITICAL STORY OPENING LENGTH (SIDE) Metre		
VERTICAL OPENING LAYOUT	REGULAR ()	F. REGULAR ()	IRREGULAR ()
LOCATION OF BUILDING	SEPARATED ()	ADJ. MIDDLE ()	ADJ. CORNER ()
BUILDING HEIGHT DIFFERENCE	NO ()	YES ()	
FLOOR ELEVATION DIFFERENCE	NO ()	YES ()	
PREVIOUS DAMAGE	NO ()	YES ()	
ADJACENT TO HISTORICAL BUILDING	NO ()	YES ()	
OBSERVATIONS INSIDE THE BUILDING (See -3-)			
TYPICAL STORY HEIGHT Meters		
TYPICAL WALL THICKNESS Meters		
UNCONSTRAINED WALL LENGTH (L_m) > 5.0 m ?	YES () TIMES	NO ()
WALL LENGTH BTW TWO OPENINGS (L_b) < 1.0 m ?	YES () TIMES	NO ()
WALL LENGTH BTW CORNER & OPENING (L_k) < 1.5 m ?	YES () TIMES	NO ()
GENERAL OBSERVATIONS (See -4-)			
MASONRY WALL TYPE	SOLID BRICK ()	HOLLOW BRICK ()	SOLID CMU ()
	HOLLOW CMU ()	AAC ()	CUT STONE ()
	RUBBLE STONE ()	ADOBE ()	
MORTAR TYPE	CEMENT ()	LIME ()	MUD ()
			NO ()
WORKMANSHIP	GOOD ()	MODERATE ()	
		POOR ()	
FLOOR TYPE	RC ()	WOODEN ()	ARCHED ()
HORIZONTAL BOND BEAM ?	OVER WINDOW ()	FLOOR LEVEL ()	NO ()
VERTICAL BOND BEAM ?	YES () metre interval	NO ()	
LINTEL ?	YES ()	NO ()	
LINTEL/BEAM MATERIAL?	RC ()	WOODEN ()	
ROOF TYPE	FLAT ()	SHED ()	GABLE ()
			HIPPED ()
ROOF MATERIAL	TILE ()	RC ()	METAL SHEET ()
			EARTHEN ()
CONNECTIONS	GOOD ()	POOR ()	
SOFT/WEAK STORY	YES ()	NO ()	

Figure 1.2 a) Data collection form of masonry buildings in the context of Istanbul Earthquake MasterPlan Project (front page)

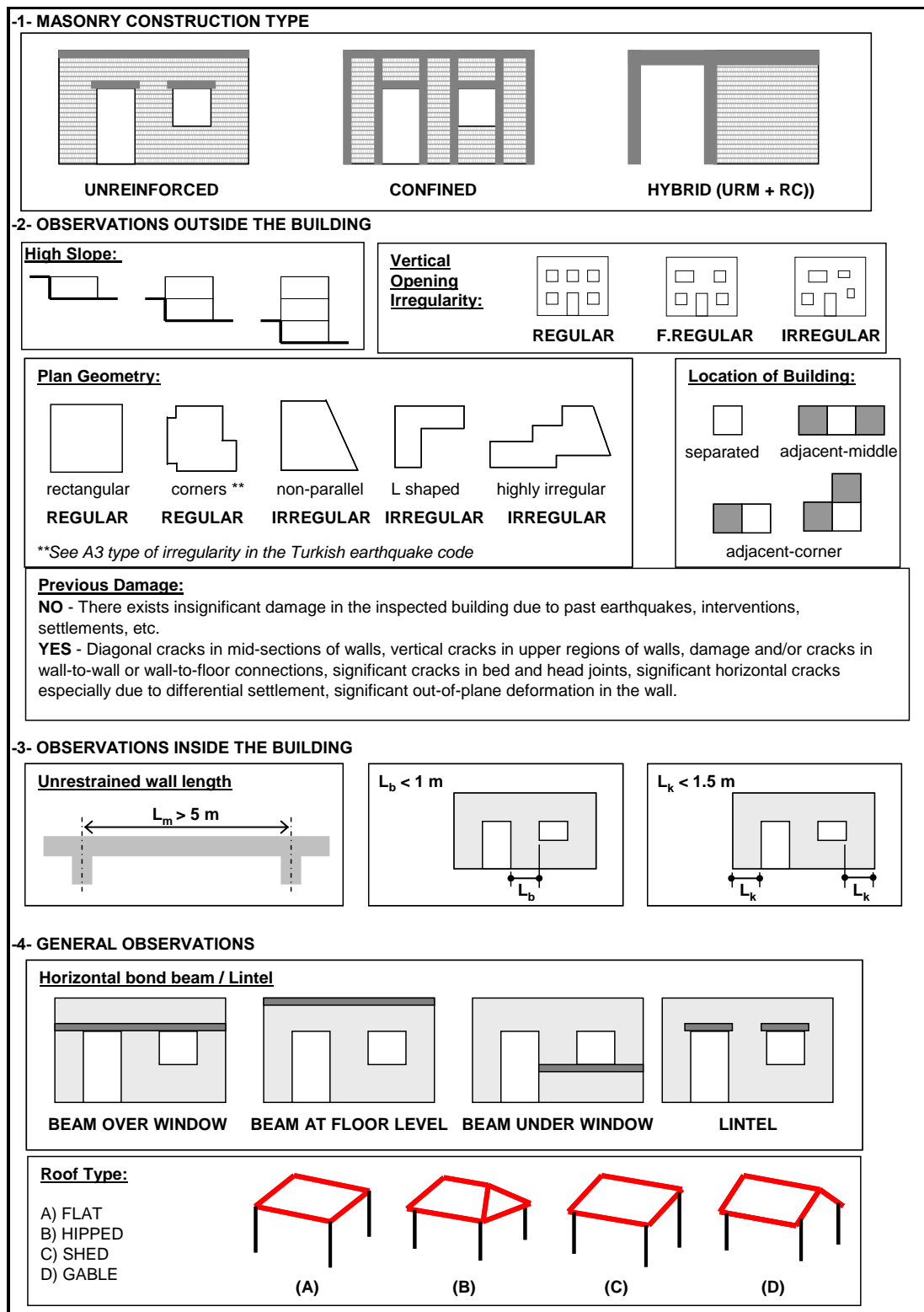


Figure 1.2 b) Data collection from of masonry buildings in the context of Istanbul Earthquake MasterPlan Project (information page)

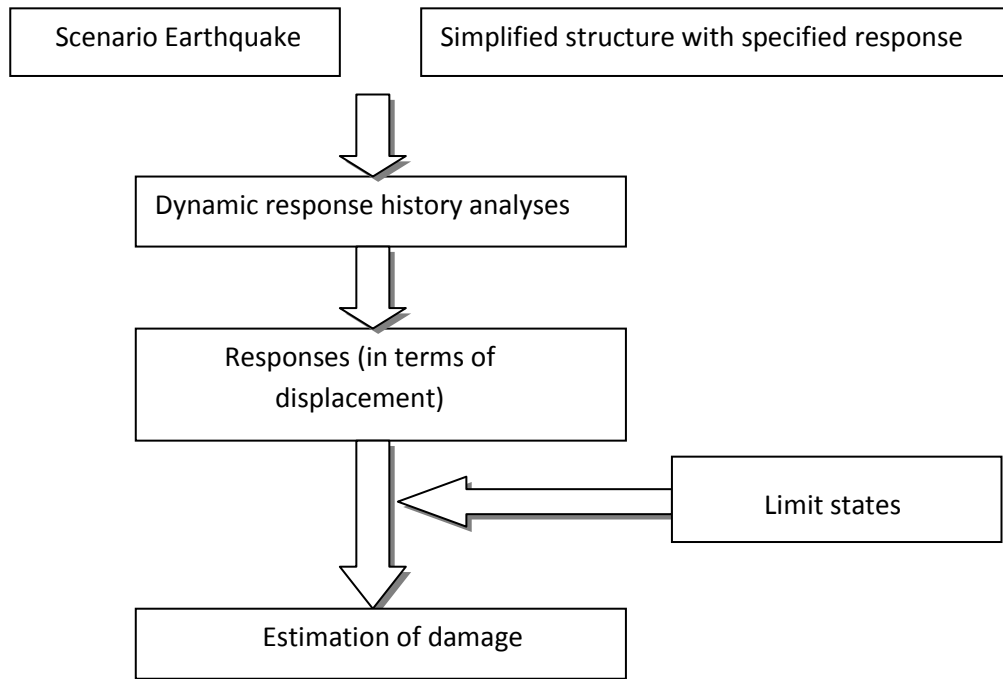


Figure 1.3. Structure of the damage estimation

Chapter 2 describes the generation of single degree of freedom system from a multi-degree of freedom system. In addition, modified Clough hysteretic model that is used in the SDOF analyses is introduced with all the model parameters.

Chapter 3 presents the structural data generated for the evaluation of seismic performance of masonry buildings followed by the corresponding equivalent SDOF model parameters.

Chapter 4 includes the determination of the SDOF model parameters for reinforced concrete buildings categorized as frame, shearwall and dual buildings by making use of the previous studies and available building data.

Chapter 5 presents the case study which is an application of the proposed approach in Erzincan. First seismic hazard is identified and the ground motion records obtained from pre-defined scenario earthquakes are discussed. Then seismic damage prediction is carried out for the residential buildings in four different districts of the Erzincan city.

Finally, Chapter 6 is the summary and conclusion of this study.

CHAPTER 2

IDEALIZED MODELS FOR BUILDING STRUCTURES

2.1 General

This chapter focuses on the basics of the proposed methodology by emphasizing the main assumption of using idealized models instead of actual building models. The employment of idealized models enables the damage assessment of a large population of buildings or building sub-classes in a comparatively short period of time. In addition, it becomes possible to use nonlinear dynamic analysis to obtain realistic seismic response statistics. Hence equivalent single degree of freedom (ESDOF) systems are employed in this study to represent different building sub-classes instead of complex analytical models.

In this chapter, first the studies in the literature, which have made use of idealized structural models are reviewed. Then the selected hysteresis model to simulate the inelastic behavior of the building structures is presented together with its model parameters.

2.2 Previous Studies That Use Idealized Structural Models

The idea of representing complex structural systems by using simple idealized models date back to 1970's when Gulkan and Sozen (1974) and Shibata and Sozen (1978) proposed the "substitute structure" method, which was actually the realization of ESDOF concept. In 1975, Freeman used to same concept to develop one of the today's well-known approaches of earthquake engineering, called as the "Capacity Spectrum Method". Also in 1979, Saiidi and Sozen develop Q-model to obtain nonlinear seismic response of reinforced concrete structures.

Another method that makes use of the conversion from a multi degree of freedom (MDOF) system to an ESDOF system is the N2 method, which was originally proposed by Fajfar and Fischinger (1987). This method was later recommended in Eurocode 8 (CEN 1995). According to this method, after obtaining the pushover curve of a MDOF system, it is converted to a capacity curve for an ESDOF system by using the equations 2.1 and 2.2.

$$D^* = \frac{D_t}{\Gamma} \quad (2.1)$$

$$F^* = \frac{V}{\Gamma} \quad (2.2)$$

In Equations 2.1 and 2.2, parameters D^* and F^* are the displacement and force of the ESDOF system, respectively. D_t is the top displacement and V is the base shear of the MDOF system and it is defined as in Equation 2.3,

$$V = p \phi^T M s = m^* p \quad (2.3)$$

where m^* is the equivalent mass of SDOF system. In the equation ϕ represents modal displacement shape. In Equations 2.1 and 2.2, parameter Γ denotes the transformation factor, which controls the conversion from MDOF to SDOF system and it is defined as;

$$\Gamma = \frac{m^*}{\sum m_i \phi_i^2} \quad (2.4)$$

The curve that shows the relationship between V and D_t for the MDOF system is the same with the F^* and D^* relationship curve of ESDOF system, except the scale of the axes that is the result of the transformation factor, Γ . As a result of the bilinear idealization of the curve, F_y^* and D_y^* which are the yield strength and displacement of the SDOF system, are estimated. The elastic period of the bilinearized equivalent SDOF system is;

$$T^* = 2 \pi \sqrt{\frac{M^*}{K^*}} \quad (2.5)$$

ESDOF concept also encouraged the use of nonlinear static procedures (NSP) for the seismic assessment of structural systems with the introduction of the documents like

ATC-40 (1996) and FEMA-273 (1997). According to the ATC-40 document, structures can be represented by an ESDOF system instead of complex MDOF systems, as shown in Figure 2.1. The basic conversion of MDOF systems to ESDOF systems is obtained by using the capacity spectrum method. In this method, MDOF systems are represented by ESDOF systems by defining effective mass M^* and effective period T_{eff} .

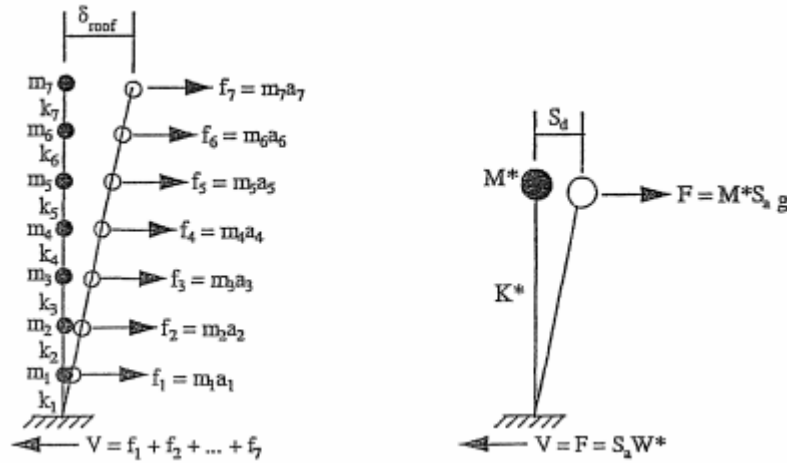


Figure 2.1 MDOF System Represented By a Single Mass System (ATC 40, 1996)

In capacity spectrum method, the capacity curve, that shows the relationship between force - displacement, is converted to acceleration - displacement response spectra (ADRS) format by using the Equations 2.6 and 2.7.

$$S_a = \frac{V}{\alpha_1 W} \quad (2.6)$$

$$S_d = \frac{\Delta_{\text{roof}}}{PF \phi_{\text{roof},1}} \quad (2.7)$$

In the above equations, V is the base shear, W is the weight of the structure, α_1 is the modal mass coefficient for the first natural mode, Δ_{roof} is the roof displacement, PF_1 is the modal participation factor for the first natural mode and $\phi_{\text{roof},1}$ is the amplitude of the first mode at the roof level. The parameters α_1 and PF_1 which are used in above equations are defined as ;

$$\alpha_1 = \frac{\left[\sum_{i=1}^N \frac{w_i \phi_{i,1}}{g} \right]^2}{\left[\sum_{i=1}^N \frac{w_i}{g} \right] \left[\sum_{i=1}^N \frac{(w_i \phi_{i,1}^2)}{g} \right]} \quad (2.8)$$

$$PF_1 = \frac{\left[\sum_{i=1}^N \frac{(w_i \phi_{i,1})}{g} \right]}{\left[\sum_{i=1}^N \frac{(w_i \phi_{i,1}^2)}{g} \right]} \quad (2.9)$$

where w_i/g is the mass assigned to level i , $\phi_{i,1}$ is the amplitude of the first mode at level i and N is the number of stories.

On the capacity curve, at each point V and Δ_{roof} are converted to S_a and S_d by using the Equations 2.6 and 2.7 and in this way, the required parameters to obtain ADRS spectrum are calculated (Figure 2.2).

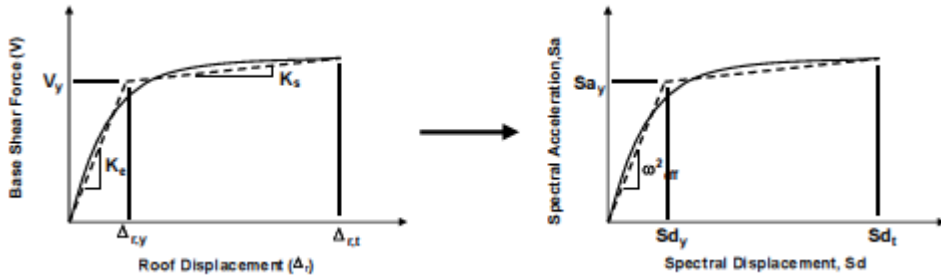


Figure 2.2. Conversion of capacity curve to capacity spectrum (ATC-40, 1996)

After the bilinearization of the capacity spectrum, from the initial slope, effective frequency (i.e. w_{eff}^2) of the equivalent SDOF system is determined and the force-deformation relationship of equivalent SDOF system is estimated according to the Equations 2.10, 2.11 and 2.12.

$$M^* = \alpha_1 M \quad (2.10)$$

$$K^* = w_{eff}^2 M^* \quad (2.11)$$

$$F_y = V_y = S_{a_y} M^* \quad (2.12)$$

where F_y is the yield force, V_y is the yield base shear and S_{a_y} is the yield spectral acceleration. The effective frequency of the ESDOF system is defined as;

$$w_{\text{eff}} = 4\pi^2 / T_{\text{eff}}^2 \quad (2.13)$$

As the final product, the force- displacement relationship of the ESDOF system is as shown in Figure 2.3. In the figure, parameter a_p is the ratio of post-yielding stiffness (K_u) to the initial elastic stiffness (K_e) of the bilinearized capacity curve. The elastic period of the bilinearized equivalent SDOF system can be defined as;

$$T^* = 2\pi \sqrt{\frac{M^*}{K^*}} \quad (2.14)$$

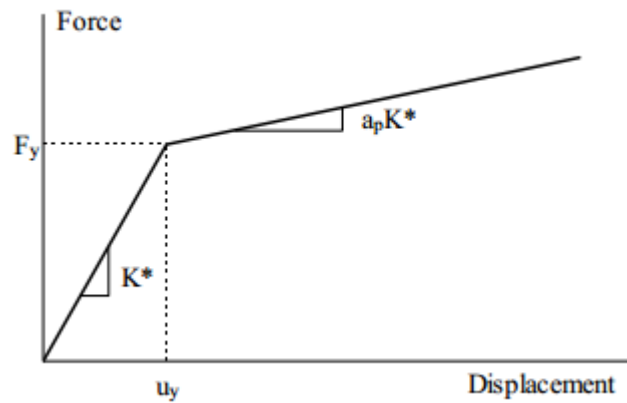


Figure 2.3 Force-displacement relationship of the ESDOF system. (ATC-40, 1996)

Chopra and Goel (2002) also used ESDOF concept while proposing their improved pushover analysis procedure called as modal pushover analysis. They idealized the pushover curve by using a bilinear force–deformation relationship that defines the inelastic SDOF system of each mode. Vibration properties were assumed to be in the linear range that are the same as those of the elastic SDOF system of the considered mode.

In 2007, Jeong and Elnashai proposed parameterized fragility method for practical application of analytical fragility curves to estimate seismic damage for a large number of structural configurations in a timely manner. They used ESDOF systems to characterize different structural systems and obtained fragility curves through SDOF analyses.

As observed from the previous studies, the concept of idealizing the response through an ESDOF system has been used in many different methods in earthquake

engineering since it is a simple and straight-forward approach. However the underlying assumptions of using such simplified models should always be kept in mind while interpreting the seismic response obtained through these models.

2.3 Hysteresis Model Selection for the ESDOF System

In order to simulate the inelastic behavior of idealized building structures in the form of ESDOF models, a force-deformation relationship, which is called as a hysteresis model, should be used. Hysteresis models prescribe a set of rules governing the behavior of the model under all possible cyclic loading histories (Stojadinovic and Thewalt, 1996). As the complexity of the model increases, it becomes computationally more expensive and versatile.

Bilinear hysteretic model is the simplest one to be used in nonlinear dynamic analysis of structural systems. It has also been the most popular model, especially at the initial development stages when the computational facilities were not so involved.

In 1966, Clough and Johnston proposed a hysteretic model with a bilinear primary curve. In fact, their original model is an enhanced version of bilinear model by considering the degradation of the reloading stiffness. There are two main rules of the model. First, the unloading stiffness remains parallel to the initial elastic stiffness, and second, reloading aims at the previous maximum response point in the direction of loading (see Figure 2.4). Since the model basically does not consider strength degradation, it may be employed to simulate the behavior of well-detailed reinforced concrete members.

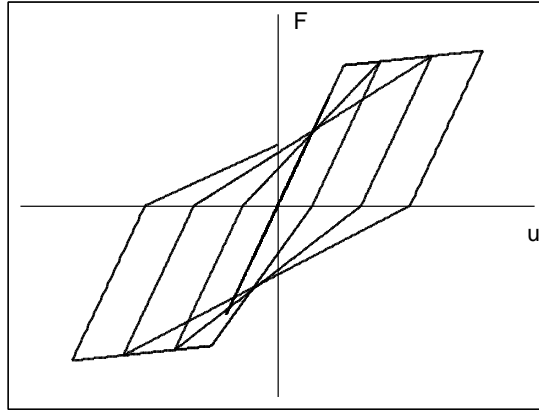


Figure 2.4 Degrading stiffness model by Clough and Johnston (1966)

There exist many other complex hysteresis models in the literature that take into account modeling features like reloading and unloading stiffness degrading, capping and cyclic strength degrading and pinching (Takeda et al. 1970, Roufaiel and Meyer 1987, Park et al. 1987, Otani 1993, Stojadinovic and Thewalt 1996, Sivaselvan and Reinhorn 1999, Sucuoglu and Erberik 2004). These models estimate the inelastic response in a more accurate way whereas they possess many model parameters to be determined by the user.

In this study, a modified version of the Clough and Johnston model, which also simulates stiffness and strength degrading, is employed to determine the seismic response of ESDOF models. The hysteresis model has been implemented into an academic purpose analysis platform called as USDP (Utility Software for Data Processing) that was developed in Middle East Technical University. The USDP program is able to conduct nonlinear dynamic analysis of SDOF systems by using a variety of hysteresis models, including the one used in this study.

The backbone curve of the considered model is shown in Figure 2.5. In the figure, parameters f_m , f_y and f_r are the maximum strength, yield strength and residual strength, respectively. Besides, u_y is the yield displacement, u_m is the maximum displacement and u_r is the residual displacement. These are the major model parameters from which the period, strength ratio and ductility of the SDOF system can be determined.

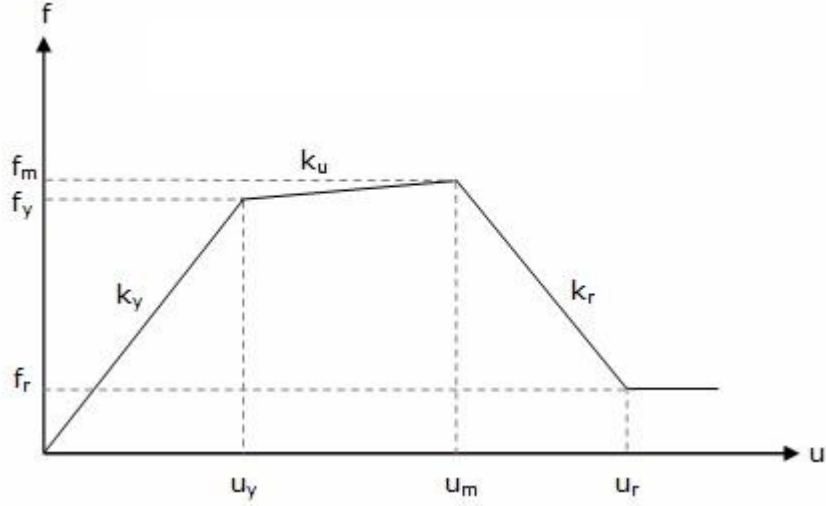


Figure 2.5. Backbone curve of the stiffness and strength degrading Clough model

As shown in Figure 2.5, the available stiffness definitions are k_y (initial elastic stiffness), k_u (post-yielding stiffness) and k_r (post-capping stiffness). In this study these parameters are considered in terms of stiffness ratios. Hence, two stiffness ratios, which are α_u (post-yielding stiffness ratio) and α_r (post-capping stiffness ratio), are employed as they are defined in Equations 2.15 and 2.16.

$$\alpha_u = \frac{k_u}{k_y} \quad (2.15)$$

$$\alpha_r = \frac{k_r}{k_y} \quad (2.16)$$

Another model parameter used in this study is the residual to yielding strength ratio (λ) which is given as;

$$\lambda = \frac{f_r}{f_y} \quad (2.17)$$

The cyclic response of the model is characterized by some degrading model parameters. The simple sketch that presents the cyclic response of the hysteretic model is given in Figure 2.6. In the model, the stiffness degradation factor is used as β_0 . The elastic stiffness of the structures degrades due to the yielding of the members. However, after yielding the unloading stiffness decreases as formulated in Equation 2.18. Stiffness degradation occurs both in unloading and reloading phases.

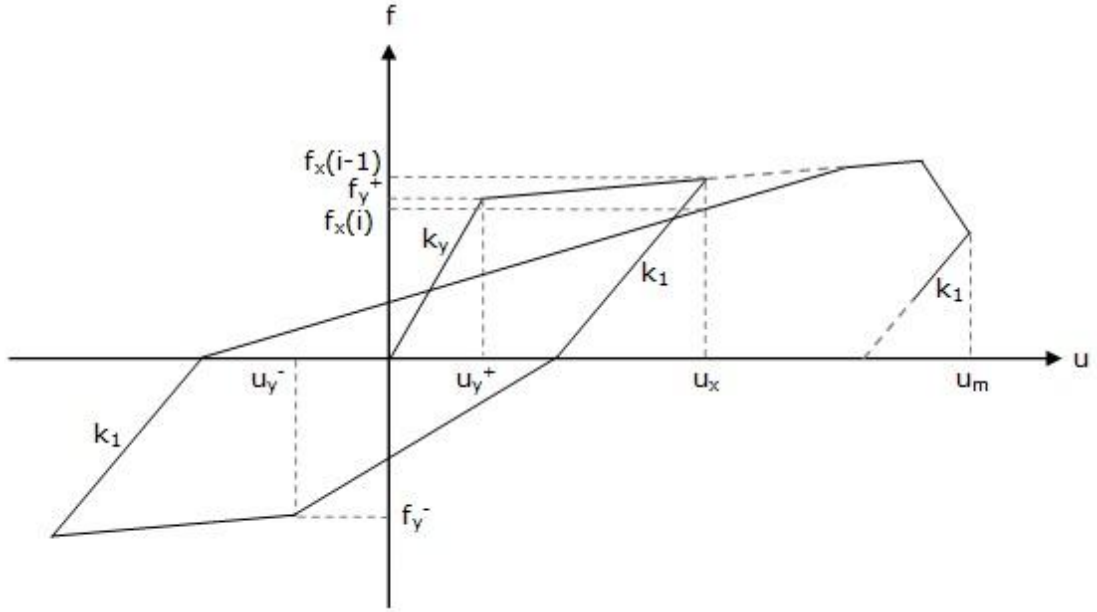


Figure 2.6. Stiffness and strength degrading Clough hysteretic model

$$k_1 = k_y \left(\frac{u_y}{u_x} \right)^{\beta_0} \quad (2.18)$$

The strength degradation parameters are β_a and β_b . Parameter β_a is used to calculate the strength capacity of the cycle by using the value of the previous cycle in the hysteretic model and parameter β_b is related to the rate of degradation within the cycles. The strength degradation is formulated as ;

$$f_x(i) = \beta_a f_x(i-1) \left(1 - e^{-\beta_b n \frac{u_x}{u_y}} \right) \quad (2.19)$$

According to the equation, if β_a is equal to 0.0, it means that there is no strength degradation. In the case of β_a being equal to 1.0, it shows that the strength capacity decreases depending on the rate parameter β_b . In Equation 2.19, $f_x(i-1)$ is the maximum strength before degradation and $f_x(i)$ is the maximum strength after degradation.

The values assigned to the hysteresis model parameters for different structural systems are discussed in Chapters 3 and 4.

CHAPTER 3

EQUIVALENT SDOF PARAMETERS FOR MASONRY BUILDINGS

3.1 General

Masonry buildings are one of the oldest construction types that have been widely used in Turkey, especially in rural areas due to their economical feasibility because these buildings are constructed by using local materials and in general, without engineering knowledge and expertise.

Masonry buildings have low ductility capacity since they are constructed with brittle materials, which in turn affects the seismic energy dissipation capacity, making it lower than that of reinforced concrete buildings. Since the probability of occurrence of destructive earthquakes in Turkey is so high, seismic damage assessment of Turkish masonry structures is crucial in order to prevent severe seismic damage and collapse. With the aim of determining the seismic performance of Turkish masonry buildings, in this study, the equivalent SDOF system approach is used by considering the major parameters as period, strength ratio and ductility. Since observational data to obtain these SDOF parameters is rather scarce or even unavailable, generic masonry buildings are generated to maintain the required statistical data to estimate structural parameters.

3.2 Generation of Structural Data for Masonry Buildings

Since there are few studies that have focused on the seismic performance of Turkish masonry buildings, the available data is not sufficient to determine equivalent SDOF parameters of this building type. Hence the required data is obtained by using generic masonry buildings with different structural characteristics. Generic buildings are classified according to the following parameters:

- Number of stories
- Material type and quality
- Plan geometry
- Amount and distribution of structural walls in plan

The same classification was used previously in order to develop seismic fragility curves of Turkish masonry buildings (Erberik 2008).

Number of stories is a simple but important structural parameter that plays an important role to estimate the seismic performance of masonry buildings. Since in Turkey, the number of storey of masonry buildings mostly vary from one to three, the story plans of generic buildings are reproduced up to three stories. These sub-classes can be denoted as N1, N2 and N3, respectively. There are also 4 and 5 story masonry buildings, especially in large cities of Turkey. However since these are few in number, they have not been considered as a separate sub-class.

The next classification is carried out for the combination of two parameters: material type and quality. In general, the materials used in Turkish masonry buildings are solid or hollow clay bricks, cellular concrete blocks, stone and adobe. The quality is an important parameter, which affects the capacity of masonry walls. Hence four different classes are generated by considering these two parameters: D1, D2, D3 and D4. Subclass D1 represents masonry buildings that have walls with good quality solid local brick. Subclass D2 represents masonry buildings that have walls with good quality hollow factory brick or moderate quality solid local brick whereas subclass D3 represents masonry buildings that have walls with good quality stone or adobe, moderate quality hollow factory brick or poor quality solid clay brick. Finally, subclass D4 represents masonry buildings that have walls with moderate and poor quality stone or adobe or poor quality hollow factory brick.

The buildings are also classified with respect to their plan geometries as regular (R1) and irregular (R2) buildings. Subclass R1 represents a regular masonry building with nearly or completely uniform distribution of structural walls. The rectangular buildings or buildings that do not have A3 type of plan irregularity defined in TEC (2007) are considered in this subclass. Masonry buildings that have irregularities in the plan and the ones with unsymmetrical, L or U shaped story plans are included in subclass R2.

The last classification is due to the amount and distribution of structural walls in plan. There exist three subclasses: W1, W2 and W3. The criteria used in the generation of the sub-classes are L_d / A ratio and the conformity of the walls to the rules given in the current version of the Turkish seismic code regarding the placement of structural walls in plan. By definition in L_d / A ratio, parameter L_d is the total length of masonry load-bearing walls in one of the orthogonal directions in plan whereas parameter A is the gross floor area. This parameter is quite simple, but field observations after earthquakes have indicated that it is correlated with seismic damage. Accordingly, subclass W1 represents masonry buildings which conform to the code requirements regarding the placement of structural walls and L_d / A ratio is 0.30. Subclass W2 contains buildings which violate some of the requirements in the code. For this sub-class, L_d / A ratio is taken as 0.25. Subclass W3 represents masonry buildings that do not conform to most of the code principles in the code with a L_d / A ratio of 0.2. Details of this classification can be found elsewhere (Erberik 2008).

In total, there are 72 sub-classes of masonry buildings that are generated with the aforementioned structural parameters. Six different generic story plans are developed (R1W1, R1W2, R1W3, R2W1, R2W2, R2W3) with the same floor area as seen in Appendix A. These plans are reproduced for different number of stories and for different material types to make up 72 different subclasses of masonry buildings, which are assumed to cover a significant portion of the Turkish masonry building stock with local characteristics. However it should be mentioned as a serious limitation of the study that the parametric variation of the generic models is not considered in this study. Hence the response obtained from the analyses of generic masonry buildings represents the average value and lacks some precision in this sense.

The abbreviation used in this study to define generated masonry building sub-classes is a five digit alphanumeric code, which starts with the letter “M”, denoting masonry buildings. The remaining digit is numbers, representing the sub-classes for number of stories, material type / quality, plan geometry and amount / distribution of structural walls, respectively. For instance, M3212 represents the class of 3-story and regular masonry buildings with good quality hollow factory brick or moderate quality solid

local brick walls that do not strictly follow the code requirements regarding the placement of structural walls.

The generated buildings are modelled by using the computer program MAS, that can be used for the three-dimensional, linear and nonlinear earthquake analyses of reinforced and unreinforced brick masonry buildings. There are two assumptions in MAS: the first one is to assume the floors of the masonry building as reinforced concrete and infinitely rigid in their own planes. Therefore, there is a rigid diaphragm modelling. As a second assumption, for unreinforced masonry buildings, the bending rigidities of the elements in their own planes are assumed to be large in comparison to their shear rigidities and therefore the rigidities in the out-of-plane direction of the wall elements are negligible. Furthermore, masses of the stories are assumed as lumped at floor levels. (Mengi et al, 1992).

In MAS program, as an input parameter, the story height, coordinates and properties of each wall assemblies and masses of each story are used. The story masses and mass moment of inertias of masonry models are shown in Table 3.1. In the buildings that are in subclass D1, the linear limit of secant shear modulus (G) is assumed as 640MPa. The value of G is assumed as 480 MPa, 320 MPa and 160 MPa for the buildings in sub-classes D2, D3 and D4.

Table 3.1 Story mass and mass moment of inertias of masonry building models

	Story mass (t)	Mass moment of inertia (tm^2)
R1W1	87	2630
R1W2	80	2260
R1W3	65	1240
R2W1	72	2710
R2W2	68	2500
R2W3	65	2420

3.3 Classification of Masonry Buildings

In the previous section, masonry buildings were classified according to some major parameters for generation and modelling. Now, a different classification will be carried out to represent the masonry building sub-classes to be used in regional

seismic damage assessment studies. This should be a broader classification when compared to the previous one in order to carry out seismic damage analysis in a practical manner. Therefore, number of stories and the level of compliance with the seismic design and construction principles are used as the major parameters for classification. Accordingly 9 groups of Turkish masonry buildings are defined by the following abbreviations: MU1A, MU2A, MU3A, MU1B, MU2B, MU3B, MU1C, MU2C and MU3C, where the first two letters indicate unreinforced masonry buildings, the number in the next digit stands for the number of stories (1, 2 or 3) and the letter in the last digit (A, B or C) denotes the level of compliance with seismic design and construction principles. The letters A, B and C represent high, moderate and low levels of compliance, respectively.

This sub-classification deserves some additional discussion. Obviously, it is not possible to determine the level of compliance of any building with seismic code by just examining the building through street survey in a few minutes. Such a determination is much more complex and requires some effort. Hence in order to classify the buildings accordingly, one should have this information before conducting the seismic damage estimation analysis. An alternative approach is to classify the buildings according to their apparent condition, which is an easily obtained structural information during field work. Then the buildings can be classified by considering their structural deficiencies (weak or soft story, excessive overhang, irregularities in plan and elevation), material quality, workmanship, etc.

The following sections are focused on the determination of equivalent SDOF parameters for these 9 groups of masonry buildings by making use of the information gathered from the analysis of 72 sub-classes of generated masonry buildings and some other information from the literature.

3.4 Major SDOF Parameters for Masonry Buildings

This section focuses on the attainment of major SDOF parameters for sub-classes of masonry buildings by using the generated masonry building database. This information is will be used to estimate the seismic performance of this structural type under varying levels of ground motion intensity.

3.4.1 Fundamental Period

In order to represent the structure as an equivalent SDOF model, fundamental period of the structure is one of the most important parameters. An accurate estimation of the period of the structure is important to determine the seismic forces accurately. This section first deals with the empirical formulations that predict the fundamental period of masonry buildings. Then the periods obtained from the eigenvalue analyses of generic masonry buildings are introduced. The period values obtained through analyses are accepted as the reference values since they reflect the local characteristics of Turkish masonry construction. New empirical formulations after regression analyses are proposed for masonry buildings. These new formulations are more enhanced with more parameters like plan geometry and material type in addition to the number of stories. Then the best formulation that fits to the analytical data is obtained by using root mean square error.

The empirical period formula that has been proposed for the fundamental vibration period in the United States codes (NEHRP (1994), SEAOC (1996) and UBC (1997) is;

$$T = 0.02 H^{0.75} \quad (3.1)$$

According to Eurocode 8 (1995), a similar period formulation is proposed;

$$T = 0.05 H^{0.75} \quad (3.2)$$

In the study of Bal et al (2008), 28 different existing structures with varying number of stories with timber and reinforced concrete slabs, were chosen and it was stated that the type of the slab has an influence on the period of vibration. As a result of the analysis on real structures of the existing building stock, the empirical formulas for masonry buildings with timber floors and reinforced concrete floors were defined as;

$$T = 0.039 H \quad (\text{with timber floors}) \quad (3.3)$$

$$T = 0.062 H^{0.87} \quad (\text{with reinforced concrete floors}) \quad (3.4)$$

In these equations, H represents the height of the building. The empirical formulation, which had been used in Erberik (2008) is;

$$T = 0.06 N \quad (3.5)$$

where N is the number of stories.

Although empirical formulations provide a simple period- height relationship and are easy to calculate, besides height of the structure, there are some important structural parameters that cannot be ignored such as the structural regularity in plan, structural geometry and material properties. By making use of more parameters, it is possible to make better estimations for the periods of masonry buildings.

In the next phase, the vibration periods of generic buildings are obtained by using the eigenvalue analysis option of the computer program MAS as listed in Table 3.2 for all 72 sub-classes. As mentioned before, these values are used as reference for the statistical study carried out in the next phase.

During the regression analyses, plan geometry and material type are also used as input variables for the proposed empirical formulations although building height or number of stories had been the only input parameter for the equations in the literature as discussed before.

The new empirical relationship to predict the fundamental period of masonry buildings are proposed by conducting linear, nonlinear and multivariable linear regression analyses. The regression equations are obtained by using SPSS (Statistical Package for the Social Sciences) program. In the analysis, the dependent variable is period (T). Number of stories (N), plan geometry (R), and material type (G) are considered as independent variables that are used to obtain period formulations. In SPSS, the variable N is named as 1 for 1 story, 2 for 2 story and 3 for 3 story buildings. Parameter R is defined as regular and irregular by the identifiers of 0 and 1, respectively. Besides, material type (G), which refers to previous definitions of sub-classes D1, D2, D3 and D4 are represented by the integers 1, 2, 3 and 4, respectively.

Table 3.2 Major SDOF parameters obtained from MAS program

Building No	Class	Period	η	μ
1	M1111	0.03	3.54	3.080
2	M1112	0.03	2.825	2.825
3	M1113	0.04	3.14	3.336
4	M1121	0.04	4.28	3.076
5	M1122	0.06	3.08	4.466
6	M1123	0.1	2.541	2.541
7	M1211	0.04	2.76	2.773
8	M1212	0.04	2.48	2.847
9	M1213	0.05	2.32	3.504
10	M1221	0.05	3.22	3.126
11	M1222	0.07	2.31	4.534
12	M1223	0.12	1.43	2.425
13	M1311	0.05	1.77	3.069
14	M1312	0.05	1.66	3.135
15	M1313	0.06	1.62	3.391
16	M1321	0.06	2.19	3.217
17	M1322	0.08	1.68	3.877
18	M1323	0.14	0.99	2.561
19	M1411	0.06	1.01	3.055
20	M1412	0.07	0.9	3.151
21	M1413	0.08	0.84	3.350
22	M1421	0.08	1.15	3.467
23	M1422	0.11	0.81	5.094
24	M1423	0.2	0.55	2.348
25	M2111	0.05	1.78	2.180
26	M2112	0.06	1.58	2.306
27	M2113	0.06	1.52	2.564
28	M2121	0.07	2.13	2.240
29	M2122	0.09	1.5	3.364
30	M2123	0.16	0.92	1.897
31	M2211	0.06	1.34	2.300
32	M2212	0.07	1.21	2.325
33	M2213	0.07	1.23	2.307
34	M2221	0.08	1.62	2.298
35	M2222	0.11	1.14	3.448
36	M2223	0.19	0.71	1.930

Table 3.2 Continued

Building No	Class	Period	η	μ
37	M2311	0.07	0.86	2.551
38	M2312	0.08	0.76	2.640
39	M2313	0.09	0.8	2.556
40	M2321	0.1	1.08	2.343
41	M2322	0.13	0.75	3.539
42	M2323	0.23	0.48	1.939
43	M2411	0.1	0.46	2.472
44	M2412	0.11	0.42	2.483
45	M2413	0.13	0.43	2.445
46	M2421	0.14	0.54	2.613
47	M2422	0.18	0.4	3.481
48	M2423	0.32	0.26	2.115
49	M3111	0.07	1.12	2.066
50	M3112	0.08	1.03	2.021
51	M3113	0.09	1.05	1.928
52	M3121	0.09	1.35	2.064
53	M3122	0.13	1	2.708
54	M3123	0.22	0.62	1.699
55	M3211	0.08	0.82	2.130
56	M3212	0.09	0.77	2.003
57	M3213	0.1	0.77	2.031
58	M3221	0.11	0.98	2.212
59	M3222	0.15	0.76	2.618
60	M3223	0.26	0.48	1.591
61	M3311	0.1	0.57	1.996
62	M3312	0.11	0.49	2.167
63	M3313	0.12	0.51	2.083
64	M3321	0.13	0.67	2.102
65	M3322	0.18	0.5	2.653
66	M3323	0.32	0.3	1.906
67	M3411	0.15	0.29	1.982
68	M3412	0.16	0.26	2.019
69	M3413	0.18	0.26	2.123
70	M3421	0.19	0.35	2.034
71	M3422	0.26	0.26	2.604
72	M3423	0.45	0.16	1.820

Table 3.3 presents the results of linear regression analyses that are carried out for different alternatives of empirical formulations, where a, b, c and d are the regression coefficients. In the calculation process, when the number of story, plan geometry and proposed material type are taken into consideration separately, it is obvious that the proposed empirical equations are unrealistic. However, in the linear empirical equation obtained by multivariable regression analysis, when three of the parameters are used as an input parameter, a better prediction is obtained as revealed by the R² statistics. The exact form of the multivariable linear equation to predict period of masonry buildings is given in Equation 3.6.

Table 3.3. Linear empirical equations for predicting fundamental periods of masonry buildings

T = aN + bR + cG + d					
The relationships between dependent (T) and independent variables	a	b	c	d	R ²
T and N	0.16	-	-	0.027	0.216
T and R	-	0.07	-	0.08	0.205
T and G	-		0.27	0.048	0.149
Multivariable	0.044	0.07	0.027	-0.075	0.586

$$T = 0.044N + 0.07R + 0.027G - 0.075 \tag{3.6}$$

Nonlinear regression is a technique that predicts the relationship between the dependent variable and several independent variables in the form of a nonlinear model. Multivariable linear regression, on the other hand assumes linear relationships between the dependent variable and independent variables. Before performing nonlinear regressions, conducting a multivariable linear regression can assist for the prediction of the model because the effects of the dependent variables on the independent variable can be recognised by linear regression. In this study, the proposed nonlinear formulation to predict the fundamental period of masonry buildings is given in Equation 3.7.

$$T = \frac{c_1 * N}{c_3 * R + e^{(G * c_2)}} \tag{3.7}$$

In this equation, T is period, N is the number of story, R is the plan geometry (0 for regular, 1 for irregular structure), and G is the material type (1 for subclass D1, 2 for subclass D2, 3 for subclass D3, 4 for subclass D4). Coefficients c_1 , c_2 and c_3 are determined as a result of nonlinear regression analysis and their values are obtained as 0.027, -0.152 and -0.284, respectively with a high R^2 value of 0.64. To sum up, the nonlinear empirical equation to predict the fundamental period of masonry building is;

$$T = \frac{0,027 * N}{-0,284 * R + e^{(-0,152G)}} \quad (3.8)$$

The empirical equations found in the literature (Equations 3.1-3.5) and the formulations obtained in multivariable and nonlinear regression analyses are compared with the reference period values from the eigenvalue analyses by the computer program MAS in Table 3.4 for all 72 subclasses of generic masonry buildings.

Root mean square error (RMSE) measures the difference between the reference data and estimated data in the model. Therefore, in order to determine the most appropriate equation that estimates the periods of a masonry buildings in a more accurate manner, root mean square error formulation is used.

$$RMSE = \sqrt{\frac{\sum_{i=1}^n (X_{obs}-X_{est})^2}{n}} \quad (3.9)$$

In Equation 3.9, X_{obs} is the reference period, X_{est} is the estimated period and n is the total number of periods. The results of the error analysis are presented in Table 3.5 for the empirical formulations proposed in this study and in the literature. According to the results, both the multivariable linear regression equation and nonlinear regression equation perform well but the smallest error is observed in the empirical period formulation obtained by the nonlinear regression. Therefore, in order to use in damage assessment of the masonry buildings, with the aim of predicting the period of an equivalent SDOF system, Equation 3.8 is selected to predict the fundamental periods of Turkish masonry buildings.

Table 3.4. Comparison of empirical period formulation with the reference values obtained through eigenvalue analyses

No	Class	Reference Periods	Empirical Periods					Multivariable Linear Regression	Nonlinear Regression
		Period (s)	Eq 3.1	Eq 3.2	Eq 3.3	Eq 3.4	Eq 3.5	Eq 3.6	Eq 3.8
1	M1111	0.03	0.042	0.105	0.105	0.147	0.06	-0.004	0.031
2	M1112	0.03	0.042	0.105	0.105	0.147	0.06	-0.004	0.031
3	M1113	0.04	0.042	0.105	0.105	0.147	0.06	-0.004	0.031
4	M1121	0.04	0.042	0.105	0.105	0.147	0.06	0.066	0.047
5	M1122	0.06	0.042	0.105	0.105	0.147	0.06	0.066	0.047
6	M1123	0.1	0.042	0.105	0.105	0.147	0.06	0.066	0.047
7	M1211	0.04	0.042	0.105	0.105	0.147	0.06	0.023	0.036
8	M1212	0.04	0.042	0.105	0.105	0.147	0.06	0.023	0.036
9	M1213	0.05	0.042	0.105	0.105	0.147	0.06	0.023	0.036
10	M1221	0.05	0.042	0.105	0.105	0.147	0.06	0.093	0.059
11	M1222	0.07	0.042	0.105	0.105	0.147	0.06	0.093	0.059
12	M1223	0.12	0.042	0.105	0.105	0.147	0.06	0.093	0.059
13	M1311	0.05	0.042	0.105	0.105	0.147	0.06	0.05	0.042
14	M1312	0.05	0.042	0.105	0.105	0.147	0.06	0.05	0.042
15	M1313	0.06	0.042	0.105	0.105	0.147	0.06	0.05	0.042
16	M1321	0.06	0.042	0.105	0.105	0.147	0.06	0.12	0.077
17	M1322	0.08	0.042	0.105	0.105	0.147	0.06	0.12	0.077
18	M1323	0.14	0.042	0.105	0.105	0.147	0.06	0.12	0.077
19	M1411	0.06	0.042	0.105	0.105	0.147	0.06	0.077	0.049
20	M1412	0.07	0.042	0.105	0.105	0.147	0.06	0.077	0.049
21	M1413	0.08	0.042	0.105	0.105	0.147	0.06	0.077	0.049
22	M1421	0.08	0.042	0.105	0.105	0.147	0.06	0.147	0.104
23	M1422	0.11	0.042	0.105	0.105	0.147	0.06	0.147	0.104
24	M1423	0.2	0.042	0.105	0.105	0.147	0.06	0.147	0.104
25	M2111	0.05	0.071	0.211	0.177	0.269	0.12	0.04	0.063
26	M2112	0.06	0.071	0.211	0.177	0.269	0.12	0.04	0.063
27	M2113	0.06	0.071	0.211	0.177	0.269	0.12	0.04	0.063
28	M2121	0.07	0.071	0.211	0.177	0.269	0.12	0.11	0.093
29	M2122	0.09	0.071	0.211	0.177	0.269	0.12	0.11	0.093
30	M2123	0.16	0.071	0.211	0.177	0.269	0.12	0.11	0.093
31	M2211	0.06	0.071	0.211	0.177	0.269	0.12	0.067	0.073
32	M2212	0.07	0.071	0.211	0.177	0.269	0.12	0.067	0.073
33	M2213	0.07	0.071	0.211	0.177	0.269	0.12	0.067	0.073
34	M2221	0.08	0.071	0.211	0.177	0.269	0.12	0.137	0.119
35	M2222	0.11	0.071	0.211	0.177	0.269	0.12	0.137	0.119
36	M2223	0.19	0.071	0.211	0.177	0.269	0.12	0.137	0.119

Table 3.4. Continued

No	Class	Reference Periods	Empirical Periods					Multivariable Linear Regression	Nonlinear Regression
		Period (s)	Eq 3.1	Eq 3.2	Eq 3.3	Eq 3.4	Eq 3.5	Eq 3.6	Eq 3.8
37	M2311	0.07	0.071	0.211	0.177	0.269	0.12	0.094	0.085
38	M2312	0.08	0.071	0.211	0.177	0.269	0.12	0.094	0.085
39	M2313	0.09	0.071	0.211	0.177	0.269	0.12	0.094	0.085
40	M2321	0.1	0.071	0.211	0.177	0.269	0.12	0.164	0.154
41	M2322	0.13	0.071	0.211	0.177	0.269	0.12	0.164	0.154
42	M2323	0.23	0.071	0.211	0.177	0.269	0.12	0.164	0.154
43	M2411	0.1	0.071	0.211	0.177	0.269	0.12	0.121	0.099
44	M2412	0.11	0.071	0.211	0.177	0.269	0.12	0.121	0.099
45	M2413	0.13	0.071	0.211	0.177	0.269	0.12	0.121	0.099
46	M2421	0.14	0.071	0.211	0.177	0.269	0.12	0.191	0.207
47	M2422	0.18	0.071	0.211	0.177	0.269	0.12	0.191	0.207
48	M2423	0.32	0.071	0.211	0.177	0.269	0.12	0.191	0.207
49	M3111	0.07	0.096	0.316	0.240	0.383	0.18	0.084	0.094
50	M3112	0.08	0.096	0.316	0.240	0.383	0.18	0.084	0.094
51	M3113	0.09	0.096	0.316	0.240	0.383	0.18	0.084	0.094
52	M3121	0.09	0.096	0.316	0.240	0.383	0.18	0.154	0.140
53	M3122	0.13	0.096	0.316	0.240	0.383	0.18	0.154	0.140
54	M3123	0.22	0.096	0.316	0.240	0.383	0.18	0.154	0.140
55	M3211	0.08	0.096	0.316	0.240	0.383	0.18	0.111	0.109
56	M3212	0.09	0.096	0.316	0.240	0.383	0.18	0.111	0.109
57	M3213	0.1	0.096	0.316	0.240	0.383	0.18	0.111	0.109
58	M3221	0.11	0.096	0.316	0.240	0.383	0.18	0.181	0.178
59	M3222	0.15	0.096	0.316	0.240	0.383	0.18	0.181	0.178
60	M3223	0.26	0.096	0.316	0.240	0.383	0.18	0.181	0.178
61	M3311	0.10	0.096	0.316	0.240	0.383	0.18	0.138	0.127
62	M3312	0.11	0.096	0.316	0.240	0.383	0.18	0.138	0.127
63	M3313	0.12	0.096	0.316	0.240	0.383	0.18	0.138	0.127
64	M3321	0.13	0.096	0.316	0.240	0.383	0.18	0.208	0.231
65	M3322	0.18	0.096	0.316	0.240	0.383	0.18	0.208	0.231
66	M3323	0.32	0.096	0.316	0.240	0.383	0.18	0.208	0.231
67	M3411	0.15	0.096	0.316	0.240	0.383	0.18	0.165	0.148
68	M3412	0.16	0.096	0.316	0.240	0.383	0.18	0.165	0.148
69	M3413	0.18	0.096	0.316	0.240	0.383	0.18	0.165	0.148
70	M3421	0.19	0.096	0.316	0.240	0.383	0.18	0.235	0.311
71	M3422	0.26	0.096	0.316	0.240	0.383	0.18	0.235	0.311
72	M3423	0.45	0.096	0.316	0.240	0.383	0.18	0.235	0.311

Table 3.5. Error estimations in the empirical formulations

	Standard error (RMSE)
Equation 3.1	0.081
Equation 3.2	0.091
Equation 3.3	0.127
Equation 3.4	0.176
Equation 3.5	0.07
Equation 3.6	0.047
Equation 3.8	0.045

3.4.2 Strength Ratio and Ductility

In the literature, there are few experimental studies, in which the base shear ratio and ductility are determined for masonry buildings. Costley and Abrams (1996) tested two reduced scale URM buildings on a shaking table. These were two story buildings made of clay brick units. The difference between the test buildings was the arrangement of walls and openings. The envelope capacity curves of the tested buildings are shown in Figure 3.1. Accordingly, the building with less amount of openings have strength ratio of 1.2 whereas the other test building has a ratio of 0.7. Since the governing damage mode is pier rocking, which is a ductile type of response, the ductility capacities of the tested buildings are observed to be high ($\mu \approx 7-8$).

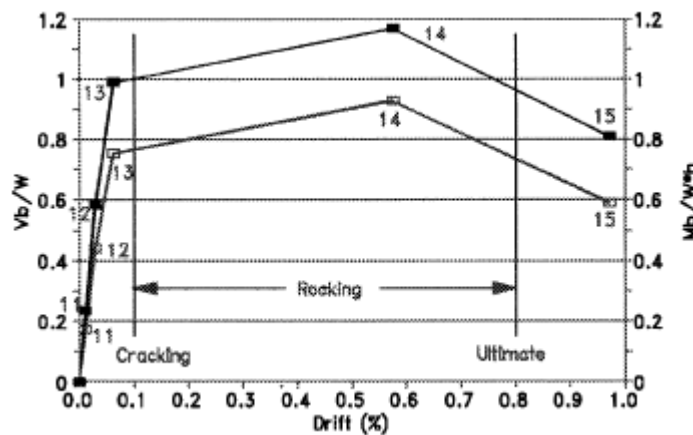


Figure 3.1. Experimental capacity curves of tested buildings (Costley and Abram, 1996)

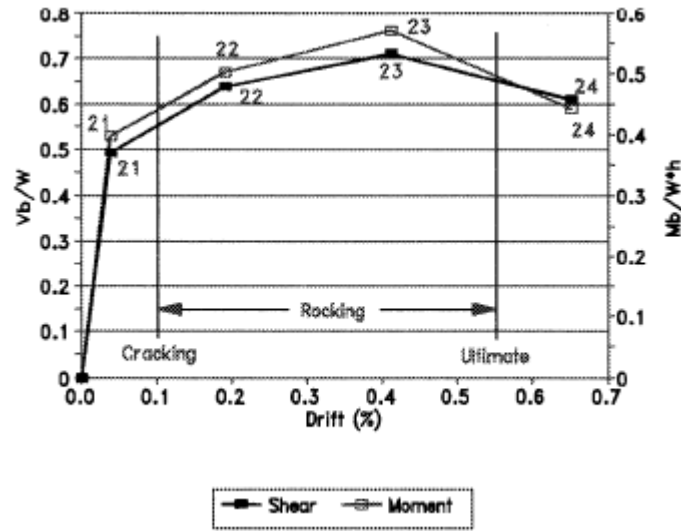


Figure 3.1. Continued

Benedetti et al (1998) conducted shaking table tests on 24 simple masonry buildings. The tested buildings were half-scaled two story structures that were constructed by using stone and brick units. The authors stated that the buildings were representing non-engineered masonry buildings with low seismic capacity. The strength ratios obtained for these buildings after the test were in the range 0.12 – 0.30, conforming that these were deficient structures. The corresponding ductility ratios were in the range 1.5 – 3.0.

Tomazevic et al (2004) tested 1 / 5 – scale multi-story masonry buildings with different types of materials on a simple uni-directional seismic simulator. At the end of the tests, the authors obtained strength ratios in a wide range from 0.4 to 1.8. Ductility ratios were obtained varying between 3 – 5.

Zavala et al. (2004) conducted on experimental study a full scale two story masonry building made of local clay bricks. The results of the cyclic test indicated that the strength ratio and the ductility capacity were approximately 1.5 and 3, respectively.

Design base shear force (V_b) proposed by the current version of Turkish seismic code can also assist for the determination of strength ratio to be assigned to the SDOF structural systems. In the code, V_b can be calculated by the following formulation

$$V_b = \frac{W A_0 I S(T)}{R_a(T)} \quad (3.10)$$

In this formulation, W is the weight, A_0 is the seismic zone coefficient, I is the building importance factor, $S(T)$ is the spectrum coefficient and $R_a(T)$ is the seismic load reduction factor. Dividing both sides of Equation 3.10 by W yields base shear coefficient.

$$\frac{V_b}{W} = \frac{A_0 I S(T)}{R_a(T)} \quad (3.11)$$

For masonry buildings, the code enforces $S(T) = 2.5$ and $R_a(T) = 2$. Hence for residential masonry buildings ($I = 1$), the enforced base shear coefficient in terms of seismic zone is presented in Table 3.6.

Table 3.6 Base shear coefficient (V_b/W) as a function of seismic zone (A_0)

A_0	0.1	0.2	0.3	0.4
V_b/W	0.125	0.25	0.375	0.5

This means that in the most severe seismic zone, one should ensure a minimum lateral capacity that is half of the weight for an earthquake resistant masonry building. However, it should not be forgotten that these legislations are rarely conformed in practice for Turkish masonry buildings.

Aforementioned studies give a physical sense concerning the two SDOF parameters; strength ratio and ductility. However there are two important issues. First, these studies do not reflect the local characteristics of Turkish masonry buildings. Second, this available data is not sufficient to determine the values of parameters that are going to be used in seismic damage estimation of masonry buildings. Hence additional data is required to achieve this task. In this study, the required data is obtained by carrying out pushover analyses on the generic masonry building models.

In pushover analysis, the structure is subjected to a predefined distributed load (or displacement) along the height of the building with the aim of evaluating the inelastic ultimate capacity of the structure. As a result of pushover analyses, the capacity curves of the 72 generic masonry building models are obtained by using the computer program MAS.

In this study, in order to obtain the strength ratio and ductility, the capacity curves are idealized by using the concepts in Tomazevic (1999) and ATC 40 (1996). According to ATC-40 (1996) method, idealization of capacity curve is obtained by the same initial slope and satisfying the equal energy rule. Bilinear idealization is performed by taking into consideration the energy conservation. In order to conserve the energy consumption, the area between the capacity curve and bilinear idealization line must be equal as in Figure 3.2. Also, the slope of the elastic portion of the idealization is the same with the initial slope of the curve.

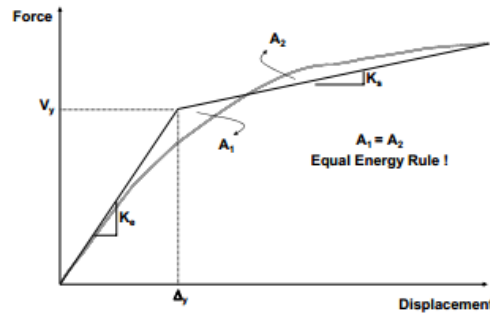


Figure 3.2 Bilinear idealization of capacity curve (ATC-40, 1996)

According to Tomazevic (1999), initial elastic stiffness (k_y) portion ends at ultimate shear strength (F_u) and post yielding stiffness (k_u) continues as straight line till the ultimate displacement (d_u). The initial slope is the ratio between the strength and displacement at crack limit. The ultimate shear strength is calculated by taking into account the conservation of energy consumption. When the area equalization between the capacity and idealization curves is achieved, the ultimate shear strength is calculated from Equations 3.12 and Equations 3.13.

$$k_y = \frac{F_{cr}}{d_{cr}} \quad (3.12)$$

$$F_u = k_y \left(d_{max} - \sqrt{d_{max}^2 - \frac{2 A_{env}}{k_y}} \right) \quad (3.13)$$

where F_{cr} and d_{cr} are the strength and displacement at the formation of the first crack, respectively. A_{env} is the area below the capacity curve and d_{max} is the maximum displacement. As it is shown in Figure 3.3, displacement at the elastic limit (d_e) is calculated by the Equation 3.14 and ductility is defined as the Equation 3.15.

$$d_e = \frac{F_u}{k_y} \quad (3.14)$$

$$\mu = \frac{d_u}{d_e} \quad (3.15)$$

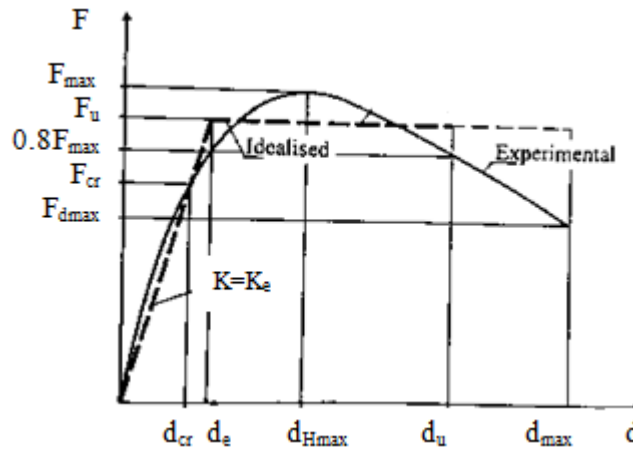


Figure 3.3 Bilinear idealization of capacity curve. (Tomatević, 1999)

Using the above procedures, the capacity curves of all 72 generic building models obtained by pushover analyses are idealized as presented in Appendix B. Then the SDOF parameters, namely strength ratio and ductility are obtained from the following equation;

$$\mu = \delta_u / \delta_y \quad (3.16)$$

$$\eta = f_y / W \quad (3.17)$$

where f_y is the idealized capacity (yield strength), W is the weight of the building, δ_u is the ultimate displacement and δ_y is the yielding displacement. The strength ratio and ductility values for building models are presented in Table 3.2.

The parameter values in Table 3.2 reveal that strength ratios are unreasonably high for all generic models in subclass D1. This subclass stands for good quality masonry material with high compressive stress and shear modulus, which is not actually representative of the non-engineered masonry buildings in Turkey. Therefore, the results obtained from the models in this subclass are disregarded. Different levels of code compliance (i.e. A, B and C as discussed before during the classification of masonry buildings) are linked with the subclasses D2, D3 and D4, respectively. Another important point is that the sub-class combination R2W3, which stands for very irregular buildings with soft or weak story yields lower capacity values than expected. This may be due to the modelling problems of such irregular structures with a computer program that has some limitations. Therefore the results obtained from buildings in this sub-class combination are considered with some caution.

In accordance with the above discussions, the values of η and μ assigned to masonry building sub-classes are presented in Table 3.7. It is observed that as the number of stories increase or as the level of code conformity is lowered, the strength ratio gets lower values as expected. The ductility capacity seems to vary between 2 – 4, which is representative for unreinforced masonry buildings.

3.4.3 Other SDOF Model Parameters

Among the other SDOF parameters, the stiffness degradation factor (β_0) is assumed as 0.0, 0.4 and 0.8 for high, moderate and low levels of code compliance with seismic design and construction principles (i.e. A, B and C). Parameters β_a is assumed as 1.0 for all sub-classes whereas parameter β_b is taken as 1.0, 0.75 and 0.6 for classes A, B and C. In addition to the degradation factors, post-yielding stiffness ratio (α_r) is taken as -0.2, -0.25 and -0.3 for all cases by considering the idealized capacity curves. Post-capping stiffness ratio (α_u) is assumed as 0.0 for sub-classes A, B and C. The parameter λ is assumed as 0.2 for all masonry building sub-classes. All the parameters for masonry building subclasses are listed in Table 3.7.

Table 3.7 Proposed SDOF parameters of masonry building subclasses

Code	T	η	μ	α_r	α_u	λ	β_o	β_a	β_b
MU1A	Eq 3.8	1.25	3.4	-0.2	0.0	0.2	0.0	1.0	1.0
MU2A		0.75	2.5	-0.2	0.0	0.2	0.0	1.0	1.0
MU3A		0.5	2.2	-0.2	0.0	0.2	0.0	1.0	1.0
MU1B		0.6	3.3	-0.25	0.0	0.2	0.4	1.0	0.75
MU2B		0.45	2.7	-0.25	0.0	0.2	0.4	1.0	0.75
MU3B		0.3	2.2	-0.25	0.0	0.2	0.4	1.0	0.75
MU1C		0.45	3.6	-0.3	0.0	0.2	0.8	1.0	0.60
MU2C		0.3	2.7	-0.3	0.0	0.2	0.8	1.0	0.60
MU3C		0.15	2.2	-0.3	0.0	0.2	0.8	1.0	0.60

CHAPTER 4

EQUIVALENT SDOF PARAMETERS FOR REINFORCED CONCRETE BUILDINGS

4.1 General

Reinforced concrete buildings are the most popular type of structures, not only in Turkey, but all over the world. Such a common use of this construction type is mostly due to the ease of supplying formworks in different geometric shapes and types and material abundance.

Because of the fast growing population and uncontrolled construction in urban regions after 1980's, there exist many reinforced concrete buildings constructed without complying with earthquake resistant design principles. In other words, people who immigrated to urban areas, have selected reinforced concrete as an economical construction material to build houses without taking into account the actual resistance of the structure. Hence, such deficient structures have been severely damaged or collapsed during major earthquakes in the last four decades.

In Turkey, most of the building stock resides close to the active faults and reinforced concrete buildings constitute approximately % 60-70 of this total building stock. Reinforced concrete buildings in the building stock are classified as moment resisting frame buildings, shear wall buildings and dual (frame + shear wall) buildings. In this study, a specific type of shear wall building, named as "tunnel form building" is considered since this specific type of construction is commonly used in Turkey, especially as shelter houses after earthquakes in earth prone regions. Owing to the fact that the behaviour of each class of reinforced concrete buildings is different under seismic loads, these building classes are considered separately in different sections. In the literature, there are many studies related to the modelling and analysis of reinforced concrete buildings in Turkey. These studies and analyses are

used in order to obtain the major equivalent SDOF parameters (period, strength ratio, ductility, etc.) as in the case of masonry buildings.

4.2 Reinforced Concrete Frame Buildings

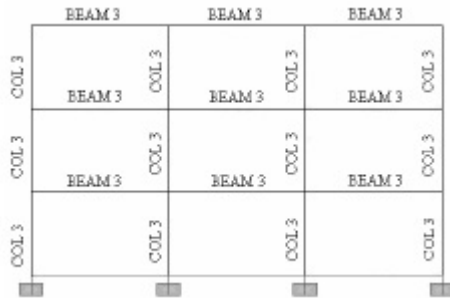
In Turkish reinforced concrete frame structures, moment resisting frames are used as structural systems which consist of columns and beams. The lateral loads and gravity loads are resisted by columns and beams. There are also infill walls that are used in the peripheral or inner frames of the building but these elements are not used as load carrying structural members. Within this scope, there exists sufficient data to construct a building database and obtain the equivalent SDOF parameters by using this database. The following section explains the details of the gathered building database for RC frame buildings.

4.2.1 Available Studies Regarding Turkish RC Frame Buildings

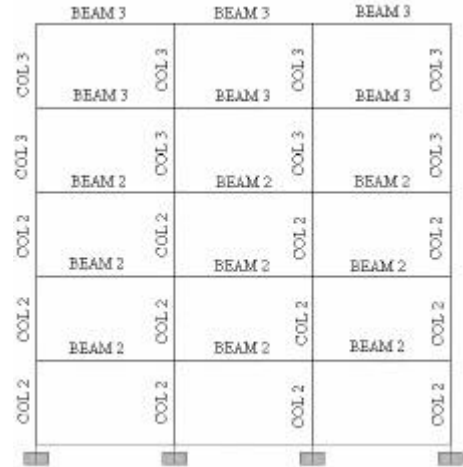
Since there are adequate numbers of studies in the literature concerning Turkish RC frame buildings, no further analyses are required. The available data is gathered in a building database and the statistical descriptors of the database are obtained in order to derive the equivalent SDOF parameters.

The studies considered for RC frame buildings belong to Ay (2006). In Ay (2006), RC frame buildings without infill walls were analyzed by taking into consideration the requirements for design and construction of RC structures (TS 500, 2000), Turkish standard regarding the previous Turkish earthquake code (TEC, 1998) and ACI Building Code (2002). The models were designed according to three different design spectra D1, D2 and D3 which are the spectra with maximum acceleration value of 0.36, 0.81 and 0.98 respectively. The structures were modelled as planar 3, 5 and 7 number of storey buildings as seen in Figure 4.1. The models were classified according to the number of stories (3S, 5S and 7S) and design spectra (D1, D2 and D3) and accordingly, 9 different structural classes were defined.

a)



b)



c)

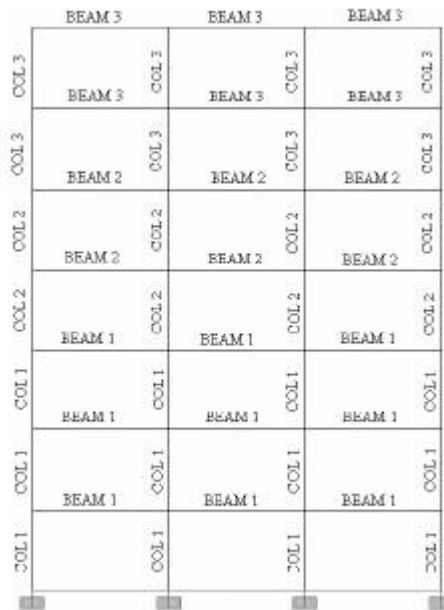


Figure 4.1a) 3 story model, b) 5 story model, c) 7 story model (Ay, 2006)

In order to reflect the local structural characteristics of RC frame buildings in Turkey, the generic structural models were further classified as superior, typical and poor building subclasses. In superior subclass, the buildings are designed according to the code regulations and adequate structural capacity with good material quality. The structures in typical subclass constitute the majority of the building stock and

violate some fundamental requirements. The poor building subclass represents the structures that do not comply with earthquake resistant design and construction principles. Hence, 9 different combinations of RC frame structures are further grouped by using the superior, typical and poor subclasses. Therefore, there are 27 number of RC frame subclasses studied by Ay (2006) and also suitable for this study to obtain equivalent SDOF parameters.

In the study, the pushover curves were obtained with the structural analysis software IDARC-2D and the idealization of the curves were obtained according to FEMA 356 (ASCE, 2000). The major SDOF parameters, base shear coefficient and ductility, are estimated by using the results of pushover analyses. Another parameter, period, was obtained from the results of eigenvalue analyses.

Ozun (2007) used the blue prints of 28 actual RC frame buildings, which were extracted from Düzce building database. This database was constructed by the field survey of METU teams after the 1999 earthquakes in Kocaeli and Düzce. The properties of these buildings and the observed damage after the earthquake are listed in Table 4.1. The buildings with 2-3 stories were categorized as low-rise buildings and the ones with 4-6 stories were considered as high-rise buildings. In order to compare the behaviours of bare and infilled frames, each building was modelled as bare frame and infilled frame separately. Therefore, the buildings were divided into four subclasses which are low-rise bare frame, mid-rise bare frame, low-rise infilled frame and mid-rise infilled frame. Accordingly, 56 RC frame buildings were analyzed by Ozun (2007) and the results of these analyses were used in this study.

In order to obtain SDOF parameters, pushover curves were obtained by nonlinear static analysis by using SAP 2000 software. The idealization of the pushover curves was carried out according to the procedure in ATC 40 (1996), which has been presented in Chapter 2.

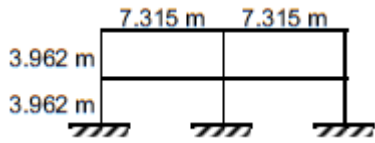
Table 4.1. General properties of the selected buildings in Düzce. (Ozun, 2007)

Building ID	Construction Year	No of stories	Building class	Building height (m)	fc (MPa)	Observed Damage
1	1985	6	MR	16.3	15	Moderate
2	1985	6	MR	16.1	14	Moderate
3	1978	5	MR	14.4	17	Moderate
4	1985	5	MR	13.8	20	Light
5	1985	3	LR	8.3	20	Moderate
6	1989	4	MR	13.5	20	Moderate
7	1977	4	MR	11.4	17	Moderate
8	1975	5	MR	14.6	22	None/Light
9	1962	2	LR	6.3	14	None
10	1975	3	LR	8.9	14	Moderate
11	1993	4	MR	11.6	17	Light
12	1999	3	LR	8.9	13	Light
13	1982	4	MR	11.6	22	Moderate
14	1980	3	LR	8.4	9	Light
15	1970	2	LR	6.3	17	Light
16	1972	2	LR	5.6	9	Light
17	1995	3	LR	8.3	14	Light
18	1990	2	LR	6.1	17	Light
19	1985	2	LR	5.8	14	None
20	1973	3	LR	9.7	17	None
21	1994	4	MR	12.3	14	Light
22	1992	5	MR	14.7	13	Moderate
23	1984	4	MR	12.5	10	Moderate
24	1981	3	LR	9.6	10	Moderate

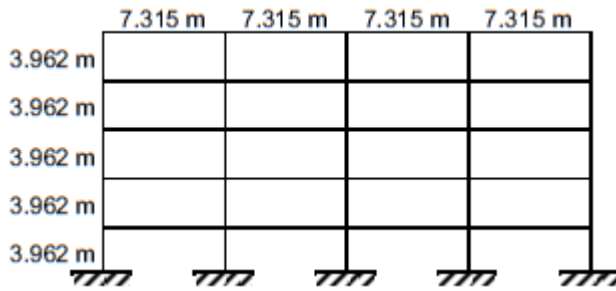
In Kadas (2006), three generic buildings, namely F2S2B, F5S4B and F8S3B, and three existing buildings in Bursa, namely F3S2B, F5S2B and F5S7B which are also shown in Figure 4.2, were used. The generic buildings were designed according to UBC (1997).

For analyses Opensees, which is an open source software framework, was used. During the generation of an equivalent SDOF system from a MDOF system, multi-idealization method was used to idealize the capacity curves. Further details can be found in Kadas (2006).

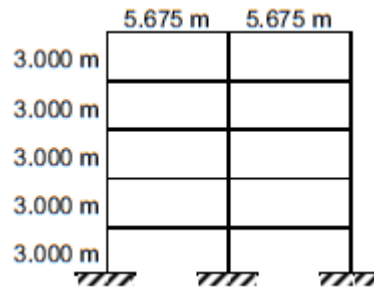
a)



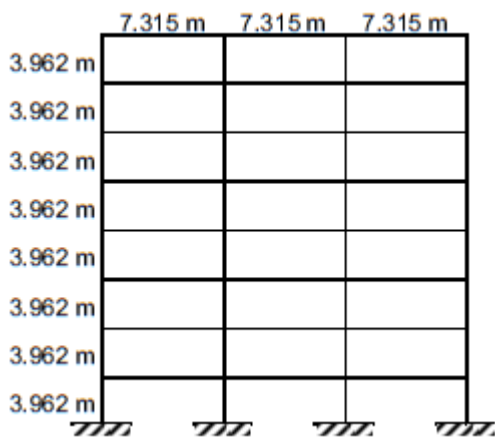
b)



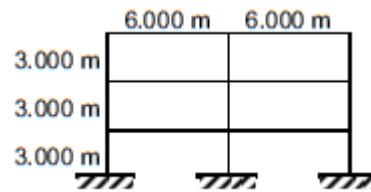
c)



d)



e)



f)

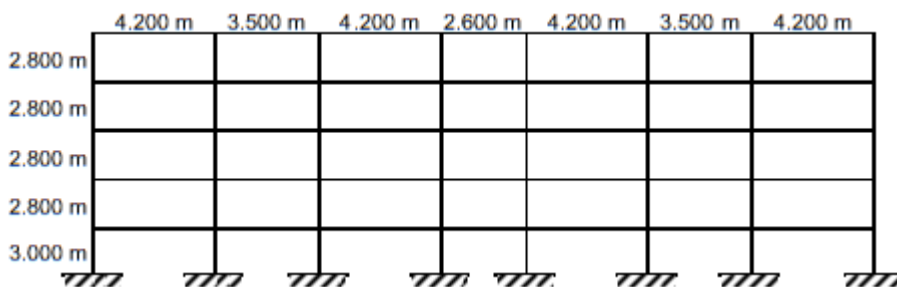


Figure 4.2a) F2S2B, b)F5S4B, c)F5S2B, d)F8S3B, e)F3S2B, f)F5S7B (Kadas, 2006)

Metin (2006) developed code-conforming generic RC frames by grouping them as standard beam-column frame and more flexible frame. The number of stories of structures were 3, 5 and 7 and in total, 12 number of RC frame structures were analyzed. The structures were designed according to ACI Building Code (2002).

In the nonlinear static analysis, the structural analysis program IDARC-2D was used and the bilinear idealization of the curves were carried out according to ATC 40 (1996) procedure which was mentioned in Chapter 2.

Yakut (2008) performed an extensive study to determine the capacity related properties of RC frame buildings in Turkey. He selected 33 sample buildings from a larger building database, which are located in the cities with the highest level of seismic risk. All buildings have number of stories between 2 and 5. After analyses, he obtained capacity curve parameters of the considered buildings and provided statistical information (mean and standard deviation) about these parameters for 2, 3, 4 and 5 story buildings, separately.

Karaca (2013) studied on the existing reinforced concrete structures in Eskişehir that vary from 4 to 7 numbers of stories. General properties of the RC frame buildings that are selected for this study are given in Table 4.2.

Table 4.2. General properties of the existing structures in Eskişehir (Karaca, 2013)

Building No	No of Stories	Height (m)	Weight (t)	Material Strength (MPa)	Design Year
1	4	11.4	253.2	C25/S420	2010
2	6	17.52	917.2	C25/S420	2005
3	6	18	725.9	C25/S420	2008
4	6	17.1	1391.4	C14/S220	1995
5	5	14	320.2	C25/S420	1993
6	7	19.6	1890.5	C25/S420	-
7	5	14	246.9	C25/S420/	1996
8	4	12.36	402.5	C20/S420	2000
9	5	14.9	609.8	C16/S420	1996
10	5	14	248.8	C25/S420	1975
11	5	13.88	322.7	C20/S420	1994
12	5	15.93	293.3	C20/S420	1980
13	4	11.8	341.6	C25/S420	2006

4.2.2 Classification of RC Frame Buildings

From the previous studies, in total, 104 RC frame buildings were selected to be used in this study. Since the database contains existing buildings from different parts in Turkey, the selected buildings seem to represent the local characteristics of Turkish RC frame buildings.

The structures are classified according to their compliance with the seismic design code and the related principles as low, moderate and high. For each study, the classification is carried out by considering the actual structural properties of the buildings in particular.

For RC frame buildings in Ay (2006), the generic structures that had been designed according to different codes were used and they were already classified as superior, typical and poor subclasses. Therefore, the same classification is also used for this study.

For buildings in Ozun (2006), the capacity curves are used to classify RC frame buildings. The ones with low force and displacement capacity are classified as ‘low’ whereas the ones with high force and displacement capacity are classified as high. When classifications are compared with the observed damage, there seems to be a reasonable match in between.

Kadas (2006) analyzed the generic buildings designed according to the earthquake codes. Therefore, in this study, since the structures obey the code regulations, they are classified as ‘high’. The existing buildings are classified according to their capacity curves.

Metin (2006) developed the analytical models of generic structures based on the design level of seismic forces. Accordingly the buildings that were designed for high level of seismicity are classified as ‘high’ and the ones designed for moderate level of seismicity are classified as ‘moderate’.

Just like in the case of Ozun (2006), the buildings studied by Karaca (2013) are also classified according to their capacity curves. The results show that the material properties (compressive strength of concrete and yield strength of steel reinforcement) have a significant effect on the capacity curves and therefore on the building classifications.

As a summary, the classification of RC frame buildings in this study is carried out by the following denotation: 'RF' represents RF frame buildings, '1' and '2' shows whether the building is low-rise (number of the storey is between 1 and 3) or mid-rise (number of stories is between 4 and 8), respectively. Finally, 'A', 'B' or 'C' represents high, moderate and low level of compliance with the seismic design and construction principles, respectively. For example, RF1A represents earthquake-resistant low-rise RC frame buildings whereas RF2C represents deficient (with many violations regarding earthquake resistant design and construction principles) mid-rise RC frame buildings. The classification of all RC frame buildings used in this study is given in Table 4.3. In Table 4.3 N , T , η , α_u and μ represents number of storey, period, strength ratio, post-yielding stiffness ratio and ductility, respectively.

Table 4.3 The classification of all RC frame buildings used in this study

Building No	Reference	N	T	η	α_u (%)	μ	Class	Note
1	Kadas (2006)	3	0.45	0.463	14.7	3.8	RF1B	Existing buildings in Bursa
2	Kadas (2006)	5	0.75	0.282	1.8	5.34	RF2C	Existing buildings in Bursa
3	Kadas (2006)	5	0.66	0.364	3.4	5.11	RF2B	Existing buildings in Bursa
4	Kadas (2006)	2	0.59	0.327	14.2	3.6	RF1A	Code-compliant buildings according to UBC
5	Kadas (2006)	5	0.95	0.304	6.8	3.98	RF2A	Code-compliant buildings according to UBC
6	Kadas (2006)	8	1.2	0.191	4.7	5.26	RF2A	Code-compliant buildings according to UBC
7	Metin (2006)	3	0.27	0.48	2.3	12.1	RF1A	Designed according to high level of seismicity
8	Metin (2006)	5	0.44	0.34	3.1	11.5	RF2A	Designed according to high level of seismicity
9	Metin (2006)	7	0.64	0.256	4.3	8.14	RF2A	Designed according to high level of seismicity
10	Metin (2006)	5	0.55	0.293	4.1	5.78	RF2B	Designed according to moderate level of seismicity
11	Metin (2006)	7	0.67	0.2	3.5	9.3	RF2B	Designed according to moderate level of seismicity
12	Metin (2006)	3	0.37	0.384	3.9	7.3	RF1A	Designed according to high level of seismicity
13	Metin (2006)	5	0.65	0.26	6.3	4.45	RF2A	Designed according to high level of seismicity
14	Metin (2006)	7	0.9	0.184	7.1	4.5	RF2A	Designed according to high level of seismicity
15	Metin (2006)	3	0.47	0.32	4.4	5.86	RF1B	Designed according to moderate level of seismicity
16	Metin (2006)	5	0.69	0.256	4.4	5.5	RF2B	Designed according to moderate level of seismicity
17	Metin (2006)	7	0.93	0.142	8.2	4.17	RF2B	Designed according to moderate level of seismicity
18	Ozun (2007)	6	0.64	0.154	2.4	5.28	RF2C	Existing buildings in Duzce city center
19	Ozun (2007)	6	0.59	0.095	1.7	7.25	RF2C	Existing buildings in Duzce city center
20	Ozun (2007)	6	0.61	0.105	1.5	5.88	RF2C	Existing buildings in Duzce city center
21	Ozun (2007)	5	0.36	0.141	5.4	4.80	RF2C	Existing buildings in Duzce city center
22	Ozun (2007)	5	0.34	0.180	0.9	4.03	RF2C	Existing buildings in Duzce city center
23	Ozun (2007)	3	0.17	0.435	0.4	13.47	RF1A	Existing buildings in Duzce city center

Table 4.3 Continued

Building No	Reference	N	T	η	α_u (%)	μ	Class	Note
24	Ozun (2007)	3	0.18	0.350	0.5	11.73	RF1A	Existing buildings in Duzce city center
25	Ozun (2007)	4	0.35	0.184	1.1	8.72	RF2B	Existing buildings in Duzce city center
26	Ozun (2007)	5	0.64	0.098	2.7	6.92	RF2C	Existing buildings in Duzce city center
27	Ozun (2007)	5	0.43	0.191	0.9	9.98	RF2B	Existing buildings in Duzce city center
28	Ozun (2007)	2	0.24	0.329	1.7	6.09	RF1B	Existing buildings in Duzce city center
29	Ozun (2007)	2	0.21	0.283	1.5	5.96	RF1B	Existing buildings in Duzce city center
30	Ozun (2007)	3	0.33	0.227	1.5	9.00	RF1B	Existing buildings in Duzce city center
31	Ozun (2007)	3	0.29	0.268	1.1	9.80	RF1B	Existing buildings in Duzce city center
32	Ozun (2007)	4	0.32	0.221	-0.1	4.91	RF2C	Existing buildings in Duzce city center
33	Ozun (2007)	3	0.47	0.160	1.5	9.22	RF1B	Existing buildings in Duzce city center
34	Ozun (2007)	3	0.44	0.182	1.5	8.46	RF1B	Existing buildings in Duzce city center
35	Ozun (2007)	4	0.44	0.127	0.8	7.78	RF2C	Existing buildings in Duzce city center
36	Ozun (2007)	3	0.46	0.153	5.3	4.71	RF1C	Existing buildings in Duzce city center
37	Ozun (2007)	3	0.26	0.243	4.4	7.50	RF1C	Existing buildings in Duzce city center
38	Ozun (2007)	2	0.22	0.438	1.4	8.91	RF1A	Existing buildings in Duzce city center
39	Ozun (2007)	2	0.19	0.393	0.5	5.63	RF1A	Existing buildings in Duzce city center
40	Ozun (2007)	2	0.25	0.280	0.9	8.04	RF1B	Existing buildings in Duzce city center
41	Ozun (2007)	2	0.24	0.295	0.8	9.87	RF1B	Existing buildings in Duzce city center
42	Ozun (2007)	3	0.31	0.265	1.4	10.64	RF1A	Existing buildings in Duzce city center
43	Ozun (2007)	3	0.25	0.317	0.9	11.20	RF1A	Existing buildings in Duzce city center
44	Ozun (2007)	2	0.23	0.420	1.0	11.96	RF1A	Existing buildings in Duzce city center
45	Ozun (2007)	2	0.13	0.559	0.4	12.19	RF1A	Existing buildings in Duzce city center
46	Ozun (2007)	2	0.21	0.450	1.0	7.42	RF1A	Existing buildings in Duzce city center

Table 4.3 Continued

Building No	Reference	N	T	η	α_u (%)	μ	Class	Note
47	Ozun (2007)	2	0.31	0.416	4.0	4.98	RF1A	Existing buildings in Duzce city center
48	Ozun (2007)	3	0.30	0.271	1.4	6.04	RF1C	Existing buildings in Duzce city center
49	Ozun (2007)	3	0.37	0.245	1.5	4.76	RF1C	Existing buildings in Duzce city center
50	Ozun (2007)	4	0.45	0.152	1.1	9.62	RF2B	Existing buildings in Duzce city center
51	Ozun (2007)	4	0.51	0.213	8.2	3.18	RF2B	Existing buildings in Duzce city center
52	Ozun (2007)	5	0.48	0.113	5.9	3.34	RF2C	Existing buildings in Duzce city center
53	Ozun (2007)	4	0.47	0.172	2.2	5.61	RF2B	Existing buildings in Duzce city center
54	Ozun (2007)	3	0.51	0.132	1.5	5.33	RF1C	Existing buildings in Duzce city center
55	Ozun (2007)	3	0.27	0.238	0.5	4.25	RF1C	Existing buildings in Duzce city center
56	Ay (2006)	3	0.76	0.28	4.8	5.73	RF1A	Generic buildings - Superior Class
57	Ay (2006)	3	0.59	0.47	3.6	8.61	RF1A	Generic buildings - Superior Class
58	Ay (2006)	5	1.06	0.23	4.8	7.00	RF2A	Generic buildings - Superior Class
59	Ay (2006)	5	0.80	0.33	4.3	7.74	RF2A	Generic buildings - Superior Class
60	Ay (2006)	5	0.70	0.47	4.4	5.74	RF2A	Generic buildings - Superior Class
61	Ay (2006)	7	1.16	0.19	4.8	7.38	RF2A	Generic buildings - Superior Class
62	Ay (2006)	7	0.97	0.27	4.3	8.30	RF2A	Generic buildings - Superior Class
63	Ay (2006)	7	0.87	0.37	4.6	6.25	RF2A	Generic buildings - Superior Class
64	Ay (2006)	3	0.84	0.22	4.1	4.34	RF1B	Generic buildings - Typical Class
65	Ay (2006)	3	0.64	0.38	2.5	7.61	RF1B	Generic buildings - Typical Class
66	Ay (2006)	3	0.49	0.56	2.6	6.14	RF1B	Generic buildings - Typical Class
67	Ay (2006)	5	1.16	0.18	3.7	5.65	RF2B	Generic buildings - Typical Class
68	Ay (2006)	5	0.87	0.25	2.9	5.46	RF2B	Generic buildings - Typical Class
69	Ay (2006)	5	0.75	0.37	2.8	5.69	RF2B	Generic buildings - Typical Class

Table 4.3 Continued

Building No	Reference	N	T	η	α_u (%)	μ	Class	Note
70	Ay (2006)	7	1.28	0.13	4.9	4.91	RF2B	Generic buildings - Typical Class
71	Ay (2006)	7	1.05	0.19	4.3	5.33	RF2B	Generic buildings - Typical Class
72	Ay (2006)	7	0.95	0.28	3.3	5.39	RF2B	Generic buildings - Typical Class
73	Ay (2006)	3	0.97	0.14	10.1	2.66	RF1C	Generic buildings - Poor Class
74	Ay (2006)	3	0.72	0.22	5.2	3.37	RF1C	Generic buildings - Poor Class
75	Ay (2006)	3	0.54	0.32	7.4	2.87	RF1C	Generic buildings - Poor Class
76	Ay (2006)	5	1.32	0.10	8.9	3.15	RF2C	Generic buildings - Poor Class
77	Ay (2006)	5	0.97	0.13	6.6	2.97	RF2C	Generic buildings - Poor Class
78	Ay (2006)	5	0.84	0.23	4.5	3.77	RF2C	Generic buildings - Poor Class
79	Ay (2006)	7	1.45	0.07	5.1	4.42	RF2C	Generic buildings - Poor Class
80	Ay (2006)	7	1.18	0.11	3.5	4.58	RF2C	Generic buildings - Poor Class
81	Ay (2006)	7	1.04	0.17	5.1	3.58	RF2C	Generic buildings - Poor Class
82	Karaca (2013)	4	0.44	0.46	4.1	5.00	RF2A	Existing Buildings in Eskişehir
83	Karaca (2013)	6	0.54	0.46	2.3	9.47	RF2A	Existing Buildings in Eskişehir
84	Karaca (2013)	6	0.44	0.47	3.1	9.50	RF2A	Existing Buildings in Eskişehir
85	Karaca (2013)	6	0.53	0.16	1.2	3.40	RF2C	Existing Buildings in Eskişehir
86	Karaca (2013)	5	0.40	0.46	4.4	7.27	RF2A	Existing Buildings in Eskişehir
87	Karaca (2013)	7	0.65	0.27	8.9	5.40	RF2C	Existing Buildings in Eskişehir
88	Karaca (2013)	5	0.53	0.35	4.1	5.88	RF2B	Existing Buildings in Eskişehir
89	Karaca (2013)	4	0.58	0.27	3.6	6.85	RF2B	Existing Buildings in Eskişehir
90	Karaca (2013)	5	0.50	0.39	4.9	3.38	RF2B	Existing Buildings in Eskişehir
91	Karaca (2013)	5	0.59	0.24	5.5	5.75	RF2C	Existing Buildings in Eskişehir
92	Karaca (2013)	5	0.88	0.23	4.0	5.93	RF2C	Existing Buildings in Eskişehir

Table 4.3 Continued

Building No	Reference	N	T	η	α_u (%)	μ	Class	Note
93	Karaca (2013)	4	0.44	0.45	5.2	5.80	RF2A	Existing Buildings in Eskişehir
94	Karaca (2013)	6	0.54	0.42	3.4	8.22	RF2A	Existing Buildings in Eskişehir
95	Karaca (2013)	6	0.53	0.10	2.1	7.20	RF2C	Existing Buildings in Eskişehir
96	Karaca (2013)	5	0.40	0.38	5.1	4.88	RF2A	Existing Buildings in Eskişehir
97	Karaca (2013)	7	0.65	0.19	10.1	4.62	RF2C	Existing Buildings in Eskişehir
98	Karaca (2013)	5	0.53	0.39	4.4	5.77	RF2B	Existing Buildings in Eskişehir
99	Karaca (2013)	4	0.58	0.30	4.3	6.70	RF2B	Existing Buildings in Eskişehir
100	Karaca (2013)	5	0.50	0.20	4.0	6.50	RF2B	Existing Buildings in Eskişehir
101	Karaca (2013)	5	0.59	0.21	7.4	6.10	RF2C	Existing Buildings in Eskişehir
102	Karaca (2013)	5	0.75	0.41	8.9	5.90	RF2B	Existing Buildings in Eskişehir
103	Karaca (2013)	5	0.69	0.22	4.6	5.93	RF2C	Existing Buildings in Eskişehir
104	Karaca (2013)	6	0.58	0.37	3.4	6.10	RF2B	Existing Buildings in Eskişehir

4.2.3 Major SDOF Parameters for RC Frame Structures

This section focuses on the estimation of major SDOF parameters for sub-classes of RC frame structures by using the constructed building database. This information is then will be used to estimate the seismic performance of this structural type under varying levels of ground motion intensity.

One of the major SDOF parameter is period and in this study, as a reference period, the periods of the constructed building database that are obtained from the previous studies are used. The buildings are classified according to the number of stories (low-rise and mid-rise) and also level of compliance with the seismic design and construction principles (A, B and C) as they were mentioned in the last section. The relationship between period and number of storey of low-rise, mid-rise and all buildings are shown in Figure 4.3. The corresponding mean and standard deviation values are displayed in Table 4.4.

Table 4.4. Mean and standard deviation of low-rise, mid-rise and all buildings

T	Mean	Std dev
Low-rise	0.394	0.203
Mid-rise	0.701	0.268
All Buildings	0.592	0.287

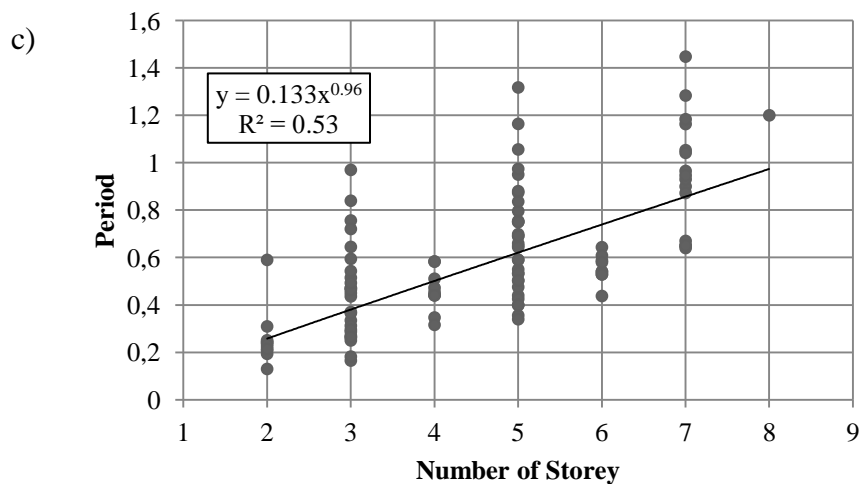
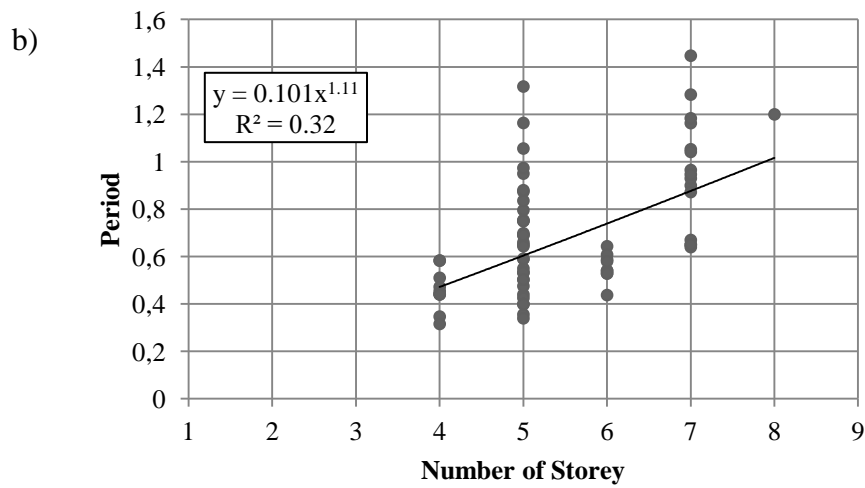
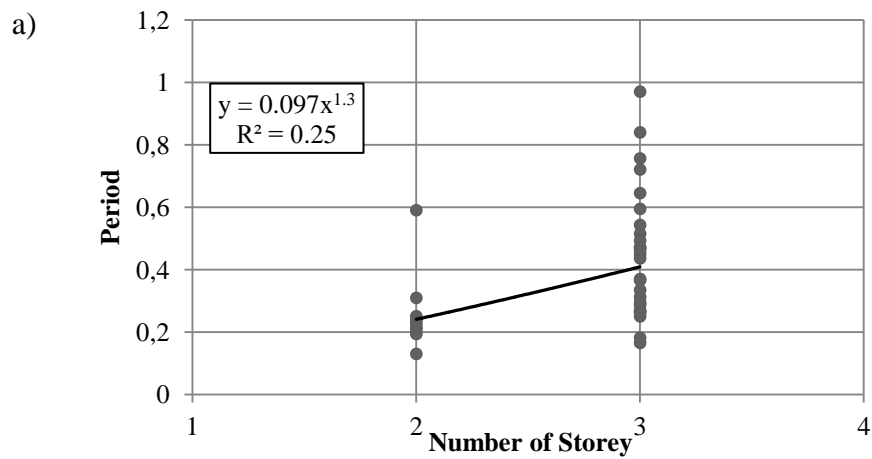


Figure 4.3 The relationship between period and number of storey a) Low-rise buildings. b) Mid-rise buildings. c) All buildings

The relationship between period and number of storey of the buildings that have A, B and C level of compliance with the seismic design and construction principles and all buildings are shown in Figure 4.4. The mean and standard deviation values are given in Table 4.5.

Table 4.5. Mean and standard deviation of buildings

T	Mean	Std dev
A	0.539	0.305
B	0.587	0.257
C	0.651	0.296
All Buildings	0.592	0.287

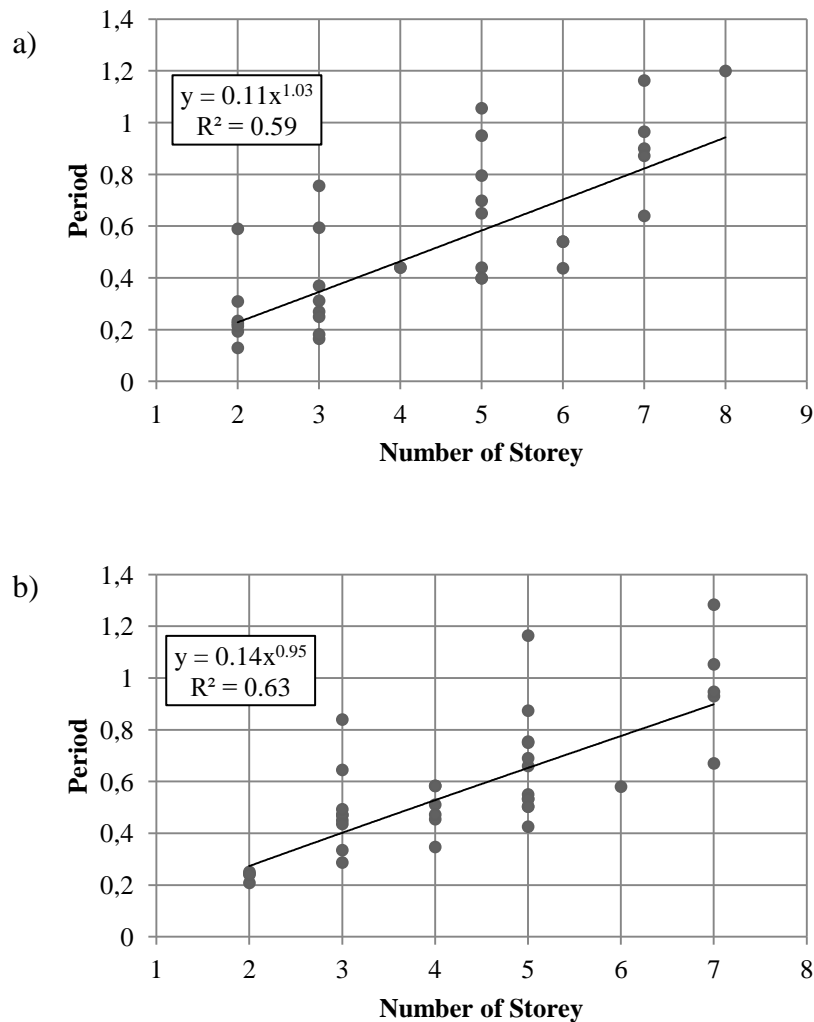


Figure 4.4 The relationship between period and number of storey a) Level A, b) Level B

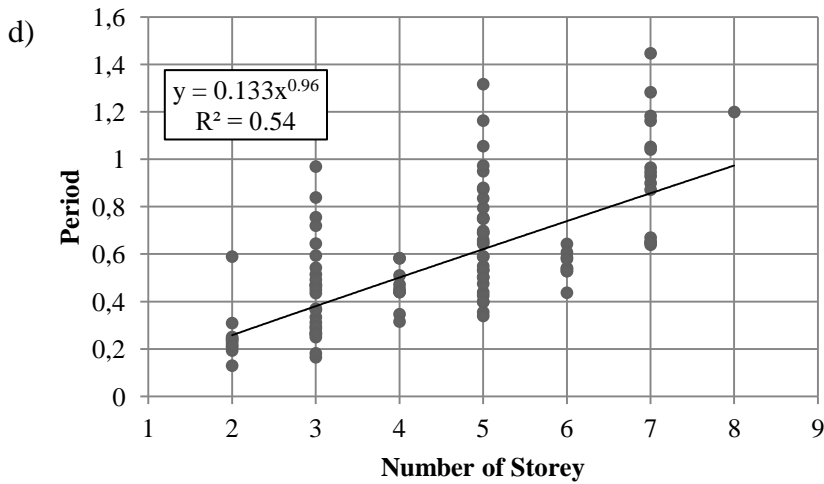
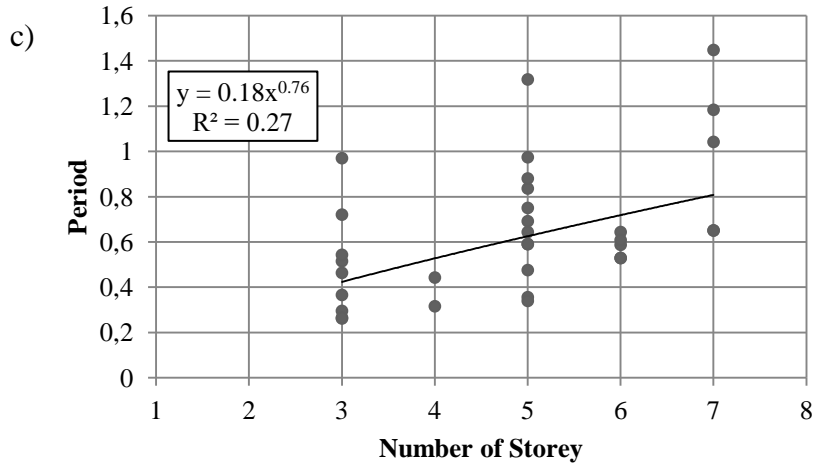


Figure 4.4 Continued c) Level C, d) All buildings

According to the Figure 4.3 and Figure 4.4, it is obvious that in the period estimations, classifying the buildings according to being low-rise and mid-rise or level of compliance with the seismic design and construction principles are not case sensitive. Therefore, without taking into consideration the classifications, for all reinforced concrete frame structures, in period estimation all the building data are used. The equation that fits most to the relationship between period and number of storey is a power function;

$$T = 0.133 N^{0.96} \quad (4.1)$$

where T is period and N is the number of storey. The reason of selecting power function for RC frame buildings is that R^2 value seems to rather higher ($R^2 = 0.54$).

In the literature, there are some code-based equations and some derived empirical formulas as a result of some studies and analyses.

As it is also recommended in NEHRP (1994), in common practices, for RC frame structures, period is estimated by using the equation 4.2 which is;

$$T = 0.1 N \quad (4.2)$$

In US practices, in period calculations the equation 4.3 is used.

$$T = 0.03 H^{0.75} \quad (4.3)$$

The empirical period formulas for the fundamental vibration period are proposed in NZSEE (2006) and NEHRP (2003) as follows, respectively;

$$T = 0.09 H^{0.75} \quad (4.4)$$

$$T = 0.0467 H^{0.9} \quad (4.5)$$

According to Goel and Chopra (2000), the formulation is defined as;

$$T = 0.067 H^{0.9} \quad (4.6)$$

In the study of TEC (1998), an alternative formula which is Equation 4.7 is recommended.

$$T = 0.07 H^{0.75} \quad (4.7)$$

The comparison between the reference periods that are obtained from the previous studies and the ones that are calculated from the empirical formulas and nonlinear regression formula are shown in Figure 4.5. For comparison, in the Equations 4.1 and Equation 4.2, instead of number of storey (N), height of the storey is referred to 3 m.

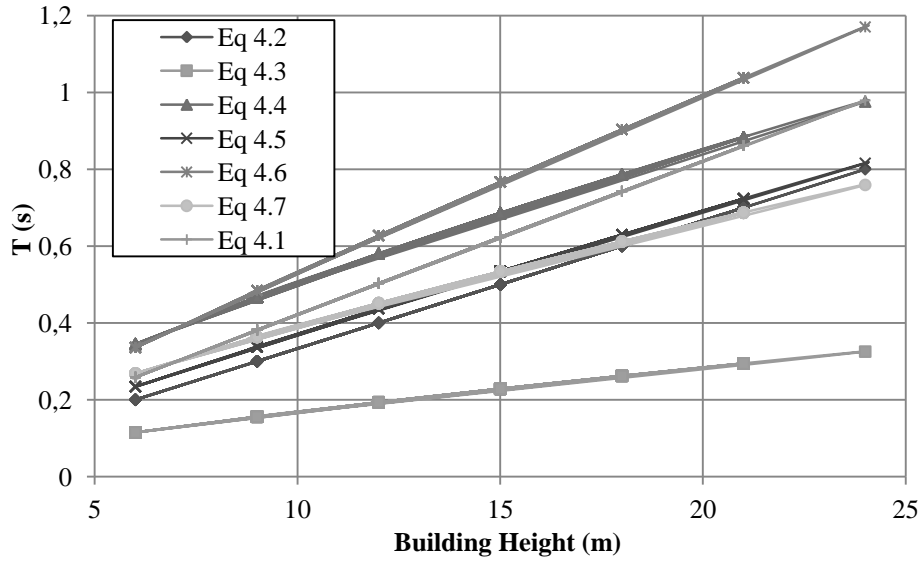


Figure 4.5 Comparison of fundamental periods in terms of building height

According to the standard error values, the smallest error is obtained in the regression equation using all building database periods. Therefore, to estimate an approximate period of RC frame buildings, Equation 4.1 is selected.

Table 4.6 Error estimations in the period formulations

	Standard Error (RMSE)
Equation 4.2	0.255
Equation 4.3	0.458
Equation 4.4	0.214
Equation 4.5	0.239
Equation 4.6	0.234
Equation 4.7	0.243
Equation 4.1	0.211

The other major parameters, strength ratio (η) and ductility (μ) are estimated from the bilinear idealization of the pushover curves as they are presented in the last part. As an example, from the study of Metin (2006), a sample bilinear idealization of the pushover curve is shown in Figure 4.6.

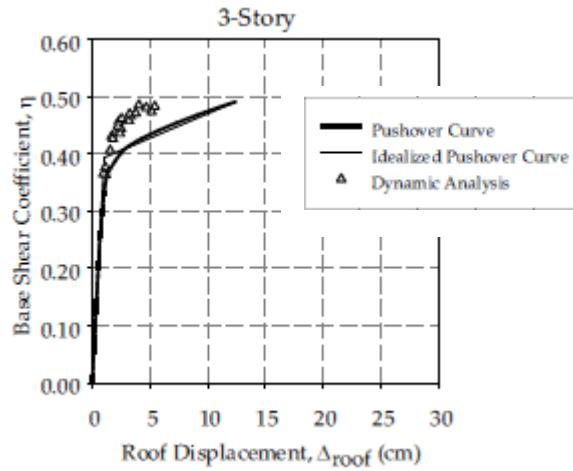


Figure 4.6 Idealization of pushover curve (Metin, 2006)

As it was already presented in the Chapter 3, the strength ratio and ductility are calculated by using the Equations 3.16 and 3.17, respectively.

In high, moderate and low level of compliance with the seismic design and construction principles, the stiffness degradation factor (β_0) is used as 0.0, 0.4 and 0.8, respectively. The strength degradation factors, β_a and β_b are assumed as 1.0 for β_a for all code levels and 1.0, 0.75 and 0.6 for β_b for high, moderate and low code levels, respectively. In addition to the degradation factors (β_0 , β_a , β_b), post-capping stiffness ratio (α_r), post-yielding stiffness ratio (α_u), yielding strength ratio (λ) are the parameters of SDOF systems. As it can be seen in Figure 4.3, post-yielding stiffness ratio values are not so stable that they vary between 0.5% and 10% so in average, post-yielding stiffness ratio is considered as 4%. The SDOF parameters are listed in Table 4.8

Table 4.7 Major SDOF parameters for RC frame structures

No	Code	N	Code Level	Period	η	μ	α_u	α_r	λ	β_0	β_a	β_b
1	RF1A	1-3	High	Equation 4.1	0.40	9.0	0.04	-0.20	0.2	0.0	1.0	1.00
2	RF2A	4-8	High		0.30	7.3	0.04	-0.20	0.2	0.0	1.0	1.00
3	RF1B	1-3	Moderate		0.23	4.9	0.04	-0.25	0.2	0.4	1.0	0.75
4	RF2B	4-8	Moderate		0.34	7.1	0.04	-0.25	0.2	0.4	1.0	0.75
5	RF1C	1-3	Low		0.26	6.1	0.04	-0.30	0.2	0.8	1.0	0.60
6	RF2C	4-8	Low		0.17	5.1	0.04	-0.30	0.2	0.8	1.0	0.60

4.3 Reinforced Concrete Tunnel-form Buildings

The RC tunnel-form structures are generally built in regions of high seismic hazard because of its high resistance against seismic action. In RC tunnel-form buildings, instead of beams and columns, there exist walls as the load carrying members. The casting of walls and slabs together result in monolithic structures which provides high resistance to lateral loads. Figure 4.7 shows example of RC tunnel-form structure. This is also the construction type used as permanent housing after earthquakes for people that had lost their houses. According to the World Housing Encyclopaedia (WHE) report on tunnel-form buildings (Yakut and Gulkan, 2003), this type of construction can be classified with a rating of ‘very low seismic vulnerability’, or in other words. excellent seismic performance.



Figure 4.7 A typical tunnel form building (Yakut and Gulkan, 2003)

RC tunnel-form buildings enable complete load transfer through the structural members and the internal stresses can be safely conveyed to the foundation of the building. In this construction type, the thicknesses of slab and shear walls are the same and it means that the slab thickness is less than the thickness of other type of structures. Therefore, diaphragm flexibility can modify dynamic behaviour. Transverse walls, which are perpendicular to the main walls, also increase the load capacity as a result of tension-compression coupling effect. These structures are

capable of dissipating energy with tolerable deformation. This is advantageous in terms of seismic behaviour because it keeps the structure in the elastic domain when strong earthquake motion is encountered (Balkaya and Kalkan, 2003).

RC tunnel-form buildings also have some drawbacks. The torsional behaviour can be observed since torsional rigidity is low in tunnel-form structures. According to Balkaya and Kalkan (2003), when total bending is taken into account, torsional behavior is observed more in structures with rectangular plans when compared to structures with square plans. Also, rectangular plans have less bending capacity along their short sides than the square plans. Generally, tunnel form building structures show good performance against lateral loads. However, almost square plans and symmetrically distributed shear walls in plan are the best to minimize the torsional affect and increase the bending capacity.

4.3.1. Available Studies Regarding RC Tunnel-form Buildings

Unfortunately, the research on Turkish RC tunnel-form buildings is rather limited when compared to frame type of buildings. The most detailed study for this type of construction belongs to Balkaya and Kalkan (2003).

Balkaya and Kalkan (2003) designed generic structures with 2, 5, 10, 12 and 15 stories according to UBC (1997) and previous version of Turkish Seismic Code (1998) in order to provide high resistance against seismic action. The structures were generated as three dimensional models by using shell element in ETABS program. Square and rectangular building plans were considered with symmetrical wall distribution. In this study, since low-rise and mid-rise buildings up to 8 stories are considered. 2 and 5 story analytical models generated by Balkaya and Kalkan (2003) are used. This makes a total of 32 RC tunnel-form buildings.

According to the building sub-classification in this study, 2 story buildings are regarded as low-rise and 5 story buildings are regarded as mid-rise. All of the buildings are classified as group A, since RC tunnel-form buildings are generally designed and constructed by considering seismic action. Hence the denotations for the available building sub-classes are RW1A and RW2A, where the letter 'W' represents tunnel-form buildings.

4.3.2. Major SDOF Parameters for RC Tunnel-form Buildings

For Turkish RC tunnel-form buildings, determination of equivalent SDOF parameters is not as easy as in the case of RC frame buildings due to scarcity of available data. Hence the quantification of the parameters is partially based on some observations and assumptions regarding tunnel-form structures.

For the determination of the empirical relationship between period and number of stories, the data from Balkaya and Kalkan (2003) is employed as shown in Figure 4.8. A power function is fit to the scattered data.

$$T = 0.0181 N^{1.3} \tag{4.8}$$

where T is period and N is the number of stories. The reason of selecting a power fit for tunnel-form buildings just like in frame buildings is that R² value which is 0.93, for power function yields higher results for this case. However, it should also be mentioned that the best fit is obtained only by considering two different groups of scattered data. i.e., the ones with 2 and 5 number of stories. There is a lack of information for other number stories which impairs the validity of this empirical formulation although it has a high R² value.

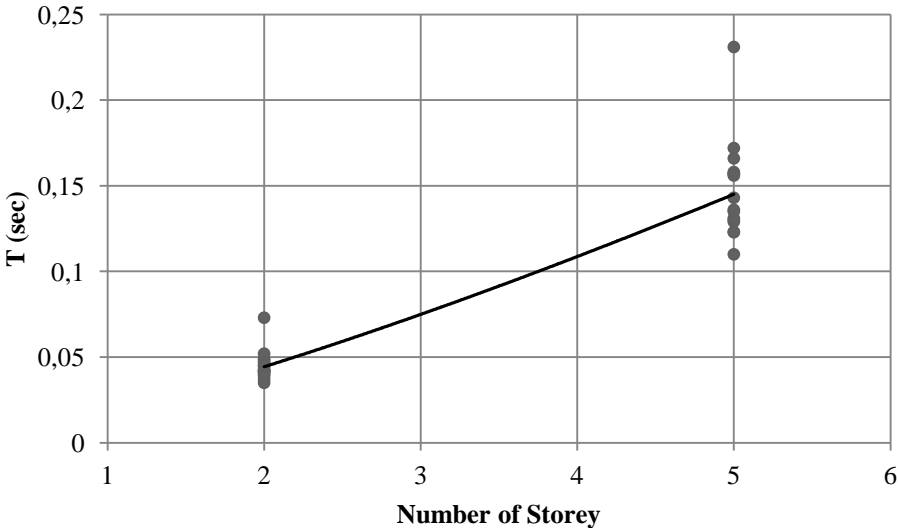


Figure 4.8. Period versus number of the stories relationship in RC tunnel-form structures

In the literature, there are some code-based equations and some derived empirical formulas as a result of some studies and analyses.

In US practices, for RC tunnel-form structures, period is estimated by using the Equation 4.9 which is;

$$T = 0.02 H^{0.75} \quad (4.9)$$

The empirical period formulas for the fundamental vibration period are proposed in Uniform Building Code (1997) as follows;

$$T = C H^{0.75} \quad (4.10)$$

From the equation above;

$$C = \frac{0.1}{\sqrt{A_C}} \quad (4.11)$$

where A_C is the combined effective area;

$$A_c = \sum_i^{NW} A_i \left(0.2 + \left(\frac{D}{H} \right)^2 \right) \quad (4.12)$$

in which A_i is the horizontal cross-sectional area, D is the dimension in the direction under consideration and NW is the total number of shear walls.

According to ATC3-06 (1978) and earlier versions of US codes, the fundamental period is defined as;

$$T = 0.05 H/\sqrt{D} \quad (4.13)$$

The comparison between the reference periods from Balkaya and Kalkan (2003) and the ones that are calculated from the empirical formulas and nonlinear regression formula are shown in Figure 4.9. For comparison, in the Equations 4.8, instead of number of storey (N), height of the storey is referred to 3 m. Because of the reason that in Figure 4.9, the relationship between building height and period is shown, Equation 4.13 is not considered.

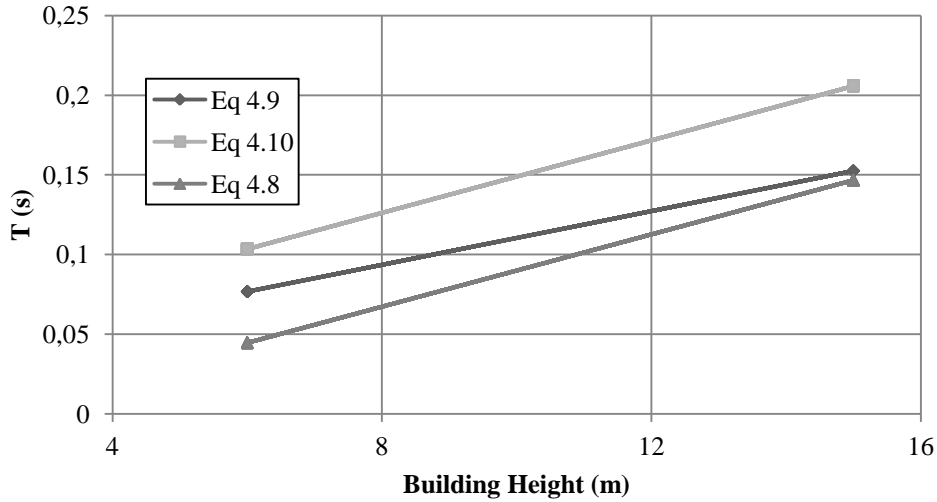


Figure 4.9 Comparison of fundamental periods in terms of building height

According to the standard error values, the smallest error is obtained from the nonlinear equation. Therefore, with the aim of estimation an approximate period of RC tunnel-form buildings, it is determined that, the Equation 4.8 can be used.

Table 4.8 Error estimations in the period formulations

	Standard Error (RMSE)
Equation 4.8	0.020
Equation 4.9	0.030
Equation 4.10	0.062
Equation 4.13	0.069

To obtain strength ratio (η) and ductility (μ), the capacity curves obtained by Balkaya and Kalkan (2004) for 2-D and 3-D models of 2 and 5 story RC tunnel-form buildings are considered (Figure 4.10). The curves show that strength ratio is very high for this type of construction, especially for 2 story (low-rise) building model whereas the ductility is rather limited. Similar results were obtained by Yuksel and Kalkan (2007), who tested two 4-story 1/5 scale building specimens under quasi-static cyclic lateral loading. There is a recent experimental study conducted by Tavafoghi and Eshghi (2013), which yielded similar results. Hence it is assumed that

for building sub-classes RW1A and RW2A, parameter η is 1.2 and 0.6, respectively. For these two building sub-classes, the ductility capacity is taken as 2.5.

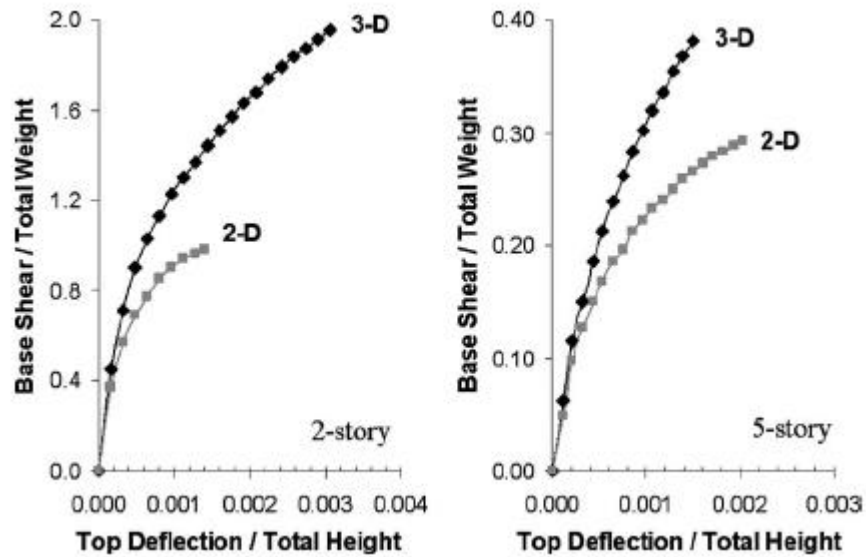


Figure 4.10 Capacity curves for 2 stories and 5 story RC tunnel-form buildings (Balkaya and Kalkan, 2004)

The post-yielding stiffness ratio is considered as higher in RC tunnel-form buildings so 8% post-yielding stiffness ratio is used. Due to the reason that RC tunnel-form buildings show high level of performance against seismic excitation, no degradation is considered. The SDOF parameters are listed in Table 4.9.

Table 4.9 Major SDOF parameters for RC tunnel-form structures

No	Code	N	Code Level	Period	η	μ	α_u	α_r	λ	β_o	β_a	β_b
1	RW1A	1-3	High	Equation 4.8	1.20	2.5	0.08	-0.20	0.2	0.0	1.0	1.00
2	RW2A	4-8	High		0.60	2.5	0.08	-0.20	0.2	0.0	1.0	1.00

4.4 Reinforced Concrete Dual Buildings

Dual reinforced concrete structures are composed of moment frames with shear walls. In this structural system, the gravity loads are resisted by the frame whereas the lateral loads are resisted by the shear walls.

RC dual buildings should be constructed in earthquake prone regions instead of RC frame buildings, especially for buildings with more than five stories. In this structural type, percentage of the total cross-sectional area of shear walls when compared to the floor are generally varies between 0.5% - 2.5%. The shear walls have the advantage of limiting the lateral deformations of the structure, which controls the damage in frame elements.

The following sub-sections present the previous studies regarding the seismic performance of RC dual structures, from which the equivalent SDOF characteristics of this type can be proposed for Turkish construction practice.

4.4.1. Available Studies Regarding RC Dual Buildings

There exists a number of studies regarding Turkish RC dual buildings. Some of these studies are considered here as discussed in the following paragraphs.

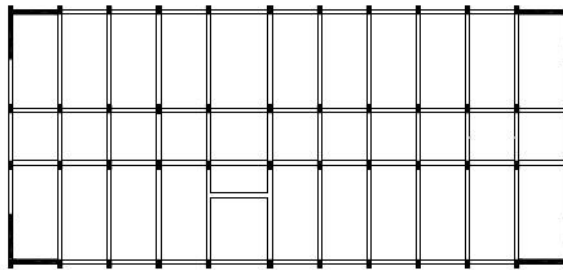
Vuran et al (2008) claimed that most of the RC dual buildings in Turkey had been constructed after the release of the 1998 version of the Turkish earthquake code. According to these researchers, before 1998 RC dual building had still been constructed, but not with the intention of earthquake resistance, as core walls around the stairs or elevators lacked proper connections to the existing frame structure.

They analyzed four 3D dual buildings with 4, 5, 6 and 8 stories, which were selected from actual buildings in northern Marmara region, representative of the existing mid-rise RC dual buildings in Turkey. They concentrated on the yield period, deformed shape and effective height in order to define SDOF characteristics of dual buildings for use in displacement based assessment.

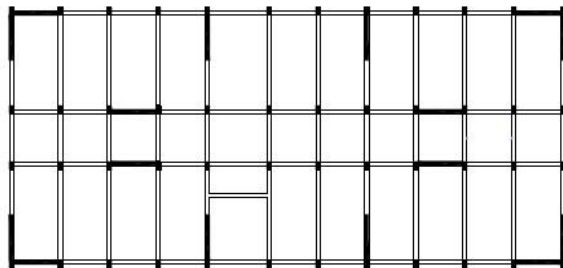
Günel (2013) studied five different existing school buildings in Istanbul. Although school buildings, i.e. public buildings, are out of the scope of this study, the study of Günel (2013) worths mentioning in the sense that it considers the effect of shear wall

area on the seismic response of dual RC structures. In order to understand the effect of the amount of shear wall on the structural performance, the structures were redesigned according to the code regulations and generic structures were obtained. One of the redesigned buildings with increasing ratio of shear wall both in longitudinal and transverse directions is shown in Figure 4.11. The buildings were designed according to Turkish Earthquake Code (2007), Turkish Standards 498 (1987) for design loads and Turkish Standards 500 (2000) for detailing. The structures were modelled in SAP 2000 and were analyzed under seven different earthquake records with changing values of PGA from 0.152g to 0.821g.

a)



b)



c)

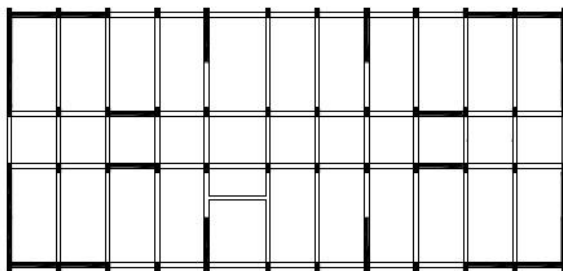


Figure 4.11 Plan view of the building with a) 0.5% shear wall ratio, b) 1.0% shear wall ratio, c) 1.5% shear wall ratio

d)

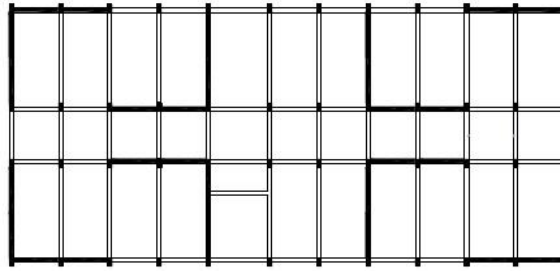


Figure 4.11 Continued, d) 2.0% shear wall ratio (Günel, 2013)

The variation in the fundamental period of the generic building (shown in Figure 4.12) with the shear wall ratio is presented in Figure 4.12. The trends reveal that the period of the building decreases with increasing shear wall ratio, as expected. In addition, the decrease seems to be quite significant for low values of shear wall ratio and as the shear wall ratio increases further, it starts to be stabilized.

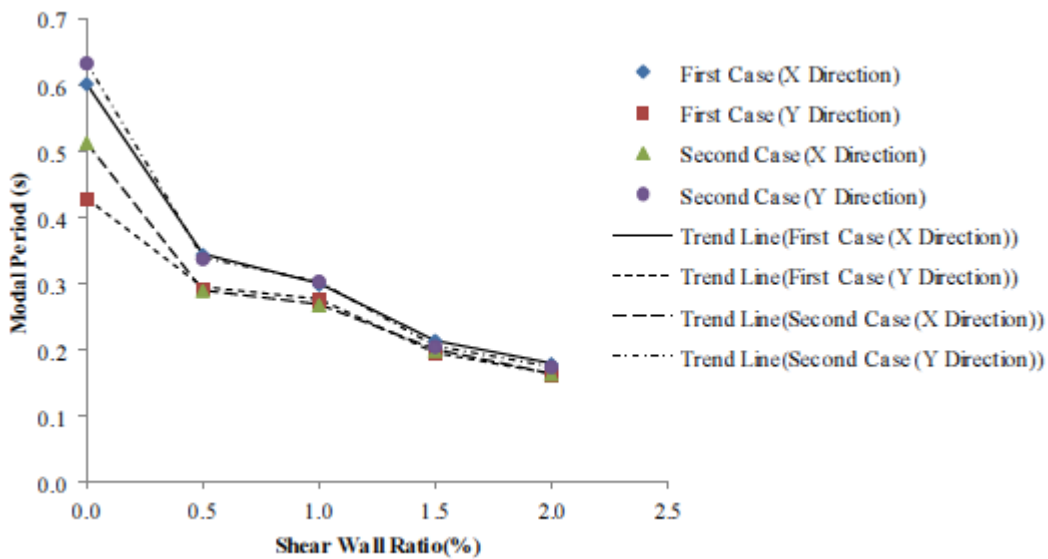


Figure 4.12 Variation of fundamental period with shear wall ratio for the generic building (Günel, 2013)

Karaca (2013) studied on the actual RC dual buildings in Eskişehir that vary from 4 to 8 number of stories. Because of the reason that these structures are existing, some detailed properties can be obtained as it is given in Table 4.10. It is also possible to

obtain response parameters of these buildings like vibration period, base shear ratio at yield and ultimate, which assist in determining the SDOF parameters of Turkish RC dual structures.

Table 4.10. General properties of the existing structures in Eskişehir (Karaca, 2013)

Building No	No of Stories	Height (m)	Weight (t)	Material Strength (MPa)	Design Year
1	6	16.8	742.6	C20/S420	1993
2	4	11.68	325.5	C25/S420	2001
3	5	14.6	754.8	C25/S420	2007
4	5	14.75	584.4	C25/S420	2006
5	6	18	884.64	C25/S420	2008
6	7	22.4	2767.7	C16/S420	1995
7	6	18.8	610.6	C30/S420	2004
8	5	11.68	581.3	C25/S420	2007
9	8	22.7	946.3	C25/S420	2010
10	6	18.7	1114.7	C20/S420	1997
11	5	14.5	547.1	C25/S420	2008
12	6	22.35	1081	C25/S420	2004
13	5	14.75	307.5	C25/S420	2007
14	5	14.96	498.4	C25/S420	2008
15	6	18	809.3	C25/S420	2007
16	5	14.6	476.7	C20/S420	2002

As it can be seen, the structural data obtained from the previous studies is limited. The main source of data to obtain SDOF parameters of RC dual buildings comes from Karaca (2013), containing 16 buildings. Günel (2013) provides the period information of some of the generic buildings whereas no detailed information can be obtained from Vuran et al (2008). The available data is presented in Table 4.11.

These types of buildings have a significant margin of safety against seismic action due to the presence of shear walls although they may possess some structural deficiencies. Therefore during sub-classification, RC dual buildings are classified as group A and B. They can be low-rise or mid-rise structures depending on the number of stories. Accordingly, the denotations for the available building sub-classes are RH1A, RH2A, RH1B and RH2B, where the letter 'H' represents dual buildings.

Table 4.11. The classification of all RC dual buildings used in this study

Building No	Reference	N	T	η	μ	Class	Note
1	Karaca (2013)	5	0.40	0.52	6.67	RH2A	Existing buildings in Eskişehir
2	Karaca (2013)	6	0.84	0.63	1.47	RH2A	Existing buildings in Eskişehir
3	Karaca (2013)	8	0.64	0.37	2.71	RH2A	Existing buildings in Eskişehir
4	Karaca (2013)	5	0.49	0.48	6.78	RH2A	Existing buildings in Eskişehir
5	Karaca (2013)	5	0.42	0.64	7.54	RH2A	Existing buildings in Eskişehir
6	Karaca (2013)	6	0.88	0.78	2.62	RH2A	Existing buildings in Eskişehir
7	Karaca (2013)	6	0.84	0.59	1.61	RH2A	Existing buildings in Eskişehir
8	Karaca (2013)	5	0.42	0.40	6.20	RH2A	Existing buildings in Eskişehir
9	Karaca (2013)	6	0.64	0.42	4.65	RH2B	Existing buildings in Eskişehir
10	Karaca (2013)	6	0.64	0.36	3.39	RH2B	Existing buildings in Eskişehir
11	Karaca (2013)	7	0.58	0.27	4.25	RH2B	Existing buildings in Eskişehir
12	Karaca (2013)	6	0.90	0.44	3.25	RH2B	Existing buildings in Eskişehir
13	Karaca (2013)	5	1.02	0.33	1.97	RH2B	Existing buildings in Eskişehir
14	Karaca (2013)	5	0.55	0.39	3.18	RH2B	Existing buildings in Eskişehir
15	Günel (2013)	4	0.33	-	-	-	Generic Buildings
16	Günel (2013)	4	0.29	-	-	-	Generic Buildings
17	Günel (2013)	4	0.3	-	-	-	Generic Buildings
18	Günel (2013)	4	0.27	-	-	-	Generic Buildings
19	Günel (2013)	4	0.21	-	-	-	Generic Buildings
20	Günel (2013)	4	0.19	-	-	-	Generic Buildings

4.4.2. Major SDOF Parameters for RC Dual Buildings

The limited information regarding the periods of Turkish RC dual buildings obtained from the available studies (Karaca (2013) and Günel (2013)) are presented in Figure 4.13 as a function of the number of stories. The form of the equation that fits most closely to the relationship between period and number of storey is a power function;

$$T = 0.02 N^{1.9} \quad (4.14)$$

where T is period and N is the number of stories. Although the number of data points is limited, the R^2 value seems to high ($R^2 = 0.71$).

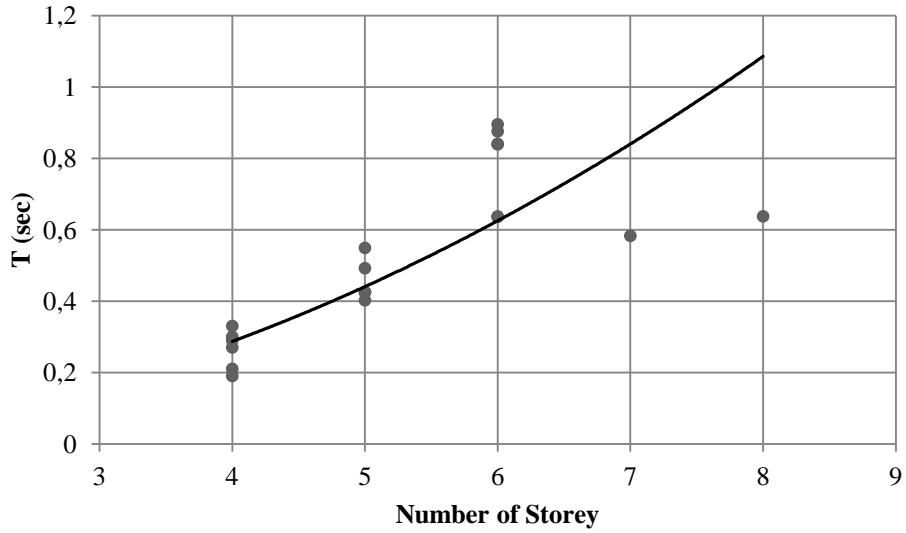


Figure 4.13. Period versus number of the stories relationship in RC dual structures

Earlier, Vuran et al (2008) proposed an alternative empirical period formulation for the fundamental vibration period as follows;

$$T = 0.075 H \tag{4.15}$$

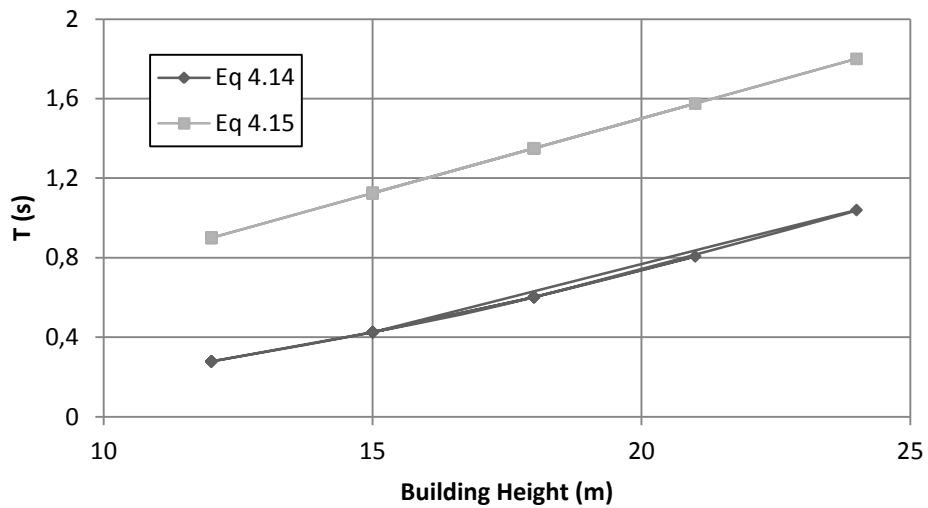


Figure 4.14 Comparison of fundamental periods in terms of building height

The smallest standard error is obtained from the nonlinear equation derived based on the period and number of stories parameters of the building database. Therefore, with the aim of estimation an approximate period of RC dual buildings, it is decided that Equation 4.14 can be used.

Table 4.12 Error estimations in the period formulations

	Standard Error (RMSE)
Equation 4.14	0.210
Equation 4.15	0.670

The strength ratio (η) and ductility (μ) values for RC dual buildings are obtained from the capacity curves in the study of Karaca (2013), as can be seen in Table 4.13. There also exist some peculiar results in the database such as unreasonably low or high values of strength ratio and ductility. Disregarding the outlier data, the representative values of η and μ for sub-classes RH1A, RH2A, RH1B and RH2B are given in Table 4.13, respectively. Other SDOF parameters assumed for the considered sub-classes (α_u , α_r , λ , β_0 , β_a , β_b) are also presented in the same table.

Table 4.13 Major SDOF parameters for RC dual buildings

No	Code	N	Code Level	Period	η	μ	α_u	α_r	λ	β_0	β_a	β_b
1	RH1A	1-3	High	Eq 4.14	0.60	5.0	0.04	-0.20	0.2	0.0	1.0	1.00
2	RH2A	4-8	High		0.50	4.5	0.04	-0.20	0.2	0.0	1.0	1.00
3	RH1B	1-3	Moderate		0.48	4.0	0.04	-0.25	0.2	0.4	1.0	0.75
4	RH2B	4-8	Moderate		0.37	3.50	0.04	-0.25	0.2	0.4	1.0	0.75

CHAPTER 5

A CASE STUDY FOR ESTIMATION OF DAMAGE RATES IN ERZINCAN

5.1 General

In this Chapter, a case study that involves the application of the proposed methodology on a group of masonry and reinforced concrete buildings is presented. The study region is urban Erzincan area located on the Eastern segment of the North Anatolian Fault zone. This area is selected for two main reasons: the recent focus of earthquake-related studies in Turkey is on the western segments due to the existence of industrial facilities and dense populations while Erzincan region is relatively more sparsely monitored and less investigated. In addition, the city center built on the Erzincan basin on deep soft sediments is under significant seismic risk due to the very short distances from the surrounding faults as well as the potential basin effects observed during major earthquakes.

To apply the proposed method in this thesis, strong ground motion data from a range of events with various magnitudes is aimed to be used. However, until recently the area was monitored sparsely thus there are not many recordings in the urban Erzincan region. Consequently, simulated ground motions for the region are employed herein.

In Section 5.2 the ground motion data used in the damage state analyses is presented. Section 5.3 introduces the results of the equivalent SDOF analyses where a verification study for the damage distribution of the 1992 Erzincan earthquake is also presented.

5.2 Synthetic Database: Simulated Ground Motions in Erzincan City Center

In this study, the simulated ground motion database generated in an ongoing national project (with grant number: TUJJB-UDP-01-12) is employed. In the mentioned project, a step-by-step algorithm is used to obtain potential seismic damage in Erzincan: the approach respectively involves estimation of site conditions, modelling of the active faults, simulations of potential ground motions from a selected set of scenario events, derivation of fragility curves based on simulated motions and finally, estimation of potential losses in anticipated future events. In this section, the synthetic ground motion database is described briefly.

5.2.1 Methodology

As mentioned earlier, the eastern parts of the North Anatolian Fault zone does not contain dense networks. Thus, the recorded ground motions do not cover a broad range of amplitude and frequency contents to be used in damage estimations. For this purpose, in the mentioned project stochastic finite fault method proposed by Motazedian and Atkinson (2005) is employed to generate a set of scenario earthquakes that would cause varying levels of ground motions in Erzincan city center.

Stochastic finite fault method relies on the fact that the far-field S-wave amplitude spectrum from an earthquake source is deterministic and known while the phase angles are incoherent (random) in nature. Any fault is modelled as a rectangular plane that consists of finite number of point sources each of which radiates waves that propagate kinematically. The method combines the amplitude spectrum with random phases in the frequency domain for every point source on the finite fault plane. Figure 5.1 displays the source mechanism employed in this method.

After constraining the source mechanism, path (wave propagation) and site parameters are chosen either from previous regional studies or derived for the region of interest. Generally, these parameters are tested in a verification exercise where a past major earthquake is simulated and simulated ground motions are compared against observed data. Further details of the method used to simulate the ground

motions can be found in Motazedian and Atkinson (2005), Askan et al. (2013) and TUJJB Project Midterm Report #4.

To generate scenario events, the stochastic finite fault method requires well-constrained input parameters for the source, path and site parameters. For this purpose, first 1992 Erzincan earthquake is simulated as outlined in detail in Askan et al. (2013); then the scenario events are designed. Before presenting the simulated ground motions, seismicity of the region is presented.

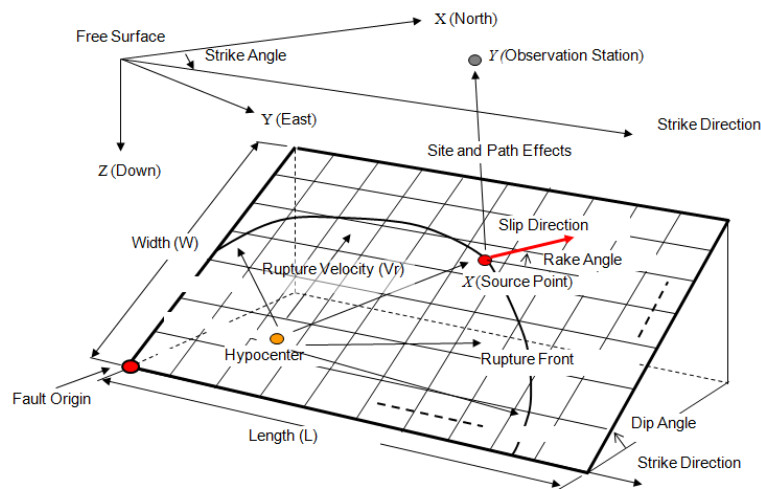


Figure 5.1. Source mechanism in stochastic finite fault method (adapted from Hisada, 2008)

5.2.2. Seismicity of the Area

Erzincan is located in the close vicinity to the triple conjunction of three active faults, namely North Anatolian, North East Anatolian and East Anatolian Fault Zones (EAFZ). Due to the interactions of these fault systems, Erzincan basin is formed which is a typical pull-apart basin structure. Historical records indicate 18 large ($M_w > 8$) earthquakes in the close vicinity of Erzincan within the past 1000 years. Due to the unfortunate combination of the seismicity and the basin structure, these events most likely generated destructive levels of ground motion amplitudes. Similarly, within the last century, Erzincan has gone through two major events: 1939 ($M_s = 8.0$) and 1992 ($M_w = 6.6$) earthquakes (Figure 5.2). Both of these events caused

significant structural losses and fatalities in Erzinçan city center and surrounding rural areas.

Despite the fact that the current focus of seismic research led in Turkey is mostly on the Western segments of the North Anatolian Fault zone, the region deserves to be studied due to the significant seismic activity as shown in Figure 5.3.

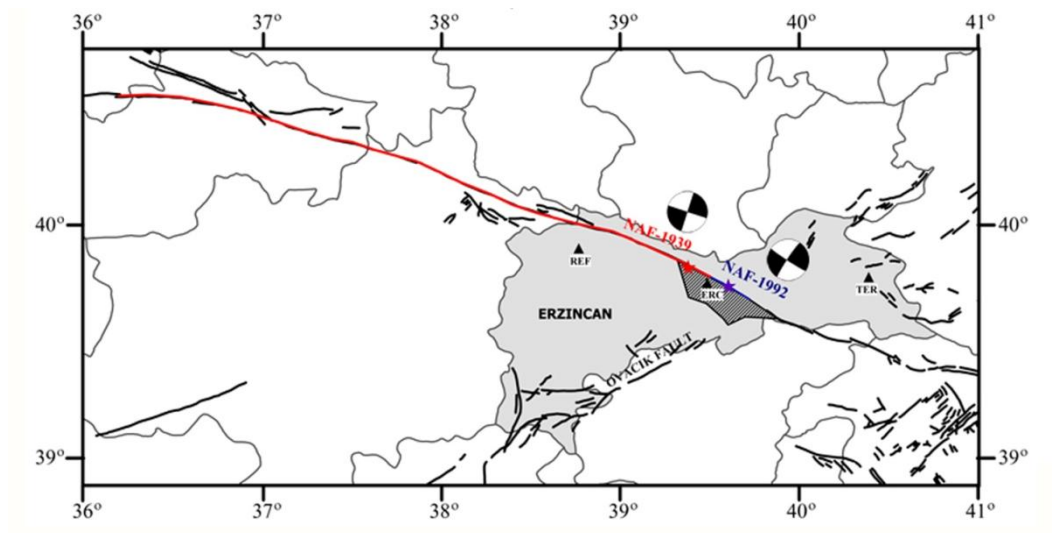


Figure 5.2. The focal mechanisms and the related faults of the 1939 (red) and 1992 (blue) Erzinçan earthquakes (Stars indicate the epicenters, triangles indicate the locations of the (three) strong motion stations that recorded the 1992 mainshock, shaded area is the Erzinçan basin)

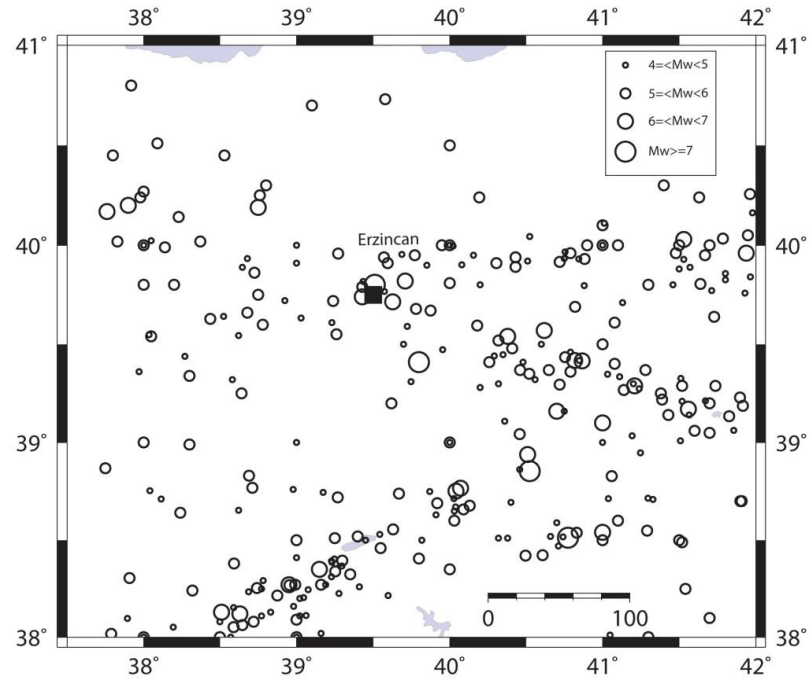


Figure 5.3. The seismic activity in Erzincan region within the instrumental era (only mainshocks are presented in this figure)

5.2.3. Simulated Ground Motion Dataset

Using the validated ground motion parameters, a set of scenario earthquakes with $M_w=5.0-7.5$ is simulated with an increment of $\Delta M_w=0.5$. In addition, 1992 earthquake is also simulated. For each event, the epicenter is assumed to be at the same location of 1992 earthquake's epicenter. It must be noted that the epicenter of 1992 earthquake is a critical location in terms of shortest distance from the fault. Thus, in the scenario events the most critical situation for the Erzincan urban area is considered.

In the simulations, In Figures 5.4, the anticipated distribution of peak ground motion parameters such as PGA, PGV and SA (0.2 sec) is shown for the 1992 event and for every scenario event considered. Out of 24 districts, 4 districts which are Cumhuriyet, Yunus Emre, Fatih and Yavuz Sultan Selim were selected for this study. In the figures, the locations of districts in Erzincan are also displayed.

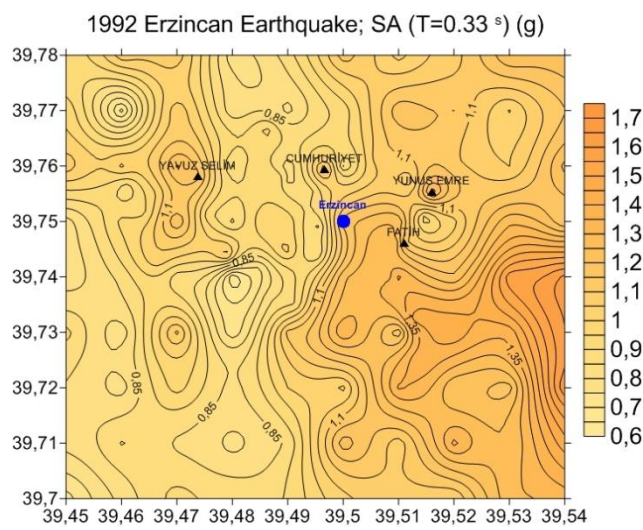
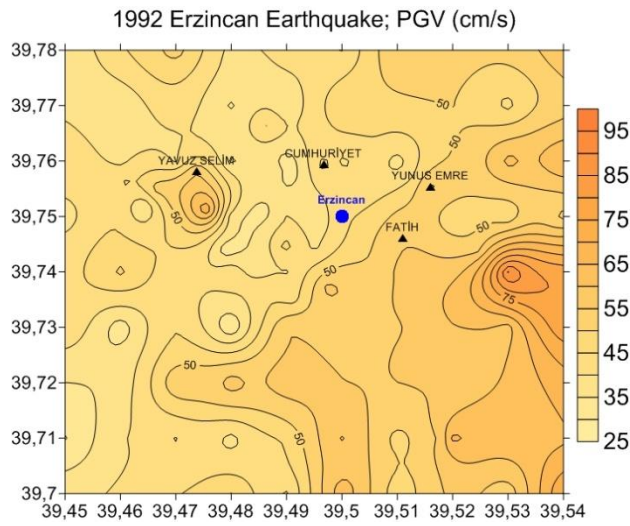
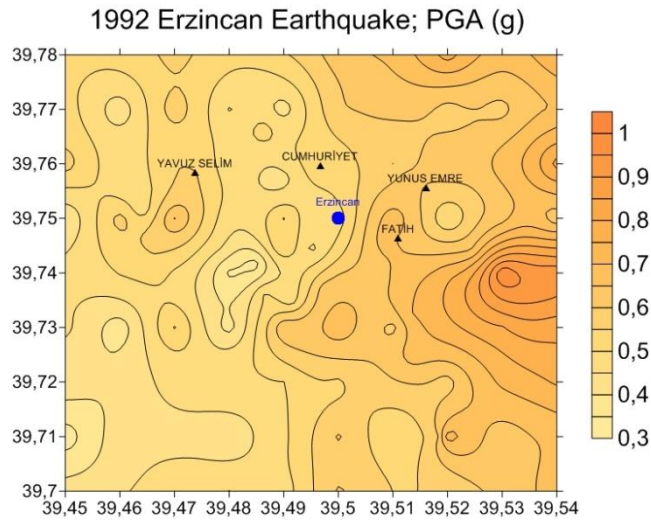


Figure 5.4 The anticipated distribution of peak ground motion parameters for each scenario earthquake

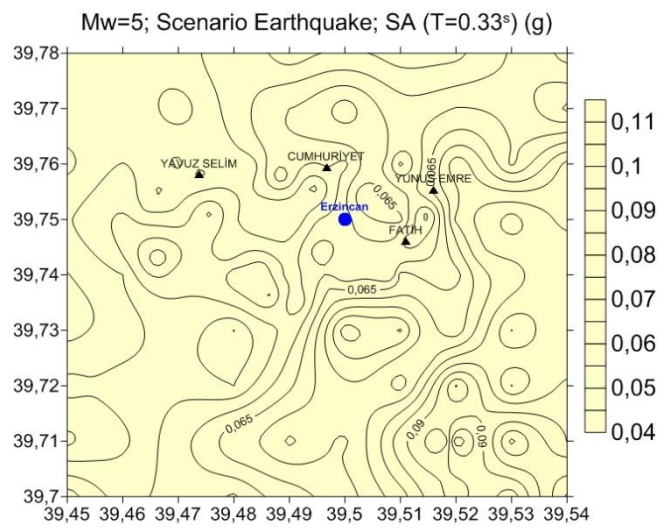
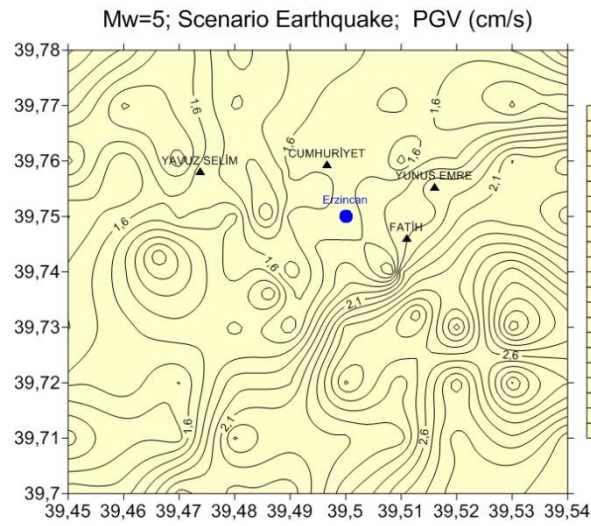
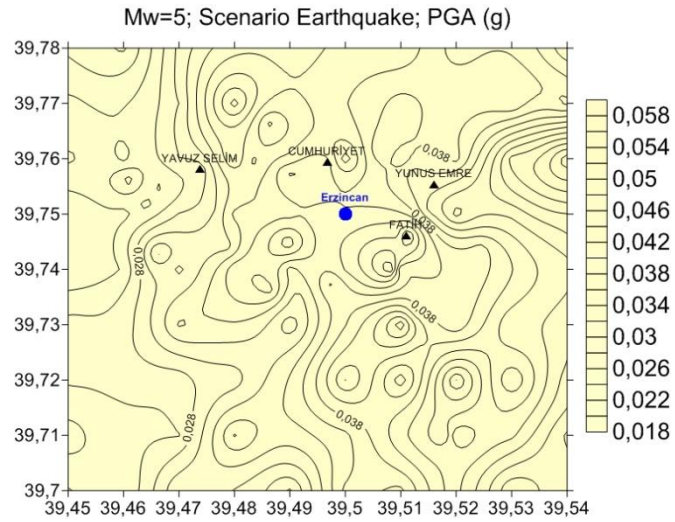


Figure 5.4 Continued

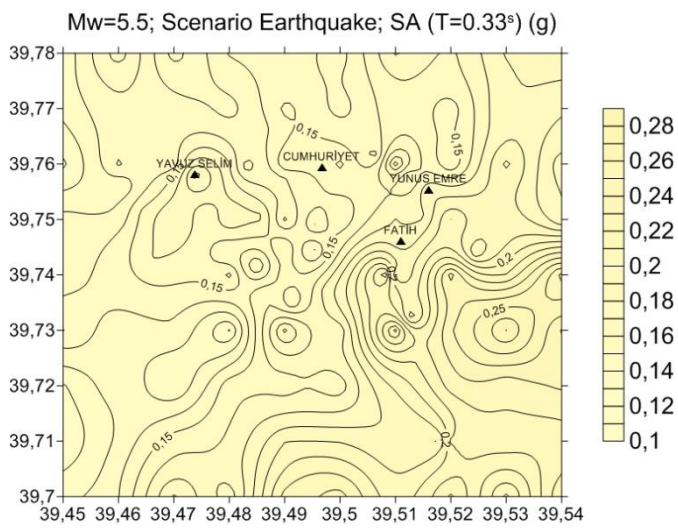
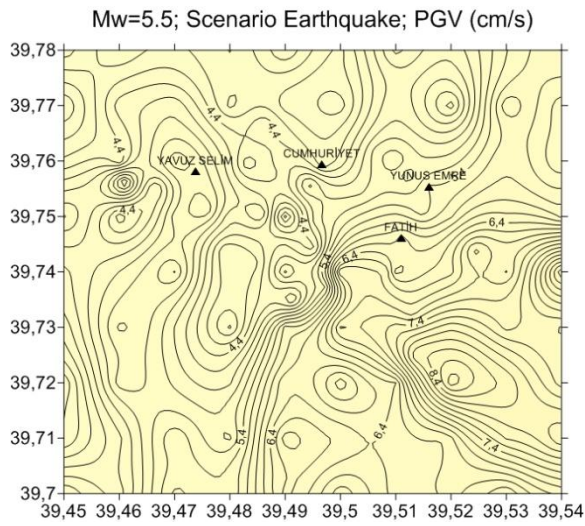
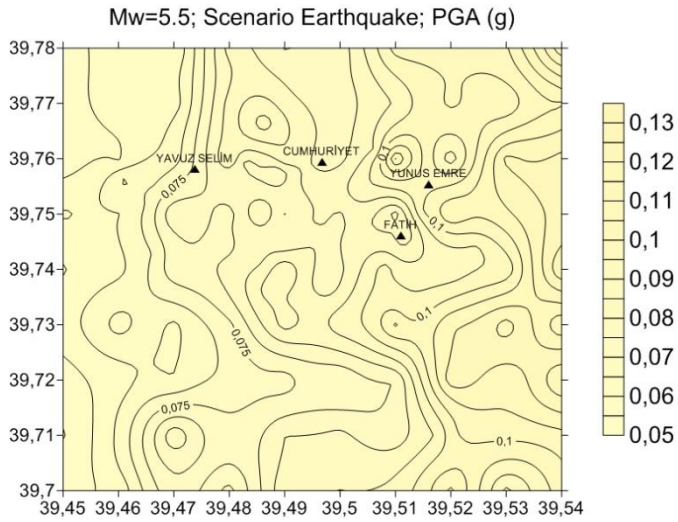


Figure 5.4 Continued

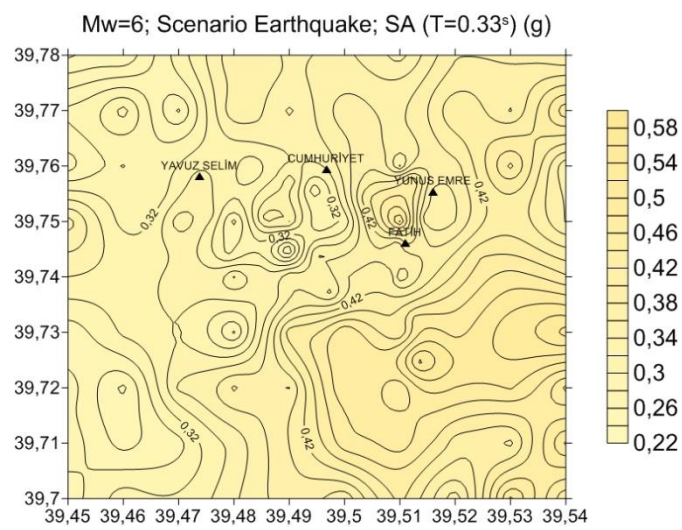
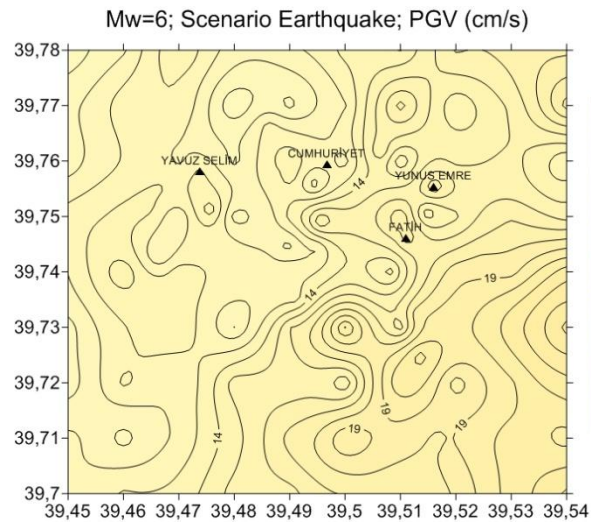
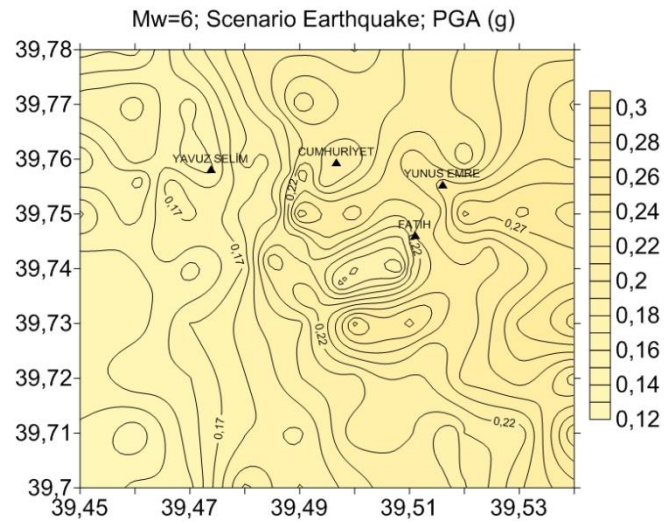


Figure 5.4 Continued

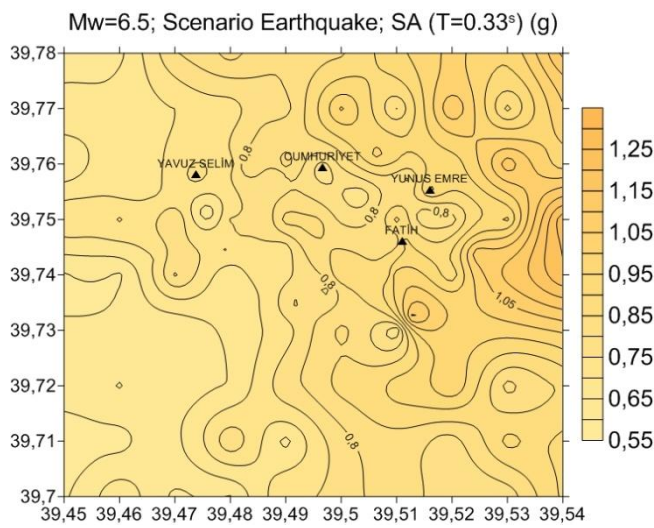
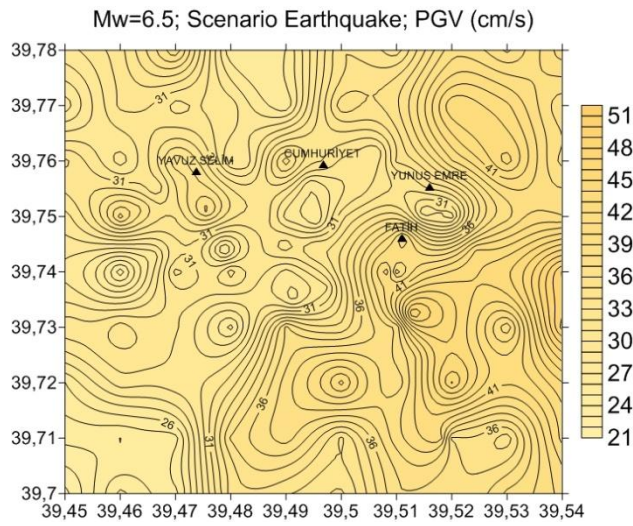
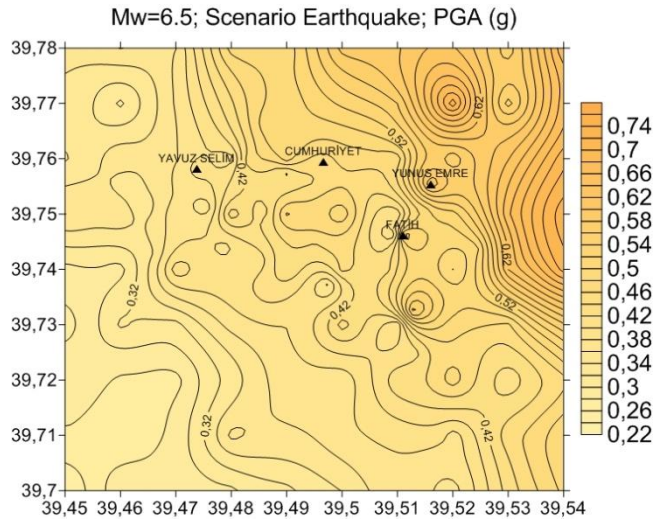


Figure 5.4 Continued

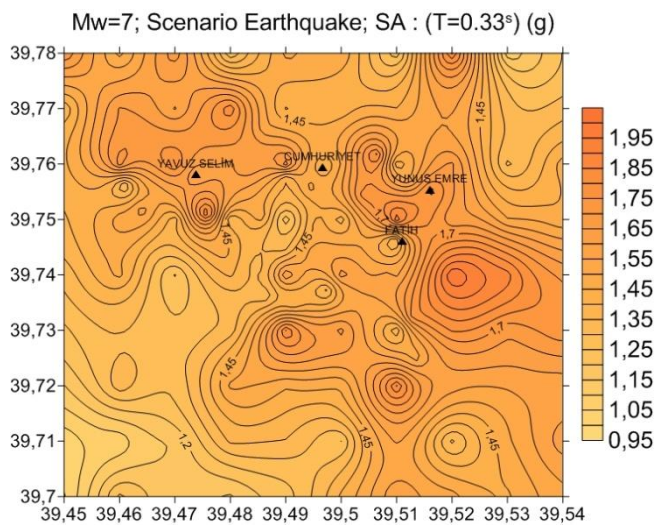
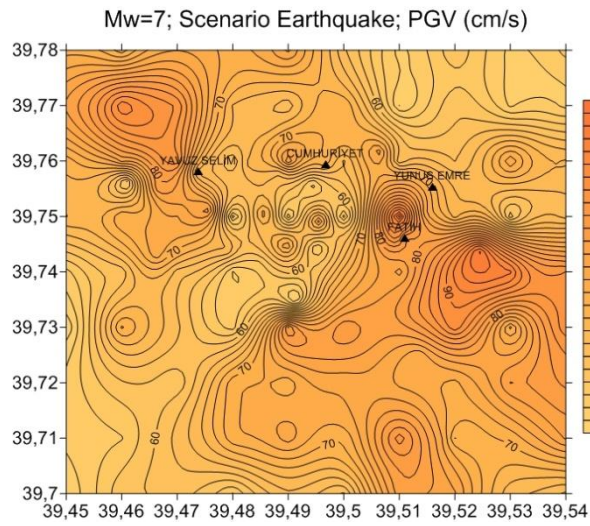
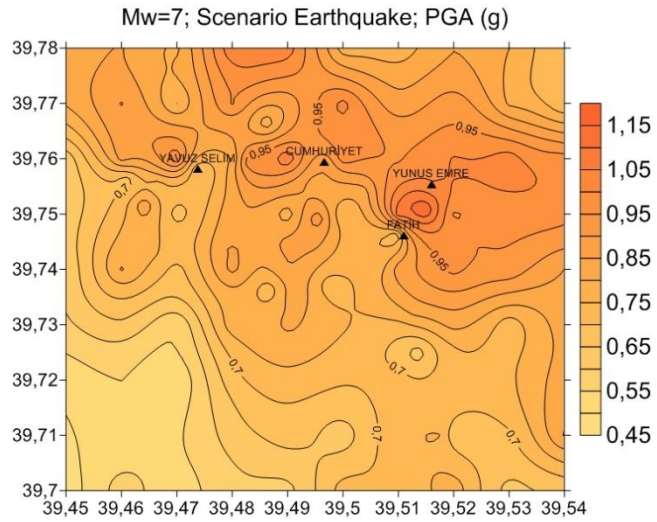


Figure 5.4 Continued

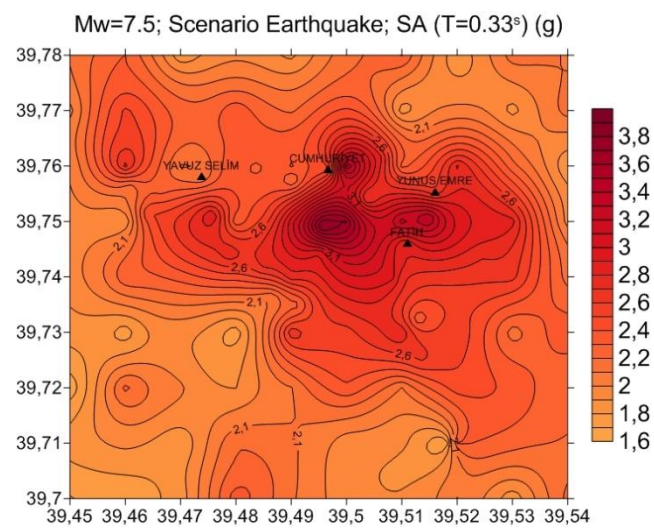
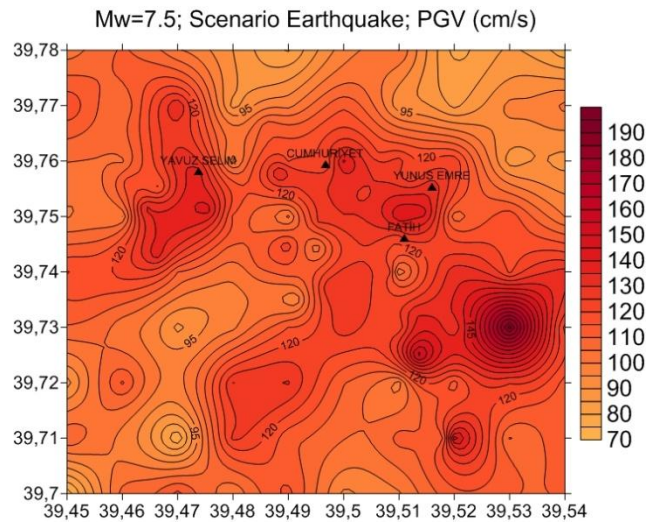
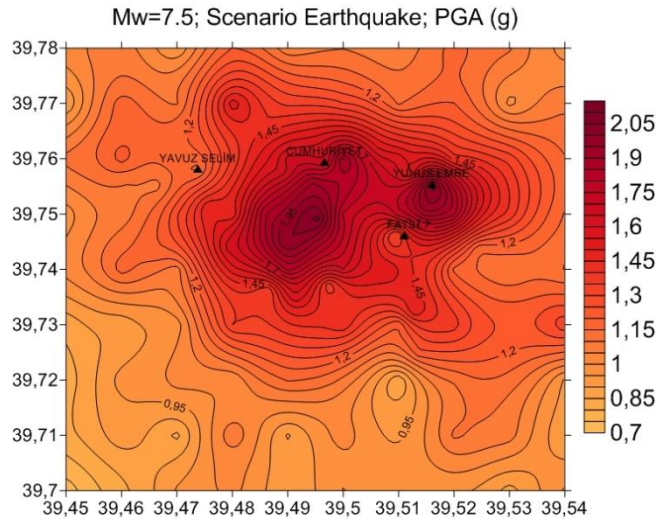


Figure 5.4 Continued

Information on location of the district centers, hypocentral and fault distances are listed in Table 5.1. It must be noted that Fatih and Yavuz Sultan Selim districts have soft soil conditions (NEHRP D) whereas Yunus Emre and Cumhuriyet districts are located on stiff soil conditions (NEHRP C). However, as mentioned previously the entire city center is on deep soil deposits of Erzincan basin.

Table 5.1 Information regarding the scenario earthquakes

District	Scenario	Latitude	Longitude	Fault Disp. (km)	Hypo Disp. (km)
Cumhuriyet	Erz 1992	39.76	39.50	4.34	14.42
Yunus Emre	Erz 1992	39.76	39.52	3.83	13.19
Fatih	Erz 1992	39.75	39.51	4.80	13.35
Yavuz Sultan Selim	Erz 1992	39.76	39.47	5.48	15.88
Cumhuriyet	Mw=5.00	39.76	39.50	14.17	16.17
Yunus Emre	Mw=5.00	39.76	39.52	12.72	14.75
Fatih	Mw=5.00	39.75	39.51	12.78	14.78
Yavuz Sultan Selim	Mw=5.00	39.76	39.47	15.77	17.70
Cumhuriyet	Mw=5.50	39.76	39.50	13.47	16.59
Yunus Emre	Mw=5.50	39.76	39.52	11.90	15.09
Fatih	Mw=5.50	39.75	39.51	12.17	15.26
Yavuz Sultan Selim	Mw=5.50	39.76	39.47	15.26	18.28
Cumhuriyet	Mw=6.00	39.76	39.50	9.10	15.10
Yunus Emre	Mw=6.00	39.76	39.52	7.47	13.61
Fatih	Mw=6.00	39.75	39.51	7.93	13.78
Yavuz Sultan Selim	Mw=6.00	39.76	39.47	11.01	16.78
Cumhuriyet	Mw=6.50	39.76	39.50	4.34	12.91
Yunus Emre	Mw=6.50	39.76	39.52	3.83	11.52
Fatih	Mw=6.50	39.75	39.51	4.80	11.70
Yavuz Sultan Selim	Mw=6.50	39.76	39.47	5.48	14.53
Cumhuriyet	Mw=7.00	39.76	39.50	1.05	14.86
Yunus Emre	Mw=7.00	39.76	39.52	1.04	13.57
Fatih	Mw=7.00	39.75	39.51	1.29	13.41
Yavuz Sultan Selim	Mw=7.00	39.76	39.47	1.85	16.20
Cumhuriyet	Mw=7.50	39.76	39.50	0.92	23.22
Yunus Emre	Mw=7.50	39.76	39.52	1.50	21.82
Fatih	Mw=7.50	39.75	39.51	0.41	21.55
Yavuz Sultan Selim	Mw=7.50	39.76	39.47	0.32	24.59

5.3 Equivalent SDOF Analyses to Estimate Seismic Damage in Selected Districts

This section of the thesis includes the equivalent SDOF analyses carried out in order to estimate the seismic damage in residential buildings in four selected districts of the Erzinan city. First, general information is provided about the building stock characteristics of the selected districts. Then, the dynamic analyses on SDOF systems, which represent the existing construction types in these districts, are carried out and the results are obtained in terms of displacement. The next step is to define the limit state definitions for the considered construction types and compare displacement demands with the corresponding displacement limit states to monitor the extent of damage predicted for the previously defined sub-classes of buildings.

5.3.1 General Characteristics of the Building Stock in the Selected Districts

As mentioned previously, four districts in Erzinan city have been selected in this study. This section focuses on the building stock characteristics of the considered districts and the building sub-classes that exist in these districts. The following information had been gathered through field surveys in Erzinan in the context of the research project with grant number TUJJB-UDP-01-12.

Cumhuriyet district is close to the urban center of Erzinan city. Most of the existing structures are old residential buildings. Approximately 80% of the building stock in this district is composed of one or two story unreinforced masonry buildings and the rest is three or four story (very few) RC frame buildings. Most of these buildings do not seem to be earthquake resistant due to structural deficiencies that they possess. Accordingly, it is assumed that the building stock in this district contains building sub-classes RF1B (N=2, 3), RF2B (N=4), RF1C (N=2, 3), RF2C (N=4), MU1B, MU2B, MU1C and MU2C. The parameter N in the parenthesis stands for the number of stories considered in the given building sub-class.

Fatih district resides in the south of the city. It is relatively far from the fault line when compared to other districts. During the field survey it had been observed that most of the structures in this district (80-85%) are single story residential masonry buildings. There also exist recently constructed four or five story RC frame and dual buildings. These buildings seem to be constructed according to the current seismic

regulations although they possess some minor structural deficiencies. Accordingly, it is assumed that the building stock in this district contains building sub-classes RF2A (N=4, 5), RF2B (N=4, 5), RH2A (N=4, 5), RH2B (N=4, 5), MU1A, MU1B and MU2B.

Yavuz Sultan Selim district is located in the western part of the city, in which nearly all the buildings (~90-95%) are used for residential purposes. The field survey results reveal that nearly 70% of the building stock is composed of RC buildings of all types and the remaining 30% belongs to one or two story old masonry buildings. This is due to the fact that the city is expanding towards west with new constructions. The recently constructed RC frame and dual buildings seem to comply with the current seismic regulations in general. There are also shelter houses that had been built after the 1992 Erzincan earthquake. These are four or five story RC shearwall (tunnel form) buildings. The old masonry buildings seem to be vulnerable to seismic action due to their structural deficiencies. Accordingly, it is assumed that the building stock in this district contains building sub-classes RF1A (N=2, 3), RF2A (N=4), RF1B (N=2, 3), RF2B (N=4), RW2A (N=4, 5), RH2A (N=4, 5), RH2B (N=4, 5), MU1B, MU1C and MU2B.

Yunus Emre district is located in the eastern part of the city, which is closest to the fault line among the selected districts. During the field survey it had been observed that the building stock is a mixture of old and new residential buildings of different types that comply or do not comply with earthquake resistant design principles. Most of the buildings (~75-80%) are four or five story RC frame or tunnel-form structures and the rest are two or three story masonry structures. Accordingly, it is assumed that the building stock in this district contains building sub-classes RF1A (N=3), RF2A (N=4, 5), RF1B (N=3), RF2B (N=4, 5), RF1C (N=3), RF2C (N=4, 5), RW1A (N=3), RW2A (N=4), MU2A, MU2B, MU2C and MU3B.

5.3.2 Dynamic Response Obtained from SDOF Analyses for the Selected Districts

The displacement responses of the SDOF systems that represent the building sub-classes in different districts are obtained through dynamic analyses by using the seven synthetic ground motion records generated for this study. The results are presented in Tables 5.2-5.5 for each district separately. In the tables, the first six columns of output data represent the SDOF displacement obtained from the scenario earthquakes with uniformly increasing magnitudes from $M=5.0$ to $M=7.5$ with $\Delta M=0.5$. The last column stands for the displacement results obtained from the simulation of the 1992 Erzincan earthquake with a magnitude $M=6.6$. Based on the SDOF analyses results, the following observations can be stated:

- There is a consistent increase in SDOF displacements as the magnitudes of the scenario earthquakes vary from $M=5.0$ to $M=7.5$. Especially for $M \geq 6.5$, the displacement values for most of the building sub-classes begin to increase drastically. For the scenario earthquake $M=7.5$, the displacements reach very high values as expected.

Table 5.2 SDOF displacement demand (in cm) for building sub-classes in Cumhuriyet district

Building Type	M=5.00	M=5.50	M=6.00	M=6.50	M=7.00	M=7.50	ERZ
RF1B (N=2)	0.099	0.486	0.716	2.458	5.436	5.436	5.436
RF1B (N=3)	0.453	0.967	1.675	3.560	12.230	12.230	7.558
RF2B (N=4)	0.587	0.466	1.861	5.202	16.564	16.564	8.465
RF1C (N=2)	0.099	0.345	0.432	2.928	2.928	2.928	2.928
RF1C (N=3)	0.453	1.214	1.184	6.589	6.589	6.589	6.589
RF2C (N=4)	0.586	0.466	2.181	7.067	8.900	8.900	8.900
MU1B	0.004	0.014	0.031	0.085	0.384	0.384	0.384
MU2B	0.019	0.095	0.212	0.878	0.878	0.878	0.878
MU1C	0.007	0.013	0.060	0.149	0.378	0.378	0.378
MU2C	0.076	0.136	0.572	0.863	0.863	0.863	0.863

- The SDOF displacements for RC frame and dual buildings seem to be significantly higher than that of RC tunnel-form and masonry buildings. This

is expected due to the flexibility of the former and rigidity of the latter building groups, respectively.

Table 5.3 SDOF displacement demand (in cm) for building sub-classes in Fatih district

Building Type	M=5.00	M=5.50	M=6.00	M=6.50	M=7.00	M=7.50	ERZ
RF2A (N=4)	0.928	1.545	2.794	6.549	20.156	12.873	13.411
RF2A (N=5)	1.009	1.133	3.874	6.816	26.831	26.492	11.781
RF2B (N=4)	0.928	1.534	2.468	7.356	16.564	16.564	16.564
RF2B (N=5)	1.009	1.133	2.932	7.672	25.881	25.881	13.575
RH2A (N=4)	0.284	0.754	1.159	3.798	9.858	9.858	6.408
RH2A (N=5)	0.511	1.700	3.229	4.825	15.633	9.801	8.709
RH2B (N=4)	0.284	0.803	1.110	5.630	5.630	5.630	5.630
RH2B (N=5)	0.511	1.855	2.594	5.479	13.277	13.277	13.277
MU1A	0.003	0.010	0.018	0.038	0.123	0.632	0.059
MU1B	0.006	0.010	0.045	0.383	0.383	0.383	0.383
MU2B	0.039	0.057	0.158	0.917	0.917	0.917	0.917

- Since building sub-classes RF2B (N=4) and MU2B exist in all the districts, they are used to compare the spatial variability of SDOF displacements. Accordingly, it is observed that the displacement values of the considered building sub-classes in all districts are close to each other whereas the ones in Fatih district yield slightly higher values.
- The increase in displacement values with number of stories can be clearly observed for the RC frame and masonry building sub-classes.
- The displacement values for RC dual buildings seem to be overestimated since these structures possess shear walls with the aim of limiting their displacement demands. But it should be noted that it is a difficult task to simulate the seismic response of this building type for two reasons. First shear wall ratio is an important parameter for this building type which has not been reflected in the basic parameters of the SDOF model. Second, more building data is required to make a reliable estimate of SDOF parameters for RC dual buildings.

Table 5.4 SDOF displacement demand (in cm) for building sub-classes in Yavuz Sultan Selim district

Building Type	M=5.00	M=5.50	M=6.00	M=6.50	M=7.00	M=7.50	ERZ
RF1A (N=2)	0.251	0.378	2.400	2.075	9.195	9.195	3.164
RF1A (N=3)	0.207	0.692	0.887	3.090	13.675	15.431	5.902
RF2A (N=4)	0.474	1.280	2.238	3.614	14.595	26.380	4.023
RF1B (N=2)	0.251	0.378	1.041	2.811	5.436	5.436	5.436
RF1B (N=3)	0.207	0.692	0.887	3.140	7.168	12.230	12.230
RF2B (N=4)	0.474	1.280	2.526	4.656	16.564	16.564	9.855
RW2A (N=4)	0.024	0.083	0.192	0.276	1.410	1.410	1.410
RW2A (N=5)	0.098	0.117	0.287	0.806	2.620	2.620	2.620
RH2A (N=4)	0.220	0.396	1.236	2.299	9.858	9.858	4.153
RH2A (N=5)	0.396	1.233	1.469	2.939	13.838	19.564	3.348
RH2B (N=4)	0.220	0.396	1.028	2.591	6.089	6.089	6.089
RH2B (N=5)	0.396	1.233	1.469	3.486	14.361	14.361	7.057
MU1B	0.006	0.010	0.022	0.384	0.384	0.384	0.384
MU1C	0.010	0.023	0.052	0.378	0.378	0.378	0.378
MU2B	0.024	0.083	0.156	0.878	0.878	0.878	0.878

Table 5.5 SDOF displacement demand (in cm) for building sub-classes in Yunus Emre district

Building Type	M=5.00	M=5.50	M=6.00	M=6.50	M=7.00	M=7.50	ERZ
RF1A (N=3)	0.211	0.529	1.930	3.030	11.853	8.563	8.976
RF2A (N=4)	0.761	1.021	2.752	4.543	13.612	10.213	9.193
RF2A (N=5)	0.939	1.431	5.144	6.485	13.800	13.760	9.039
RF1B (N=3)	0.211	0.529	1.832	4.132	12.230	12.230	8.898
RF2B (N=4)	0.761	1.021	2.650	5.696	16.564	16.564	9.666
RF2B (N=5)	0.939	1.431	4.827	10.259	15.930	25.881	9.656
RF1C (N=3)	0.211	0.529	2.593	6.589	6.589	6.589	6.589
RF2C (N=4)	0.761	1.022	2.538	8.900	8.900	8.900	8.900
RF2C (N=5)	0.939	1.431	2.791	13.907	13.907	13.907	13.907
RW1A (N=3)	0.018	0.032	0.137	0.248	0.352	1.490	0.210
RW2A (N=4)	0.037	0.066	0.148	0.273	1.409	1.409	1.409
MU2A	0.021	0.074	0.101	0.259	1.079	1.079	1.079
MU2B	0.037	0.066	0.232	0.878	0.878	0.878	0.878
MU2C	0.078	0.092	0.863	0.863	0.863	0.863	0.863
MU3B	0.068	0.289	0.612	1.280	1.280	1.280	1.280

- Low-rise and mid-rise RC frame buildings that have been designed according to seismic code regulations (i.e. RF1A and RF2A) are observed to experience heavy damage and collapse when subjected to the scenario earthquakes with magnitudes $M=7.0$ and 7.5 . This seems to be contradicting with the main philosophy of earthquake resistant design and behaviour. There may be two reasons for that. First, seismic damage is overestimated since the proposed approach contains many gross assumptions, therefore some conservatism is expected. Second, the considered districts are very close to the fault line and the ground motions generated can impose very high seismic demands on the building structures with significant near-field effects. Such effects can be more pronounced on flexible RC frame buildings.
- Finally, it must be noted that all of the districts are located on deep soil deposits in Erzincan basin which amplify the ground motions causing larger displacements.

5.4 Limit States Defined for the Building Sub-classes

In order to estimate earthquake damage, seismic demand should be compared with seismic capacity. This is generally accomplished by using a pre-defined set of performance levels, called as limit states. Estimation of the limit state values in seismic damage analyses has a paramount importance in order to make reliable estimates. This can only be achieved by considering the local characteristics of structural systems under consideration.

In this section, the definition of limit states for all building classes is discussed by making use of the findings in this study, previous studies in the literature and also engineering judgment. The limit states are presented in terms of displacement (of SDOF systems) in order to make direct comparison with the displacement values obtained through dynamic analyses. Three limit states, therefore four damage states are considered in this study. The abbreviations and definitions of damage states used in this study are given in Table 5.6. The first limit state (i.e. LS-1) is the threshold between DS-1 and DS-2. The second limit state (LS-2) is between DS-2 and DS-3 whereas the ultimate limit state (LS-3) is between DS-3 and DS-4.

For RC frame buildings, it is appropriate to use the limit state values proposed in Erberik (2008) since they had been obtained by considering the local characteristics of low-rise and mid-rise RC frame structures in Turkey. Hence limit state values in terms of SDOF displacement are determined for sub-classes RF1(A-B-C) and RF2(A-B-C) separately as shown in Table 5.7 since these two classes define low-rise and mid-rise constructions, respectively, similar to the definitions used in Erberik (2008).

For RC tunnel-form buildings, the study of Balkaya and Kalkan (2004) can be used for the determination of limit states of this building type since these researchers had worked extensively on the tunnel form RC buildings, which are the ones that exist in Yavuz Sultan Selim and Yunus Emre districts of Erzincan city as shelter houses constructed after the 1992 earthquake. The limit state values are provided in Table 5.7.

For RC dual buildings, the pushover curves obtained by Karaca (2014) can assist in the determination of limit states together with the study of Kappos and Panagopoulos (2009) that had focused on the fragility curve generation of RC buildings in Greece. It should be stated that since the lateral drift of a dual structure also depends on the ratio of shear wall area to floor area, it is not an easy task to obtain representative values for the building sub-classes considered. The proposed values for building sub-classes RH1(A-B) and RH2(A-B) are presented in Table 5.7.

In general, masonry buildings in Turkey are rigid and brittle structures with major deficiencies that impair their displacement capacity. Hence the limit states for this structural type are expected to be lower than the ones that belong to other types. To determine the limit states of masonry buildings in this study, the main source is the results obtained from the pushover curves of 72 generic building models analyzed by the computer program MAS. In addition, the study by Calvi (1999) and Moyuiannou et al. (2014) can be used for the determination of limit states for unreinforced masonry buildings. Considering all the available information, the proposed values for building sub-classes MU1(A-B-C), MU2(A-B-C) and MU3(A-B-C) are presented in Table 5.7.

Table 5.6 The abbreviations and definitions of damage states

Abbreviation	Damage State	Definition
DS1	None/Slight	Not damaged or slightly damaged, usable building (either immediately or after minor repair)
DS2	Moderate	Moderately damaged but repairable building (and can be used after repair)
DS3	Extensive	Extensively damaged, the decision of repair vs. demolition depends on the type and distribution of damage
DS4	Heavy/Collapse	Severely damaged building that should be demolished or partially/completely collapsed building

Table 5.7 Limit states of building sub-classes in terms of SDOF displacement (cm)

Building sub-class	LS-1	LS-2	LS-3
RF1(A-B-C)	1.25	4.7	9.0
RF2(A-B-C)	1.85	7.5	13.0
RW(1-2)A	0.4	1.0	2.0
RH1(A-B)	0.9	3.0	5.0
RH2(A-B)	1.0	3.5	6.5
MU1(A-B-C)	0.15	0.4	0.8
MU2(A-B-C)	0.2	0.45	0.9
MU3(A-B-C)	0.2	0.5	1.0

5.5 Estimated Damage States for Existing Building Sub-classes in the Selected Districts

When the results of the dynamic analyses that represent SDOF displacement demand is compared with the limit states that represent displacement capacity, the damage states can be predicted for all building sub-classes in the selected districts as presented in Tables 5.8-5.11. Based on the damage estimation results, the following conclusions can be drawn:

Table 5.8 Estimated damage states for building sub-classes in Cumhuriyet district

Building Type	M=5.00	M=5.50	M=6.00	M=6.50	M=7.00	M=7.50	ERZ
RF1B (N=2)	DS-1	DS-1	DS-1	DS-2	DS-3	DS-3	DS-3
RF1B (N=3)	DS-1	DS-1	DS-2	DS-2	DS-4	DS-4	DS-3
RF2B (N=4)	DS-1	DS-1	DS-2	DS-2	DS-4	DS-4	DS-3
RF1C (N=2)	DS-1	DS-1	DS-1	DS-2	DS-2	DS-2	DS-2
RF1C (N=3)	DS-1	DS-1	DS-1	DS-3	DS-3	DS-3	DS-3
RF2C (N=4)	DS-1	DS-1	DS-2	DS-2	DS-3	DS-3	DS-3
MU1B	DS-1	DS-1	DS-1	DS-1	DS-2	DS-2	DS-2
MU2B	DS-1	DS-1	DS-2	DS-3	DS-3	DS-3	DS-3
MU1C	DS-1	DS-1	DS-1	DS-1	DS-2	DS-2	DS-2
MU2C	DS-1	DS-1	DS-3	DS-4	DS-4	DS-4	DS-4

Table 5.9 Estimated damage states for for building sub-classes in Fatih district

Building Type	M=5.00	M=5.50	M=6.00	M=6.50	M=7.00	M=7.50	ERZ
RF2A (N=4)	DS-1	DS-1	DS-2	DS-2	DS-4	DS-3	DS-4
RF2A (N=5)	DS-1	DS-1	DS-2	DS-2	DS-4	DS-4	DS-3
RF2B (N=4)	DS-1	DS-1	DS-2	DS-2	DS-4	DS-4	DS-4
RF2B (N=5)	DS-1	DS-1	DS-2	DS-3	DS-4	DS-4	DS-4
RH2A (N=4)	DS-1	DS-1	DS-2	DS-3	DS-4	DS-4	DS-3
RH2A (N=5)	DS-1	DS-2	DS-2	DS-3	DS-4	DS-4	DS-4
RH2B (N=4)	DS-1	DS-1	DS-2	DS-3	DS-3	DS-3	DS-3
RH2B (N=5)	DS-1	DS-2	DS-2	DS-3	DS-4	DS-4	DS-4
MU1A	DS-1	DS-1	DS-1	DS-1	DS-1	DS-3	DS-1
MU1B	DS-1	DS-1	DS-1	DS-2	DS-2	DS-2	DS-2
MU2B	DS-1	DS-1	DS-2	DS-4	DS-4	DS-4	DS-4

- For scenario earthquakes with M=5.0 and M=5.5, nearly all the building sub-classes seem to experience none-to-slight damage (i.e. DS-1) with few exceptions. As the magnitude of the scenario earthquake becomes M=6.0, the governing damage state for the building sub-classes becomes moderate damage (i.e. DS-2). For larger magnitudes, especially for M=7.5, most of the building sub-classes seem to experience heavy damage or collapse in the selected districts.

- RC frame buildings begin to conceive significant damage for magnitudes $M \geq 6.5$ regardless of their number of stories and the level of compliances with seismic design principles. Some reasons for this discrepancy were stated in the above discussions in Section 5.3.2. This may also be due to the fact that the limit state definitions have been selected as the same for sub-types A, B, and C, hence displacement capacity is assumed to be independent of the level of compliance with the seismic code.

Table 5.10 Estimated damage states for building sub-classes in Yavuz Sultan Selim district

Building Type	M=5.00	M=5.50	M=6.00	M=6.50	M=7.00	M=7.50	ERZ
RF1A (N=2)	DS-1	DS-1	DS-2	DS-2	DS-4	DS-4	DS-2
RF1A (N=3)	DS-1	DS-1	DS-1	DS-2	DS-4	DS-4	DS-3
RF2A (N=4)	DS-1	DS-1	DS-2	DS-2	DS-4	DS-4	DS-2
RF1B (N=2)	DS-1	DS-1	DS-1	DS-2	DS-3	DS-3	DS-3
RF1B (N=3)	DS-1	DS-1	DS-1	DS-2	DS-3	DS-4	DS-4
RF2B (N=4)	DS-1	DS-1	DS-2	DS-2	DS-4	DS-4	DS-3
RW2A (N=4)	DS-1	DS-1	DS-1	DS-1	DS-3	DS-3	DS-3
RW2A (N=5)	DS-1	DS-1	DS-1	DS-2	DS-4	DS-4	DS-4
RH2A (N=4)	DS-1	DS-1	DS-2	DS-2	DS-4	DS-4	DS-3
RH2A (N=5)	DS-1	DS-2	DS-2	DS-2	DS-4	DS-4	DS-2
RH2B (N=4)	DS-1	DS-1	DS-2	DS-2	DS-3	DS-3	DS-3
RH2B (N=5)	DS-1	DS-2	DS-2	DS-2	DS-4	DS-4	DS-4
MU1B	DS-1	DS-1	DS-1	DS-2	DS-2	DS-2	DS-2
MU1C	DS-1	DS-1	DS-1	DS-2	DS-2	DS-2	DS-2
MU2B	DS-1	DS-1	DS-1	DS-3	DS-3	DS-3	DS-3

- The seismic performances of RC dual buildings seem to be similar to that of RC frame buildings. This is a contradiction as shear walls are constructed to attract the earthquake forces and limit the displacements and therefore the damage in this building type. Hence seismic damage of RC dual buildings are overestimated just like their SDOF displacements as mentioned above in Section 5.3.2. The reasons for such an inconsistent behaviour have already been mentioned in the same part of the above discussion.

Table 5.11 Estimated damage states for building sub-classes in Yunus Emre district

Building Type	M=5.00	M=5.50	M=6.00	M=6.50	M=7.00	M=7.50	ERZ
RF1A (N=3)	DS-1	DS-1	DS-2	DS-2	DS-4	DS-3	DS-3
RF2A (N=4)	DS-1	DS-1	DS-2	DS-2	DS-4	DS-3	DS-3
RF2A (N=5)	DS-1	DS-1	DS-2	DS-2	DS-4	DS-4	DS-3
RF1B (N=3)	DS-1	DS-1	DS-2	DS-2	DS-4	DS-4	DS-3
RF2B (N=4)	DS-1	DS-1	DS-2	DS-2	DS-4	DS-4	DS-3
RF2B (N=5)	DS-1	DS-1	DS-2	DS-3	DS-4	DS-4	DS-3
RF1C (N=3)	DS-1	DS-1	DS-2	DS-3	DS-3	DS-3	DS-3
RF2C (N=4)	DS-1	DS-1	DS-2	DS-3	DS-3	DS-3	DS-3
RF2C (N=5)	DS-1	DS-1	DS-2	DS-4	DS-4	DS-4	DS-4
RW1A (N=3)	DS-1	DS-1	DS-1	DS-1	DS-1	DS-3	DS-1
RW2A (N=4)	DS-1	DS-1	DS-1	DS-1	DS-3	DS-3	DS-3
MU2A	DS-1	DS-1	DS-1	DS-2	DS-4	DS-4	DS-4
MU2B	DS-1	DS-1	DS-2	DS-3	DS-3	DS-3	DS-3
MU2C	DS-1	DS-1	DS-3	DS-3	DS-3	DS-3	DS-3
MU3B	DS-1	DS-2	DS-3	DS-4	DS-4	DS-4	DS-4

- RC tunnel-form buildings do not seem to experience severe damage up to earthquake magnitudes $M=6.5$. For larger magnitudes they seem to have extensive damage. This result seems to be controversial since theoretically high code RC tunnel buildings should not conceive any serious damage at all. However it should be noted that there exist insufficient information regarding the seismic behaviour of tunnel form buildings obtained from a single source, which is a serious drawback. Second, the damage estimation is based on a single dynamic analysis, the result of which is compared to a specific limit state to estimate the damage state of that building type. Actually, the variation in demand and capacity should be considered to obtain more realistic results. Furthermore, this discrepancy can also be due to the huge damaging potential of the scenario earthquakes $M=7.0$ and $M=7.5$.
- Seismic damage of masonry buildings seems to be highly affected by the number of stories. The seismic performance of single story buildings is generally better than that of two or three story masonry buildings as expected. To a lesser extent, the compliance with the modern seismic code principles is also observed to be affecting the seismic performance of masonry buildings.

This is in accordance with the general observations regarding structural behaviour of Turkish masonry buildings.

5.6 Comparison of Estimated and Observed Damage for the 1992 Erzincan Earthquake

A destructive earthquake of magnitude $M=6.6$ struck Erzincan city in 1992, resulting in 497 fatalities and people more than 2000 injuries as declared officially. It was stated that the earthquake caused the collapse of 3200 residential dwellings whereas more than 12,000 dwellings experienced moderate or extensive damage (Sucuoğlu and Tokyay 1992). Based on the field reconnaissance by the technical teams after the earthquake, the observed damage distributions in the districts that are considered in this study are presented in Table 5.12. Accordingly, overall observed damage seems to be much more severe in districts Fatih and Yavuz Sultan Selim. In the other two districts (Cumhuriyet and Yunus Emre), slight and moderate damage states seem to govern the overall damage distribution.

Table 5.12 Observed damage distribution in the selected districts during the 1992 Erzincan earthquake

District Name	Total no of dwellings	Slight damage	Moderate damage	Extensive damage	Heavy Damage
Cumhuriyet	3500	3327	144	25	4
Fatih	1415	509	97	456	353
Yavuz Sultan Selim	1512	295	250	571	396
Yunus Emre	1500	826	568	94	12

It is not possible to make a one-to-one-comparison of observed and estimated damage distributions in these districts for some reasons. First, the estimated damage information provided in Tables 5.8-5.11 is presented in terms of building type whereas the observed damage distribution gives only the number of damage dwellings regardless of the construction type. Second, the field survey in Erzincan city was conducted in 2013, approximately 21 years after the earthquake. Hence it is obvious that the building stock characteristics had changed drastically and it is not possible to make a reliable comparison unless the building stock characteristics just

before the 1992 earthquake were known. However, a crude comparison in terms of order of magnitude of damage can be achieved. Accordingly, districts Fatih and Yunus Emre seems to be more vulnerable to seismic action as obtained from analyses whereas districts Fatih and Yavuz Sultan Selim seem to be the critical ones in the case of observed damage most probably due to softer soil conditions. Hence Fatih district can be selected for the purpose of comparing estimated and observed damage distributions. In Fatih district, damage estimation results show that mid-rise RC frame buildings and two story masonry buildings experienced heavy damage and collapsed during the 1992 earthquake. In the reconnaissance report (Sucuoglu and Tokyay 1992) it was stated that four and five story RC frame buildings in Erzincan were severely damaged in general, which is consistent with the estimated results. In the same report, it was also stated that non-engineered masonry buildings which violate seismic design principles, experienced significant damage whereas well constructed masonry buildings showed good structural performance in the earthquake. This observation can also be accepted to be in accordance with the estimated results in Fatih district (i.e. slight damage for MU1A, moderate damage for MU1B and heavy damage/collapse in MU2B).

CHAPTER 6

SUMMARY AND CONCLUSIONS

6.1 Summary

This study is focused on the regional seismic damage estimation of residential buildings in Turkey by proposing an approach. In this approach, some structural information collected from residential buildings through street surveys can be used to estimate seismic damage of the considered buildings under specified earthquake scenarios. This basic structural information includes type of construction, number of stories, materials used in the construction and apparent status of the building (i.e. structural deficiencies if any, level of conformity with earthquake design principles as evaluated from the street, etc.). Then this information can be used to classify the buildings under consideration and to adopt simple SDOF models to each building class based on the basic data obtained through street survey. Finally, dynamic analyses conducted on these SDOF models can provide a global estimation of seismic damage distribution in the region of interest. This information, although not precise, is valuable for both pre-earthquake and post-earthquake strategies to mitigate earthquake losses and to exhibit a rapid reaction to the earthquake disaster.

The study is limited to the damage assessment of residential buildings. Different construction types are considered in this study: reinforced concrete frame, reinforced concrete tunnel-form, reinforced concrete dual and unreinforced masonry buildings. Building sub-classes are formed in terms of the construction type, number of stories and the level of conformity with earthquake resistant design. A SDOF model is employed to simulate the global seismic response of each building sub-class. Major SDOF parameters required to construct the model are period, strength ratio and

ductility. There also exist some secondary model parameters for post-yield slope, post-capping slope, stiffness degradation and strength degradation. These model parameters are obtained by making use of the existing building databases as in the case of reinforced concrete frame buildings in this study. In the absence of such building databases, the building data is generated by analytical approach as in the case of unreinforced masonry buildings in this study. After the formation of the SDOF models for all building sub-classes, the next step is to carry out dynamic analysis to obtain the seismic response statistics of these building types. In this study, pre-defined limit states are assigned to each building sub-class, which is then used for comparison with seismic demand from dynamic analyses. This comparison gives the estimated damage state of the building sub-classes. In this study seismic demand and capacity are obtained in terms of SDOF displacement and the comparison is carried out on this basis. Finally, the seismic damage distribution of the residential building stock in a region can be obtained without requiring detailed structural information about different structural types within the stock. It is important to note that this will be a crude estimation of the damage distribution of the region, which can be used to develop pre-earthquake mitigation plans or post-earthquake rescue plans.

In this study, the proposed approach is implemented to Erzincan city, which is located in a very active seismic region and experienced devastating earthquakes in the past. Four districts are selected from the city and the building stock characteristics of these districts are obtained. The readily available SDOF models are assigned to the existing construction types in these districts. As a parametric study, scenario earthquakes with different magnitudes are generated together with the actual 1992 earthquake. SDOF displacements for different building types are obtained for the scenario earthquakes in the selected districts. Then by considering the pre-defined limit states, the damage states of the building types are estimated. The results show that for scenario earthquakes with small magnitudes (i.e. $M=5.0, 5.5$), nearly all the building sub-classes seem to experience none-to-slight damage whereas for larger magnitudes, especially for $M=7.5$, most of the building sub-classes seem to experience heavy damage or collapse in the selected districts. There exist some discrepancies in the results but a crude comparison of the estimated damage with the

observed damage during the 1992 earthquake encourages the use of the proposed approach.

6.2 Conclusions

Based on the limitations, assumptions and the existing building information used in this study, the following conclusions are considered:

- The study proposes an approach for the seismic damage estimation of residential building stocks by making use of basic structural information obtained from street survey. The use of the approach seems to be encouraged by the comparison of the estimated and observed damage in four different districts of the Erzincan city.
- According to the results, reinforced concrete frame and dual buildings seem to conceive the most severe damage regardless of the number of stories and level of conformity to the seismic code among all the building types considered. This may be due to the fact that soft soil conditions exist in all of the selected districts with the potential of amplifying the ground shaking and adversely affecting flexible structures rather than rigid structures. The results are in accordance with the field observations after the 1992 earthquake.
- Reinforced concrete tunnel-form buildings and engineered (high-code) masonry buildings, which can be regarded as rigid structures, exhibit a better performance when compared to the former building types. These results confirm the above discussion.
- Seismic damage in masonry buildings seem to be more related to the number of stories and code conformity. For instance non-engineered three story masonry buildings experience heavy damage in large magnitude earthquakes whereas engineered single story masonry buildings conceived slight-to moderate damage in the same scenario earthquakes. The results are in accordance with the field observations after the 1992 earthquake.
- The closest distance of the district centers from the fault line is not a parameter that affects the results since all the districts can be considered as being very close to the fault line. Soft site conditions exist in all the districts with relatively weaker soil conditions in Fatih and Yavuz Sultan Selim

districts. This may be the reason of observed and estimated severe damage distribution in Fatih district.

- Overall, it should be stated that estimation of seismic damage in Erzincan city is an interesting case study in the sense that the fault line is very close to the populated city center (only a few kilometers) and the fault system have the potential to generate very large earthquakes as it had done in the past during 1939 and 1992 events. Eventually the synthetic ground motion records generated from this fault system has very high damaging potential on the built environment. Furthermore, the generated ground motions are further amplified due to soft site conditions. Hence this can be one of the reasons of unexpected and overestimated results, especially for relatively flexible building sub-classes.
- Simulated ground motions are accurate only up to a certain level since every ground motion simulation algorithm has its own modelling assumptions. In this thesis, stochastically-simulated motions are employed. In the future, alternative methods could be used and the seismic demands could be compared for closer estimate of the potential seismic damages.
- Based on the above discussion, it can be concluded that the city of Erzincan is under high risk with many vulnerable building types. Some precautions should be taken before another major earthquake comes and hits to the city, causing the loss of many lives.
- The deterministic nature of the proposed approach is a drawback for reliable estimate of seismic damage. It is not very appropriate to judge the seismic performance of building types by using single dynamic analysis. In fact, the uncertainty in capacity should also be taken into account to generate a population of buildings in each sub-class within a probabilistic manner. Then the fragility curves for each building sub-class can be generated and used for the estimation of damage in a more reliable way.

REFERENCES

American Concrete Institute, ACI. (2002). ACI 318-02: Building Code Requirements for Structural Concrete. American Concrete Institute, Detroit.

American Society of Civil Engineers. ASCE. (2000). FEMA356. Prestandard and Commentary for the Seismic Rehabilitation of Buildings, Washington, DC.

Applied Technology Council (ATC), 1996, *Seismic Evaluation and Retrofit for Concrete Buildings*, ATC-40, Redwood City, California

Askan, A., Sisman, F.N. and Uğurhan, B. (2013). Stochastic strong ground motion simulations in sparsely-monitored regions: A validation and sensitivity study on the 13 March 1992 Erzincan (Turkey) earthquake. *Soil Dynamics and Earthquake Engineering*, 55:170-181

Askan, A. (2014). Erzincan’da olası deprem hasarlarının belirlenmesi, Project No TUJJB-UDP-01-12, Report No 4

ATC (1988a). “Rapid Visual Screening of Buildings for Potential Seismic Hazards: A Handbook”, Report ATC-21 (FEMA 154), Applied Technology Council, Redwood City, California, U.S.A.

ATC (1988b). “Rapid Visual Screening of Buildings for Potential Seismic Hazards: A Handbook”, Report ATC-21-1 (FEMA 155), Applied Technology Council, Redwood City, California, U.S.A.

ATC (2002). “Rapid Visual Screening of Buildings for Potential Seismic Hazards: A Handbook – Second Edition”, ATC-21 (FEMA 154), Applied Technology Council, Redwood City, California, U.S.A.

Ay, Ö. (2006). Fragility Based Assessment of Low-Rise and Mid-Rise Reinforced Concrete Frame Buildings In Turkey, *M.S. Thesis*, Middle East Technical University, Ankara.

Bal, I. E., Crowley, H. and Pinho, R. (2008). "Displacement-Based earthquake loss assessment of Turkish masonry structures." *14th World Conf. on Earthquake Engineering.*, Beijing, China.

Balkaya. C. and Kalkan. E. (2003). Estimation of Fundamental Periods of Shearwall Dominant Building Structures. *Earthquake Engineering and Structural Dynamics* 32:985-998.

Balkaya. C and Kalkan. E. (2004). Seismic vulnerability. behavior and design of tunnel form building structures. *Engineering Structures* 26:2081-2099.

Benedetti, D., Carydis, P. and Pezzoli, P. (1998). Shaking table tests on 24 simple masonry buildings. *Earthquake Engineering and Structural Dynamics* 27:67-90.

Calvi, G. M. (1999). A displacement based approach for vulnerability evaluation of -classes of buildings. *Journal of Earthquake Engineering* 3: 411-438.

Chopra, A.K. and Goel, R.K. (2000). Building Period Formulas for Estimating Seismic Displacements, *Earthquake Spectra* 16:2, 533–536.

Chopra, A. K. and Goel, R. K. (2002). A modal pushover analysis procedure for estimating seismic demands for buildings. *Earthquake Engineering and Structural Dynamics* 31:561-582.

Clough, R. W. and Johnston, S. B. (1966). "Effect of Stiffness Degradation on Earthquake Ductility Requirements", *Proceedings, Second Japan National Conference on Earthquake Engineering*: 227-232.

Costley, A. C. and Abrams, D. P. (1996). Dynamic response of unreinforced masonry buildings with flexible diaphragms. Report No: NCEER-96-0001, National Center for Earthquake Engineering Research, State University of New York at Buffalo, Buffalo, New York, USA.

Eurocode 8: Design provisions for earthquake resistance of structures, Part 1-2: General rules and rules for buildings - General rules for buildings. ENV 1998-1-2:1995 (CEN, Brussels, 1995).

Erberik, M. A. (2008). Fragility-based assessment of typical mid-rise and low-rise RC buildings in Turkey. *Engineering Structures* 30:1360-1373

Erberik, M. A. (2010). Seismic Risk Assessment of Masonry Buildings in Istanbul for Effective Risk Mitigation, *Earthquake Spectra* 26(4): 967–982.

Fajfar, P. and Fischinger, M. (1987). Nonlinear seismic analysis of RC buildings: implications of a case study. *European Earthquake Engineering* 1: 31-43.

Federal Emergency Management Agency, FEMA (1997). FEMA-273: NEHRP guidelines for the seismic rehabilitation of buildings, Washington DC.

Freeman, S. A., Nicoletti, J. P. and Tyrell, J. V. (1975). “Evaluations of Existing Buildings for Seismic Risk - A Case Study of Puget Sound Naval Shipyard, Bremerton, Washington”, *Proceedings of U.S. National Conference on Earthquake Engineering*, Berkeley, U.S.A.: 113-122.

Gulkan, P. and Sozen, M. (1974). Inelastic response of reinforced concrete structures to earthquake motions. *ACI Journal* 71: 604-610.

Günel, A. O. (2013). Influence of the Shearwall Area to Floor Area Ratio on the Seismic Performance of Existing Reinforced Concrete Buildings, *M.S. Thesis*, Middle East Technical University, Ankara.

Hassan, A.F. and Sozen, M.A. (1997). “Seismic Vulnerability Assessment of Low-Rise Buildings in Regions with Infrequent Earthquakes”, *ACI Structural Journal*, Vol. 94, No. 1, pp. 31-39.

Istanbul Metropolitan Municipality Construction Directorate Geotechnical and Earthquake Investigations Department (2003). *Earthquake Master Plan for Istanbul*, IMMCDGEID, Istanbul.

JBDPA (1990). “Standard for Seismic Capacity Assessment of Existing Reinforced Concrete Buildings”, Japanese Building Disaster Prevention Association, Ministry of Construction, Tokyo, Japan.

Jeong, S.H. and Elnashai, A.S. (2007). Probabilistic fragility analysis parameterized by fundamental response quantities, *Engineering Structures* 29: 1238–1251.

Kadas, K. (2006). Influence of Idealized Pushover Curves on Seismic Response, *M.S. Thesis*, Middle East Technical University, Ankara.

Kappos, A. J. and Panagopoulos, G. (2010). Fragility curves for reinforced concrete buildings in Greece. *Structure and Infrastructure Engineering* 6: 39-53.

Karaca, H. (2013). Estimation of Potential Earthquake Losses for the Evaluation of Earthquake Insurance Risks, *Ph.D. Thesis*, Middle East Technical University, Ankara.

Karbassi, A and Nollet, M. J. (2008). “Development of an index assignment procedure compatible with the regional seismicity in the province of Quebec for the rapid visual screening of existing buildings”. *Canadian Journal of Civil Engineering* 35: 925-937.

Mengi, Y., McNiven, H. D. and Tanrikulu, A. K. (1992). Models for nonlinear earthquake analysis of brick masonry buildings. Technical Report UCB-EERC 92/03, Earthquake Engineering and Research Center, University of California at Berkeley.

Metin, A. (2006). Inelastic Deformation Demands on Moment Resisting Frame Structures, *M.S. Thesis*, Middle East Technical University, Ankara.

Motazedian, D. and Atkinson, G. M. (2005). Stochastic finite-fault modeling based on a dynamic corner frequency. *Bulletin of the Seismological Society of America*, Vol. 95, 3:995-1010.

Mouyiannou, A., Rota, M., Penna, A. and Magenes, G. (2014). Identification of Suitable Limit States from Nonlinear Dynamic Analyses of Masonry Structures, *Journal of Earthquake Engineering* 18: 231–263.

NEHRP recommended provisions for the development of seismic regulations for new buildings. (1994). Building Seismic Safety Council, Washington, D. C.

NEHRP recommended provisions for seismic regulations for new buildings and other structures. (2003). Building Seismic Safety Council, Washington, D. C.

Otani, S. (1993). "Hysteresis Models for Earthquake Response Analysis", Annual Research Publications, Aoyama Laboratory, Department of Architecture, Faculty of Engineering, University of Tokyo.

Ozcebe, G., Yucemen. M. S. and Aydogan, V. (2004). Statistical Seismic Vulnerability Assessment of Existing Reinforced Concrete Buildings in Turkey on a Regional Scale, *Journal of Earthquake Engineering* 8(5): 749-773.

Ozdemir, P., Boduroglu, M. H. and Ilki, A. (2005). "Seismic Safety Screening Method", Proceedings of the International Workshop on Seismic Performance Assessment and Rehabilitation of Existing Buildings (SPEAR), Ispra, Italy, Paper No. 23.

Özün, A. (2007). Fragility Based Assessment of Low-Rise and Mid-Rise Reinforced Concrete Frame Buildings In Turkey Using Düzce Database, *M.S. Thesis*, Middle East Technical University, Ankara.

Park, Y. J., Reinhorn, A. M. and Kunnath, S. K. (1987). "IDARC: Inelastic Damage Analysis of Reinforced Concrete Frame – Shear Wall Structures", Technical Report NCEER-87-0008, State University of New York at Buffalo.

"Recommended lateral force requirements and commentary." (1996)

Roufaiel, M. S. L. and Meyer, C. (1987). "Analytical Modeling of Hysteretic Behavior of R/C Frames", *Journal of Structural Division, ASCE*, Vol.113, No.3, pp. 429-444.

Saiidi, M. and Sozen, M. A. (1979). Simple and complex models for nonlinear seismic response of reinforced concrete structures, *Civil Engineering Studies, Structural Research Series No.465*, University of Illinois at Urbana-Champaign, Urbana, IL, USA.

Shibata, A. and Sozen, M. (1976). Substitute-structure method for seismic design in R/C, *Journal of Structural Division, ASCE* 102:1-18.

Sivaselvan, M. V. and Reinhorn, A. M. (1999). "Hysteretic Models for Cyclic Behavior of Deteriorating Inelastic Structures", Technical Report MCEER-99-0018, State University of New York at Buffalo.

Stojadinovic, B. and Thewalt, C. R. (1996). "Energy Balanced Hysteresis Models", Paper No. 1734, Eleventh World Conference on Earthquake Engineering, Acapulco, Mexico.

Sucuoğlu, H. and Erberik, M. A. (2004). Energy Based Hysteresis and Damage Models for Deteriorating Systems. *Earthquake Engineering and Structural Dynamics* 33: 69-88.

Sucuoğlu, H. and Tokyay, M. (1992). Engineering Report of the 13 March 1992 Erzincan Earthquake. Prepared for the Ankara Branch of the Chamber of Civil Engineers, Ankara.

Sucuoğlu, H., Yazgan, U. and Yakut, A. (2007). A Screening Procedure for Seismic Risk Assessment in Urban Building Stocks, *Earthquake Spectra* 23(2): 441–458.

Takeda, T., Sozen M. A. and Nielsen, N.N. (1970). "Reinforce Concrete Response to Simulated Earthquakes", *Journal of Structural Division, ASCE*, Vol.96, No.ST-12, pp. 2557-2573.

Tavafoghi, A. and Eshghi, S. (2013). Evaluation of behavior factor of tunnel-form concrete building structures using Applied Technology Council 63 methodology. *The Structural Design of Tall and Special Buildings* 22:615-634.

Tomazevic, M. (1999). *Earthquake-resistant design of masonry building*, Imperial College Press.

Tomazevic, M., Bosiljkov, V. and Weiss, P. (2004). "Structural Behavior Factor for Masonry Structures." 13th World Conf. on Earthquake Engineering., Paper No. 2642 Vancouver, B.C., China.

Turkish Earthquake Code, TEC (1998) *Specifications for the Buildings to be Constructed in Disaster Areas*. Ministry of Public Works and Settlement, Ankara, Turkey.

Turkish Earthquake Code, (2007). *Specification of Building to be Built in Disaster Areas*, The Ministry of Public Works and Settlement, Ankara.

Turkish Standards Institute, (1987). Design Loads for Buildings, TS 498, Ankara, Turkey.

Turkish Standards Institute. (2000). Requirements for Design and Construction of RC Structure, TS 500. Ankara, Turkey.

Uniform Building Code, UBC (1997). International Conference of Building Officials, Whittier, California.

Vuran, E., Bal, İ. E., Crowley, H. and Pinho, R. (2008) "Determination of Equivalent SDOF Characteristics of 3D Dual RC Structures", 14th World Conf. on Earthquake Engineering., Beijing, China.

Yakut, A. (2004). Preliminary Seismic Performance Assessment Procedure for Existing RC Buildings. Engineering Structures, Vol. 26, No. 10, pp. 1447–1462.

Yakut, A. (2008). Capacity Related Properties of RC Frame Buildings in Turkey. Journal of Earthquake Engineering, Vol. 12(S2), pp. 265–272.

Yakut, A. and Gulkan, P. (2003). Tunnel form building. Housing Report. No 101. World Housing Encyclopedia. an initiative of Earthquake Engineering Research Institute and International Association for Earthquake Engineering.

Yakut, A., Ozcebe, G. and Yucemen, M.S. (2006). Seismic vulnerability assessment using regional empirical data. Earthquake Engineering Structural Dynamics 35:1187–1202.

Yuksel, S. B. and Kalkan, E. (2007). Behavior of tunnel form buildings under quasi-static cyclic lateral loading. Structural Engineering and Mechanics 27(1):1-17.

Zavala, C., Honma, C., Gibu, P., Gallardo, J. and Huaco, G. (2004). "Full Scale on Line Test on Two Story Masonry Building Using Handmade Bricks." 13th World Conf. on Earthquake Engineering., Paper No. 2885, Vancouver, B.C., China

APPENDIX A

PLAN GEOMETRY OF GENERATED MASONRY BUILDING MODELS

A.1. R1-W1 MODEL

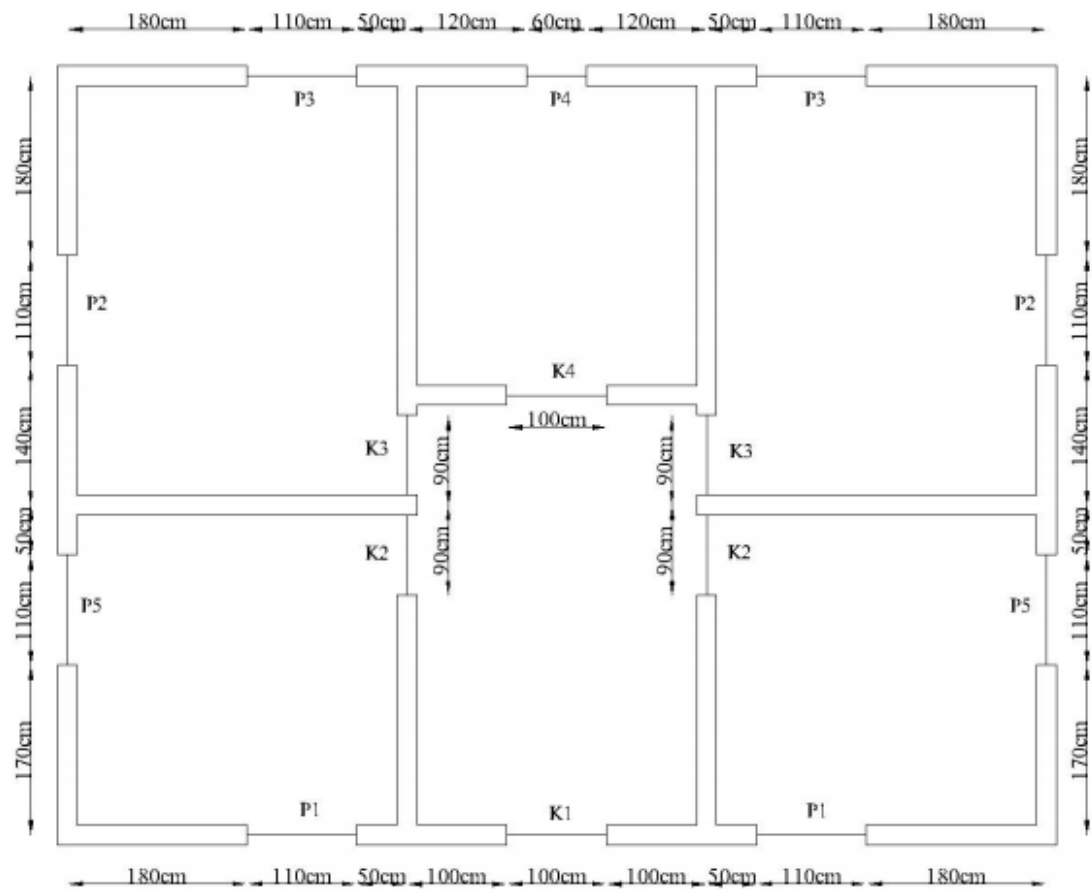


Figure A.1. 1. Plan geometry of subclass R1W1 of masonry building model

A.2. R1-W2 MODEL

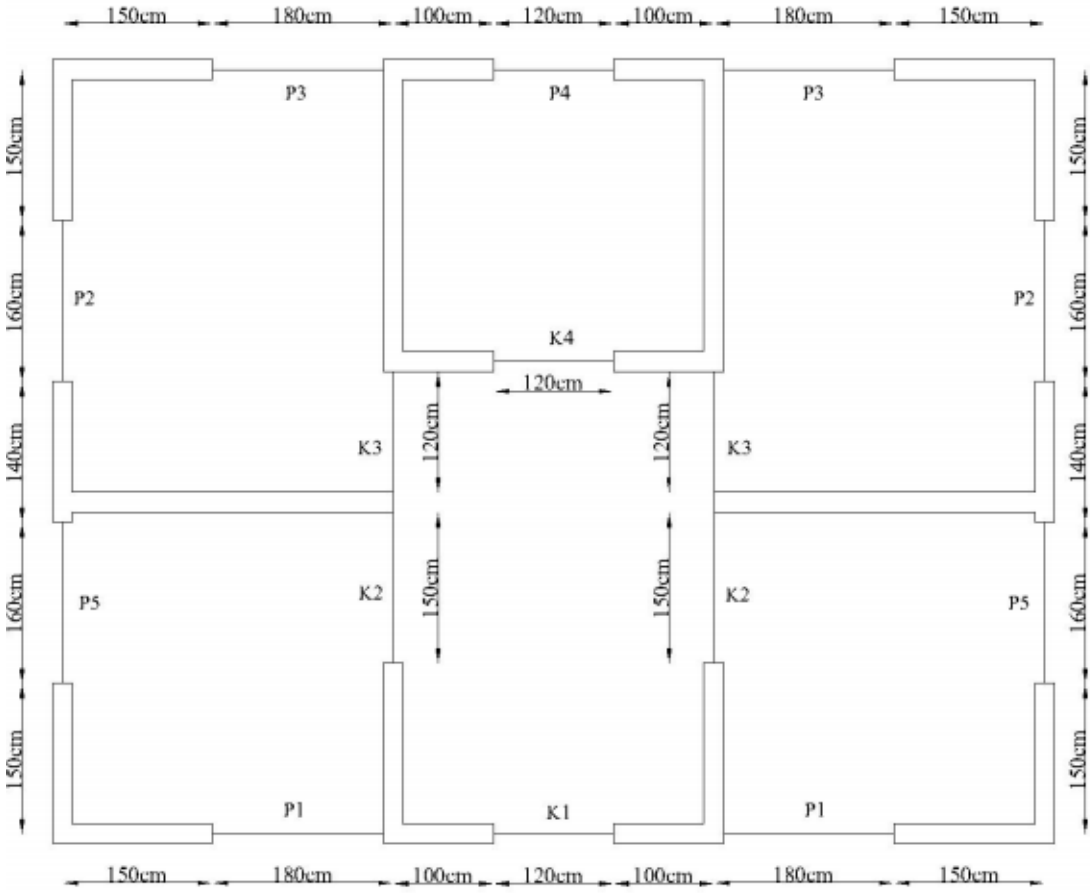


Figure A.2. 1. Plan geometry of subclass R1W2 of masonry building model

A.3. R1-W3 MODEL

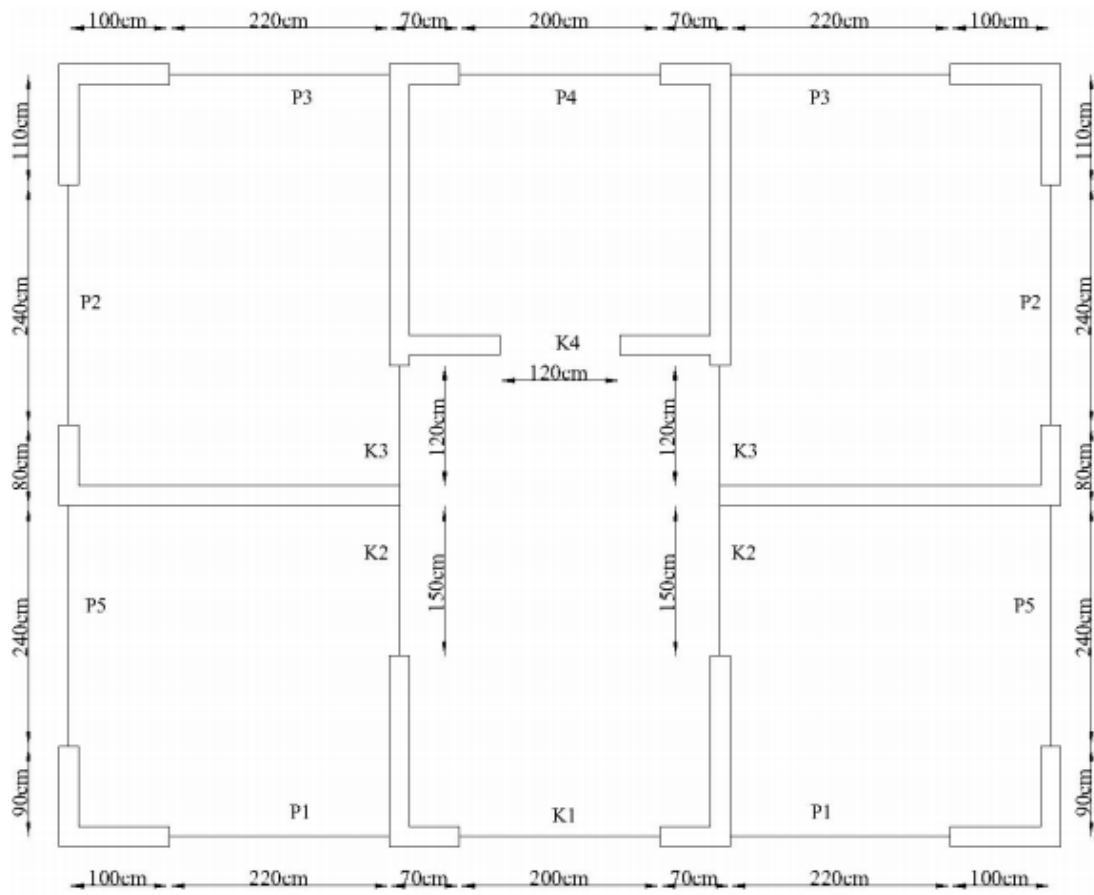


Figure A.3. 1. Plan geometry of subclass R1W3 of masonry building model

A.4. R2-W1 MODEL

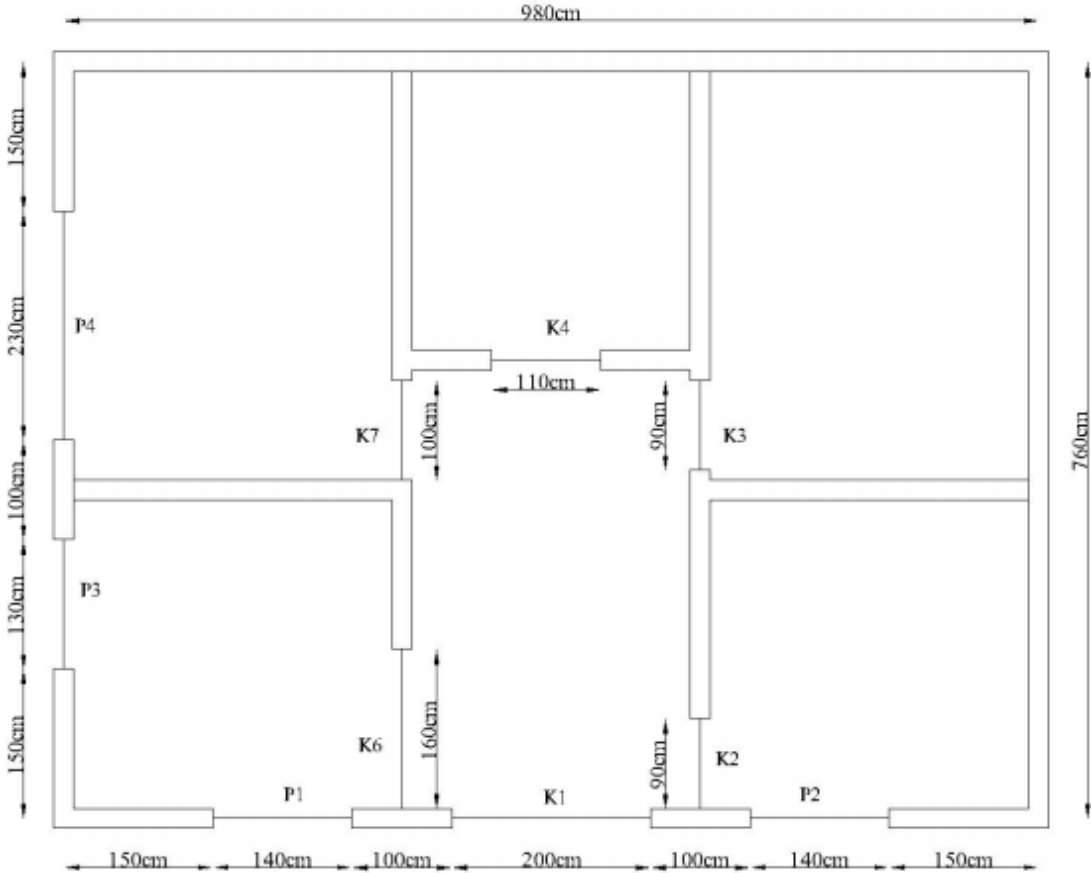


Figure A.4. 1. Plan geometry of subclass R2W1 of masonry building model

A.5. R2-W2 MODEL

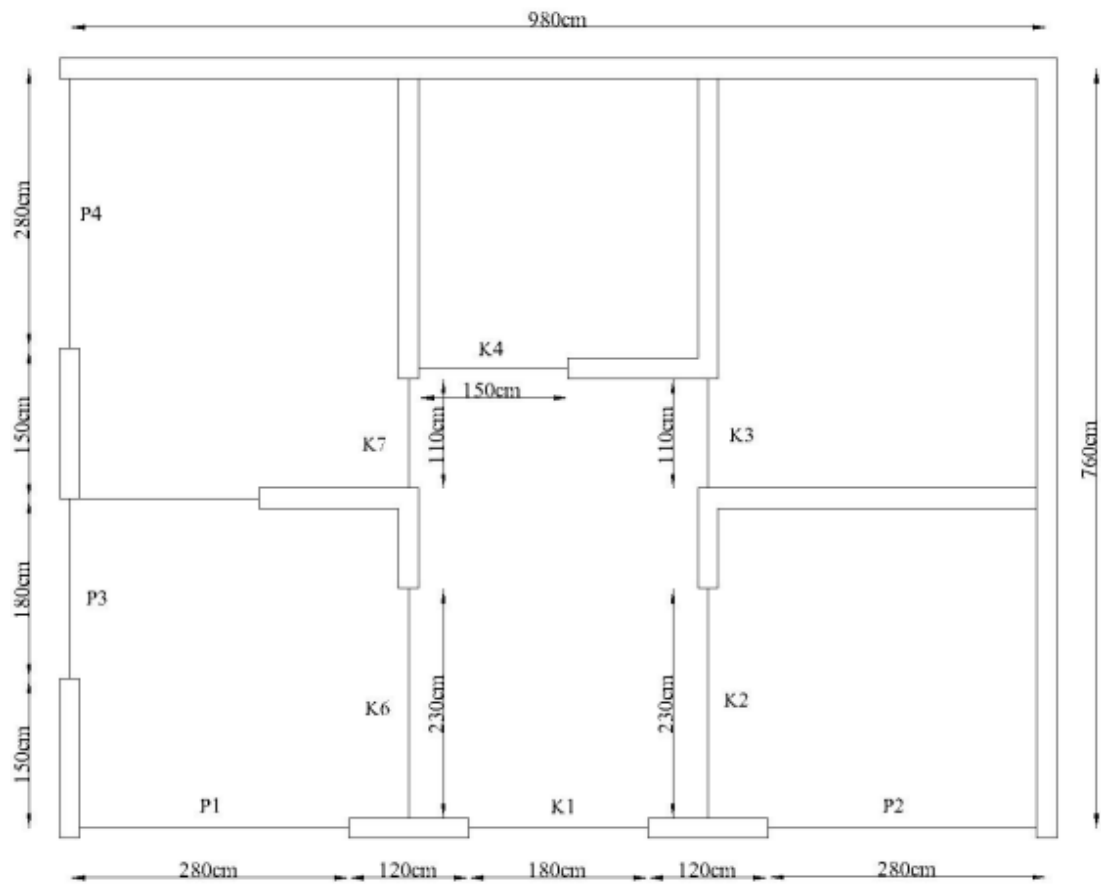


Figure A.5. 1. Plan geometry of subclass R2W2 of masonry building model

A.6. R2-W3 MODEL

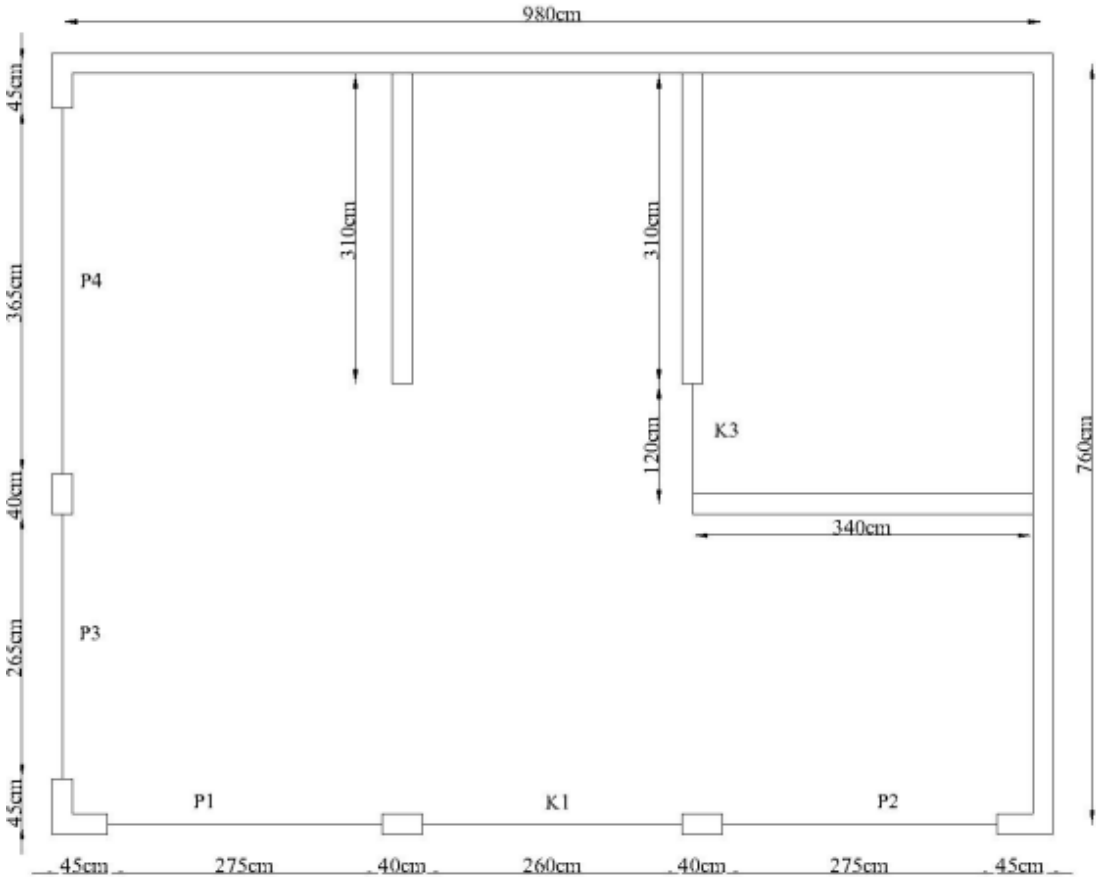


Figure A.6. 1. Plan geometry of subclass R2W3 of masonry building model

APPENDIX B

CAPACITY CURVES OF MASONRY BUILDING MODELS

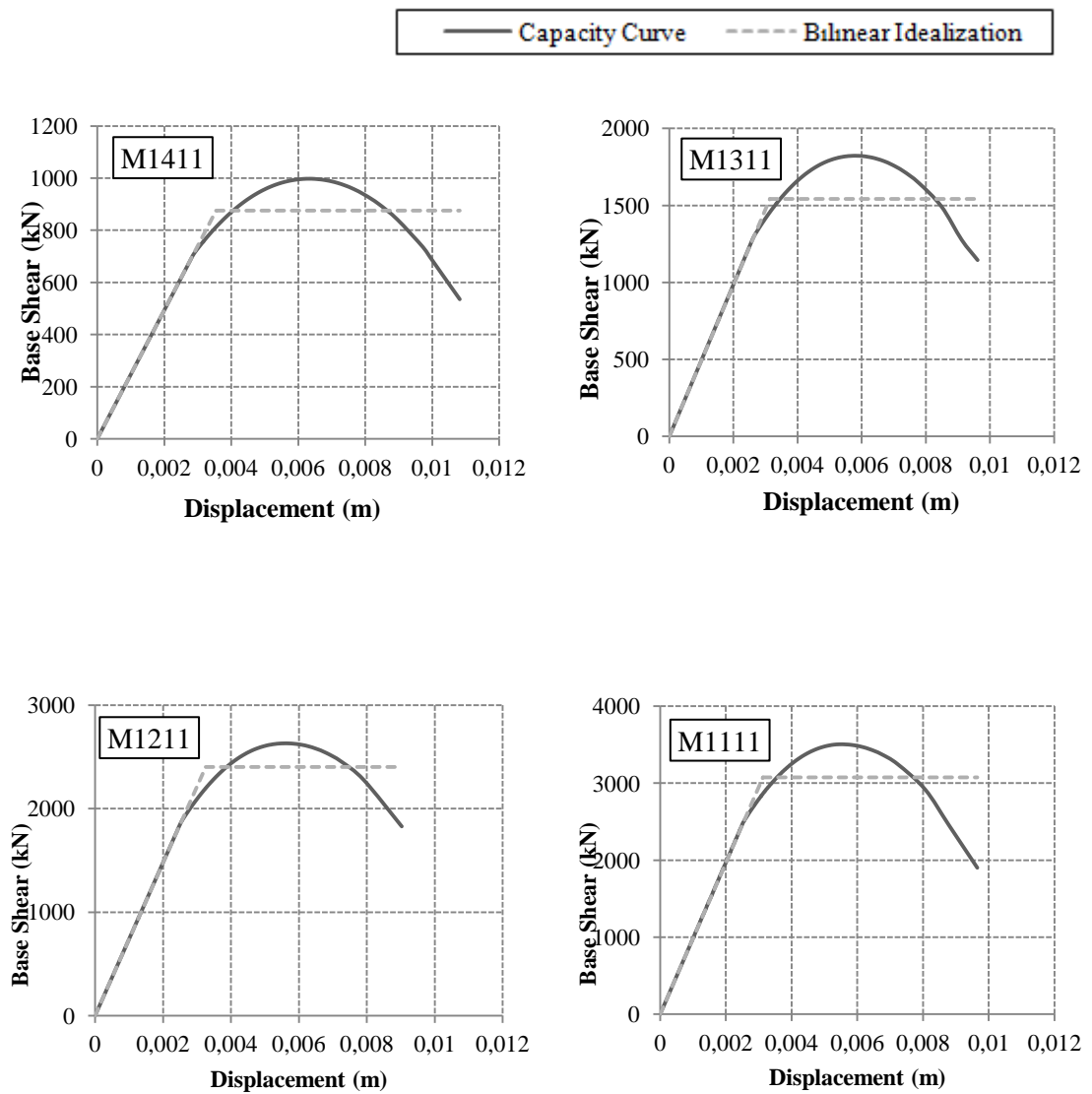


Figure B.1 Capacity Curves of subclass R1W1 of masonry building model

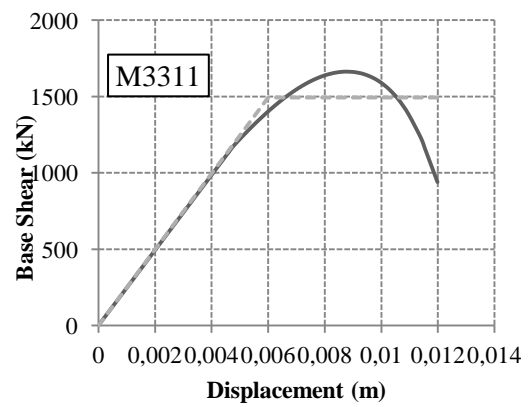
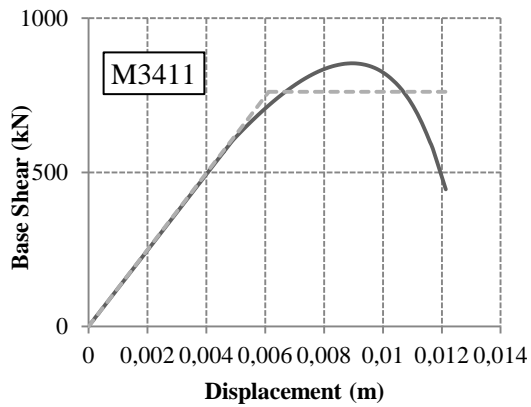
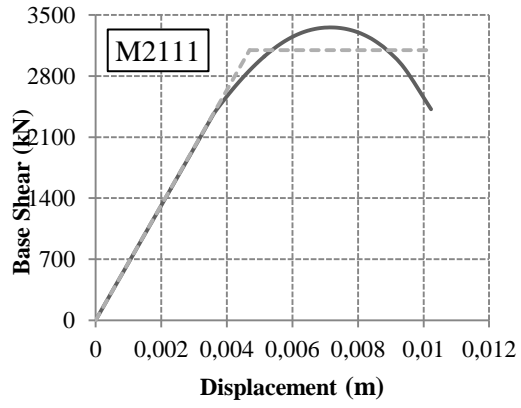
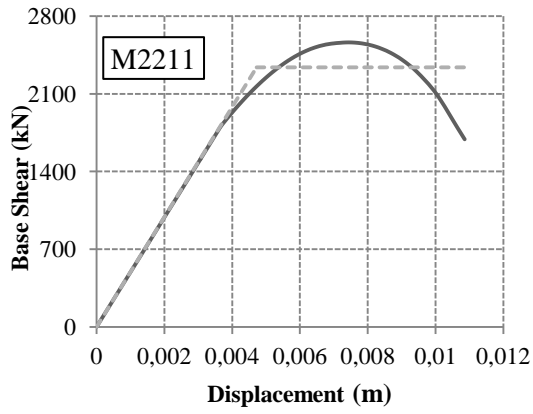
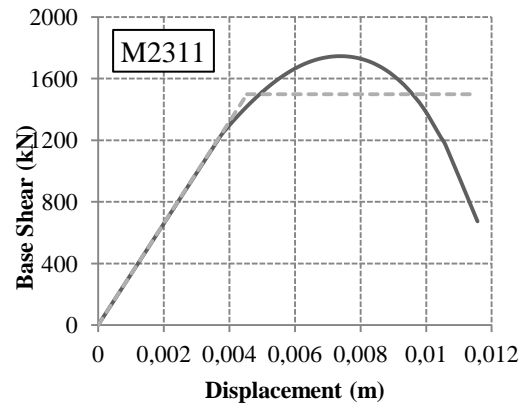
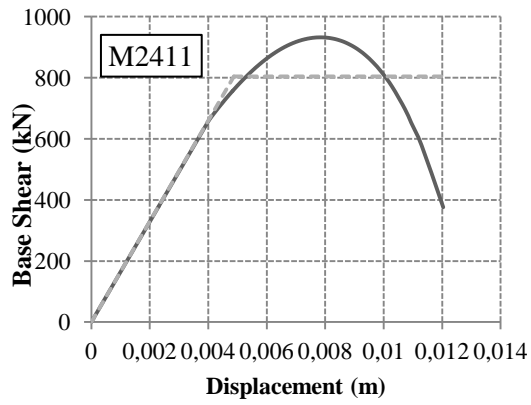


Figure B.1 Continued

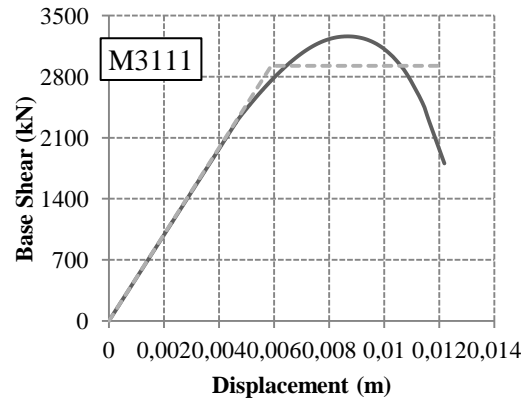
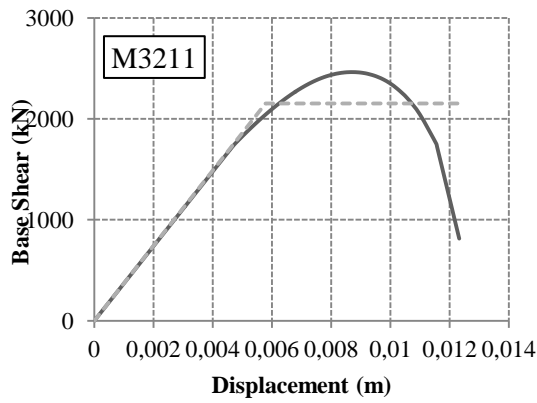


Figure B.1 Continued

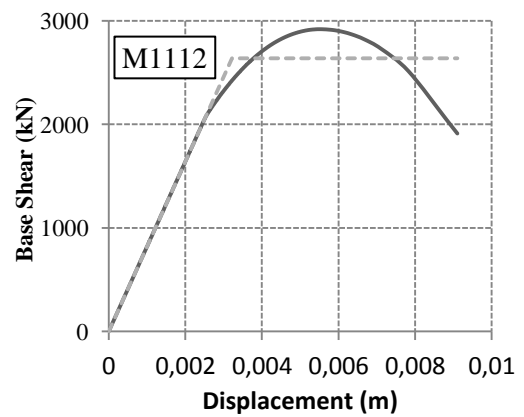
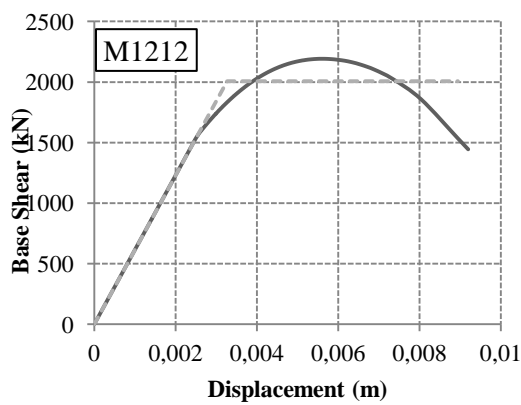
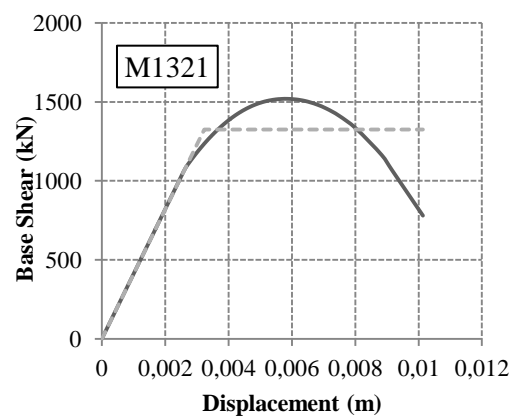
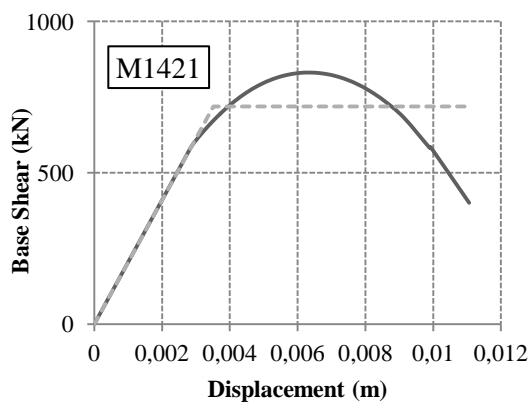


Figure B.2 Capacity Curves of subclass R1W2 of masonry building model

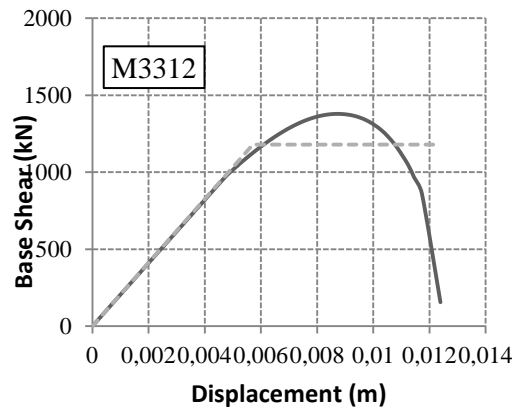
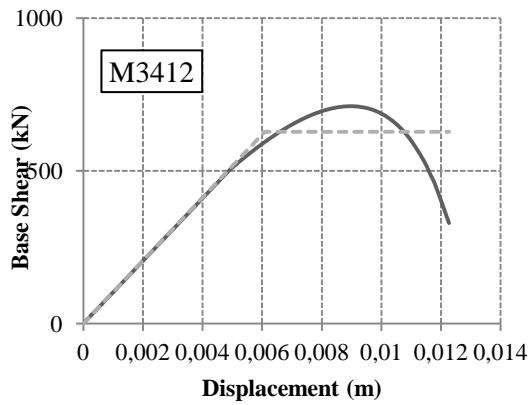
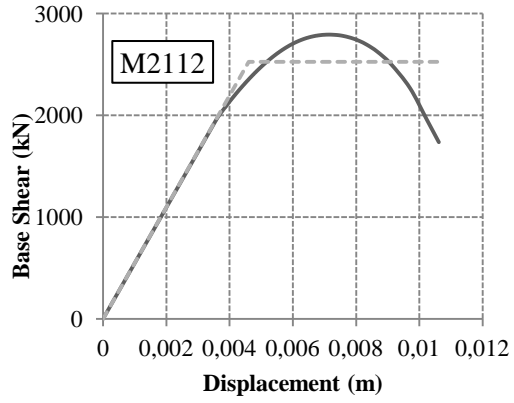
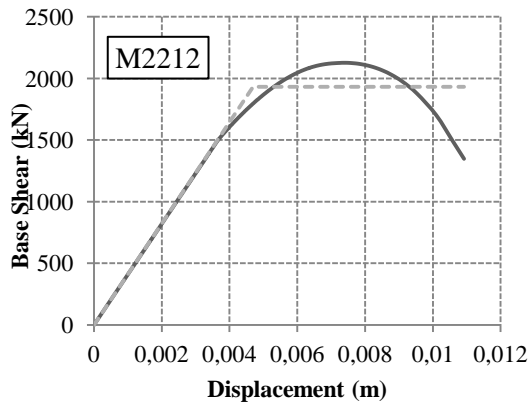
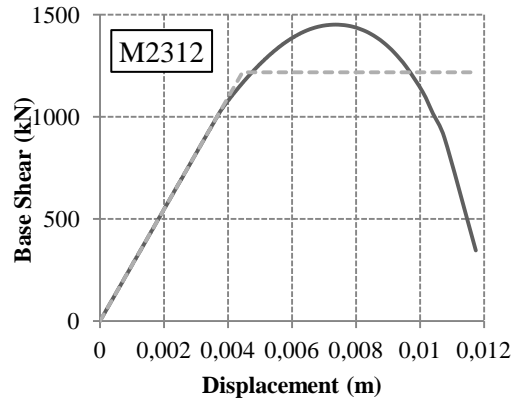
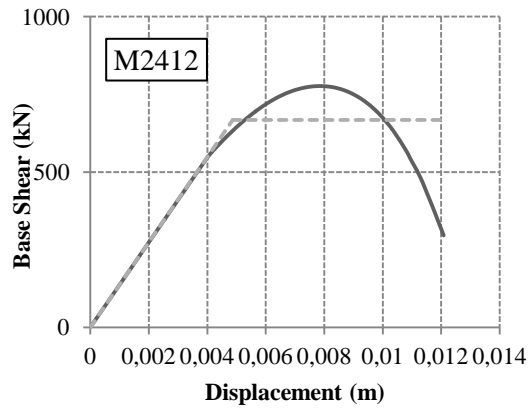


Figure B.2 Continued

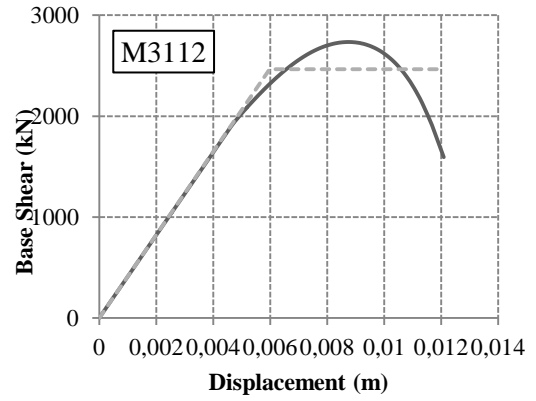
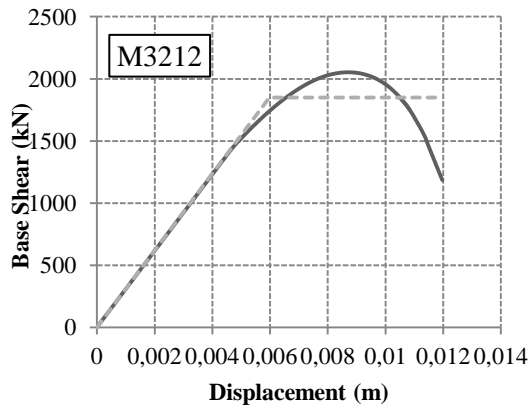


Figure B.2 Continued

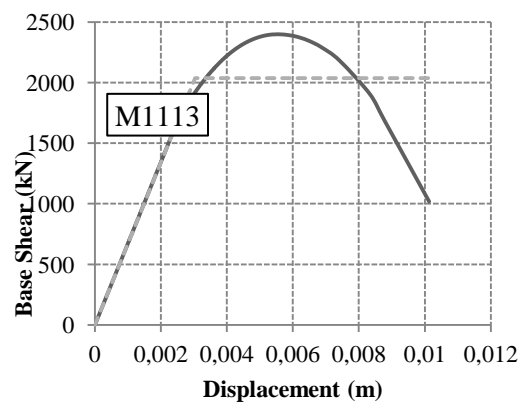
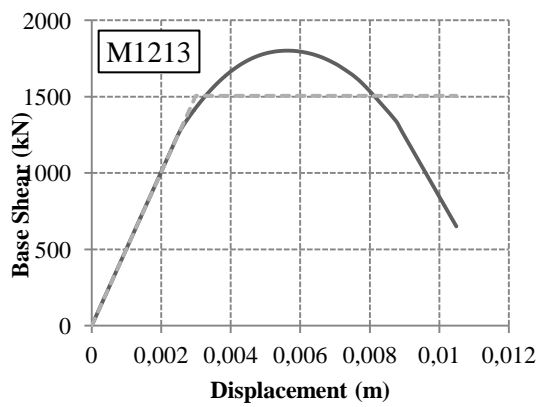
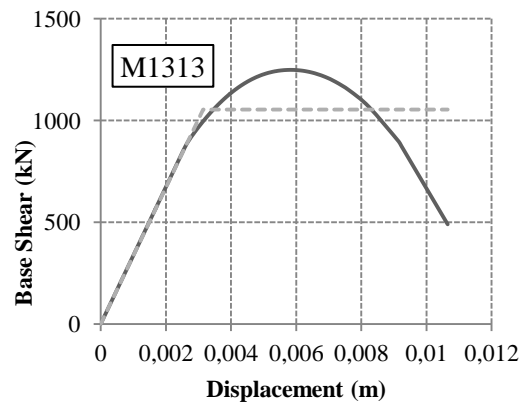
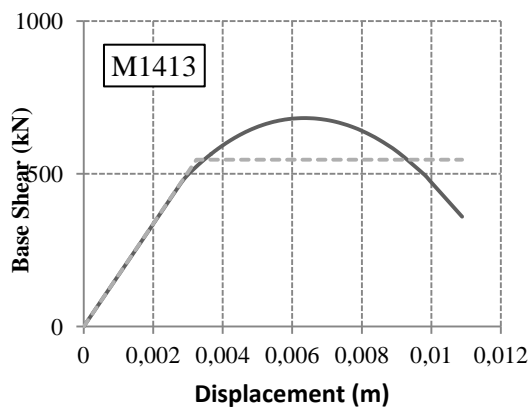


Figure B.3 Capacity Curves of subclass R1W3 of masonry building model

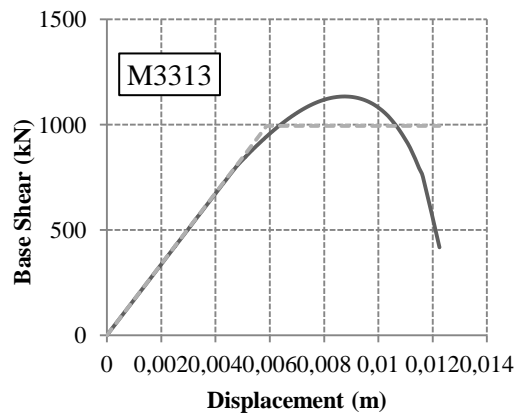
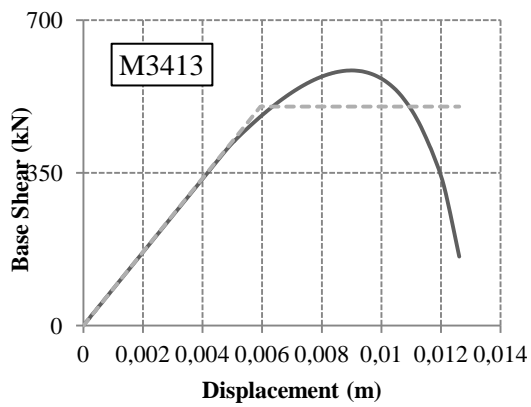
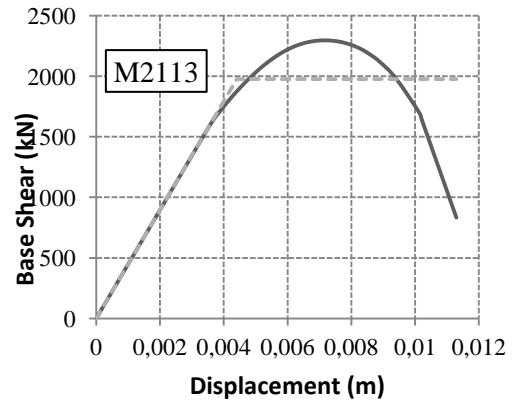
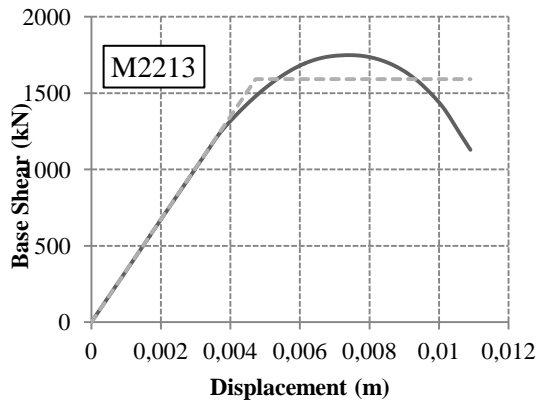
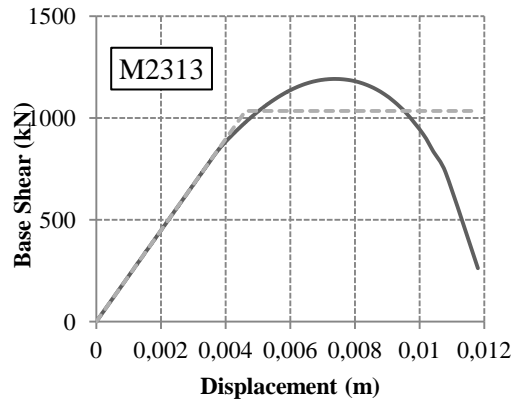
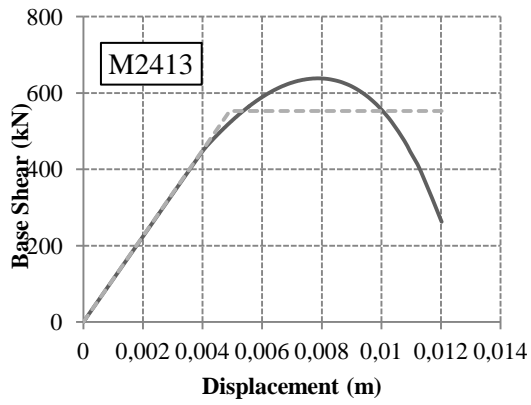


Figure B.3 Continued

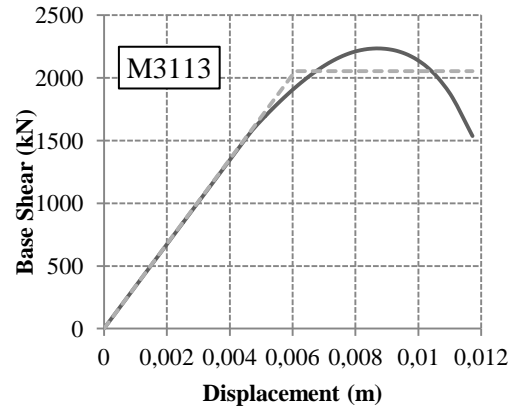
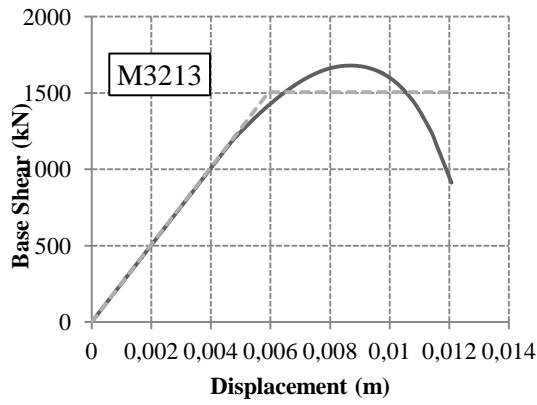


Figure B.3 Continued

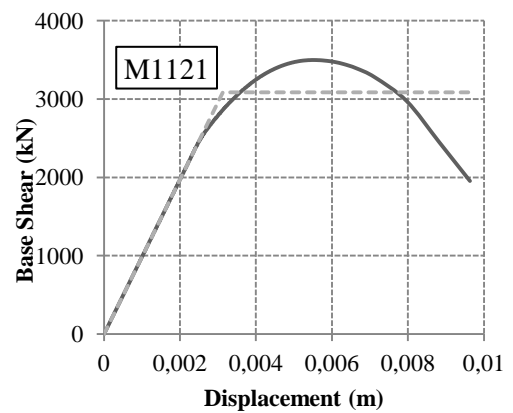
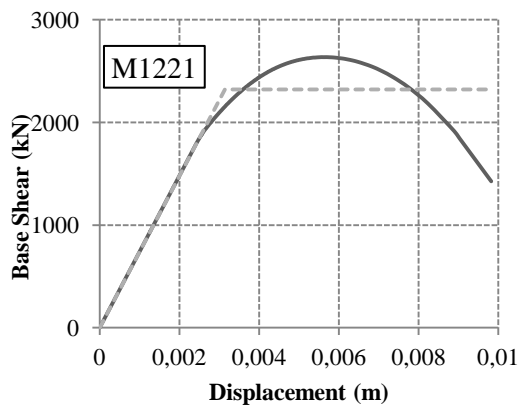
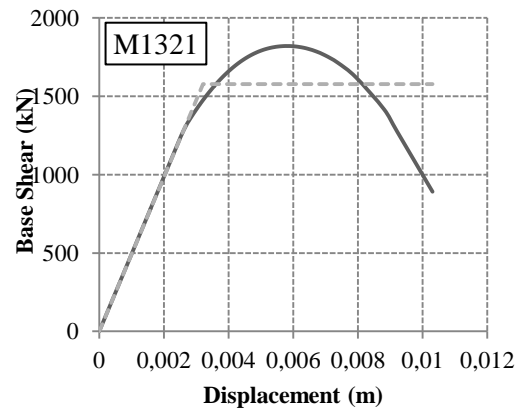
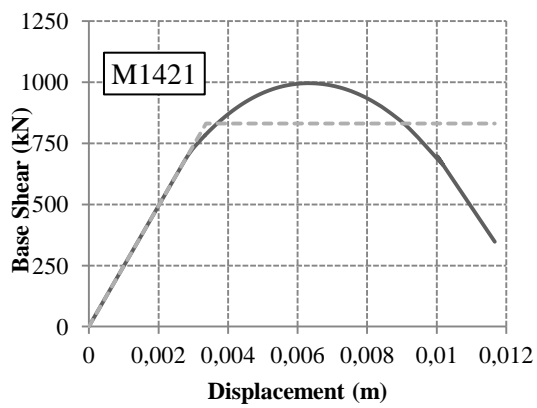


Figure B.4 Capacity Curves of subclass R2W1 of masonry building model

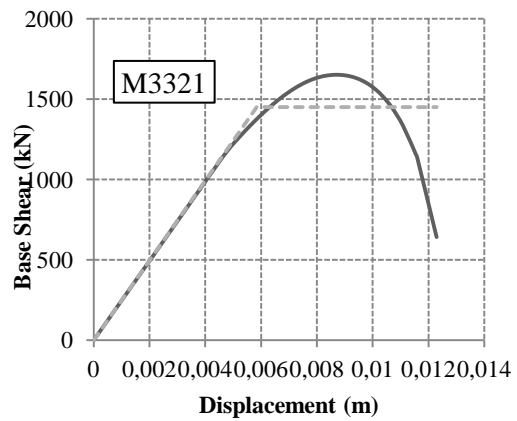
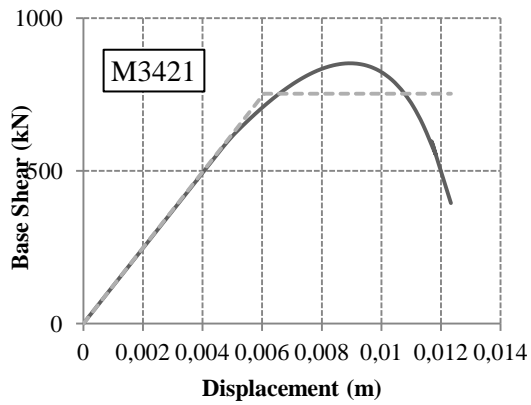
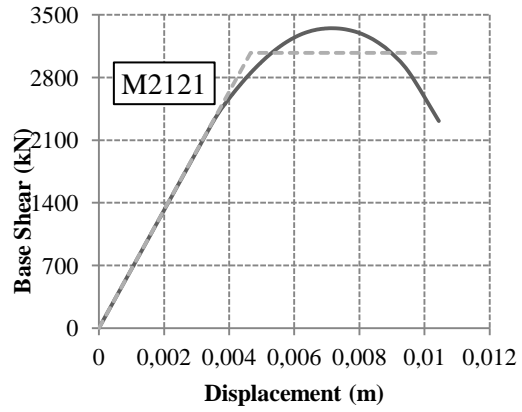
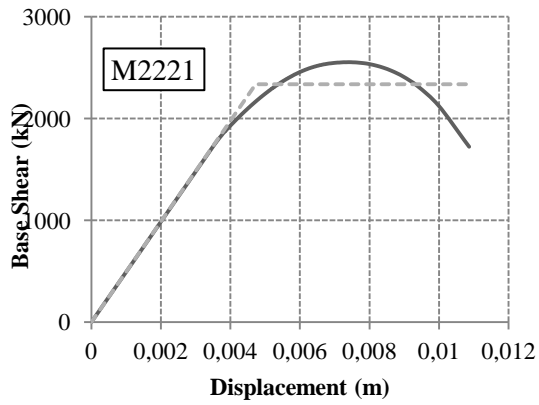
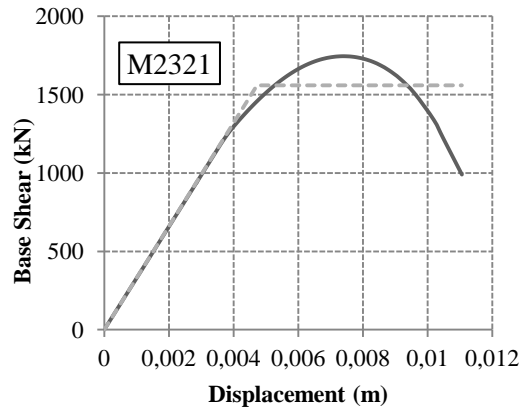
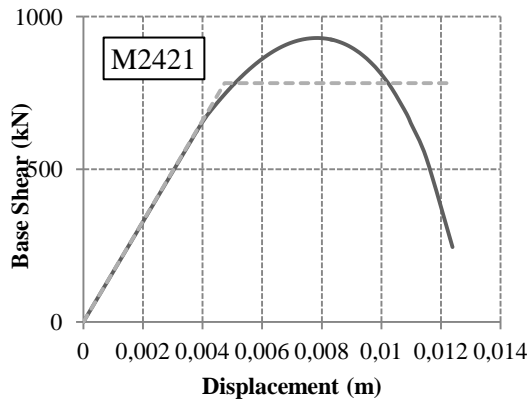


Figure B.4 Continued

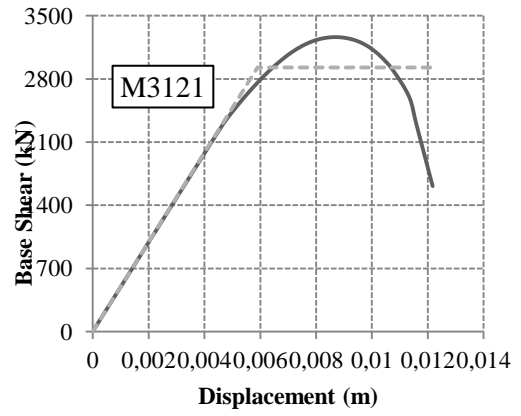
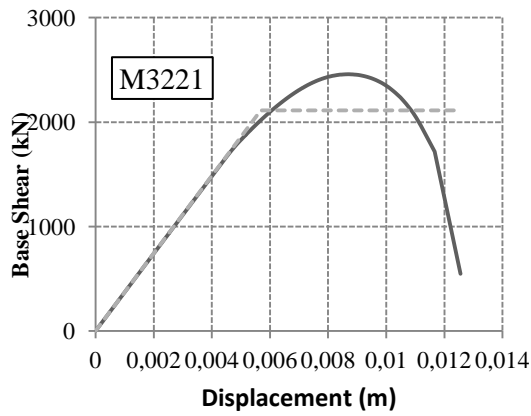


Figure B.4 Continued

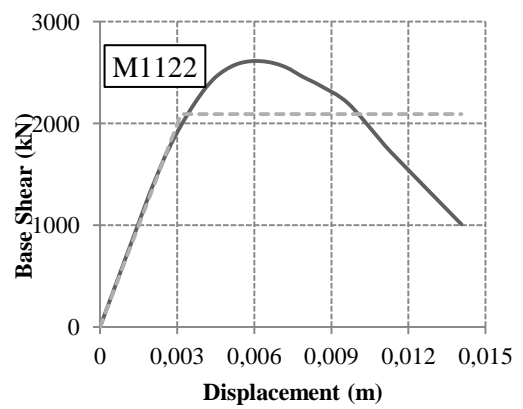
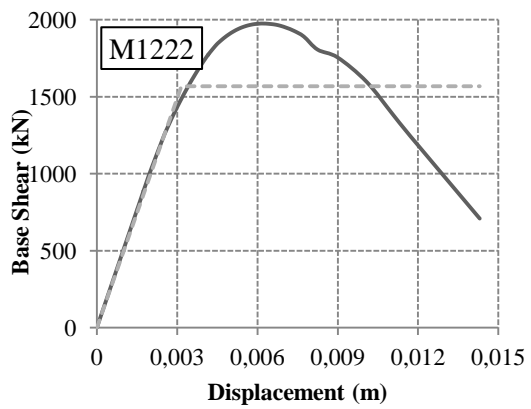
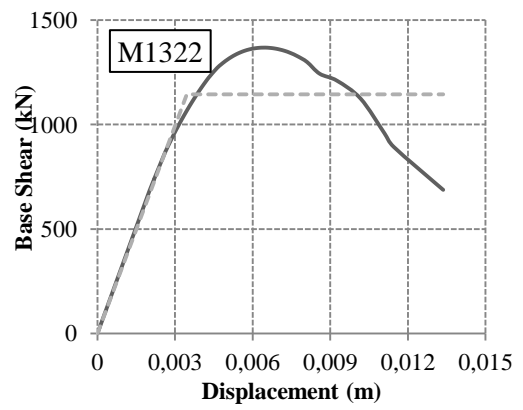
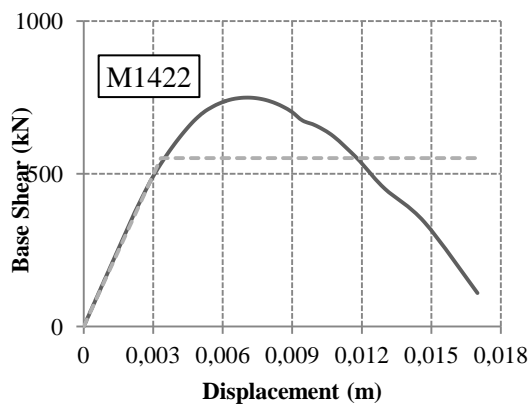


Figure B.5 Capacity Curves of subclass R2W2 of masonry building model

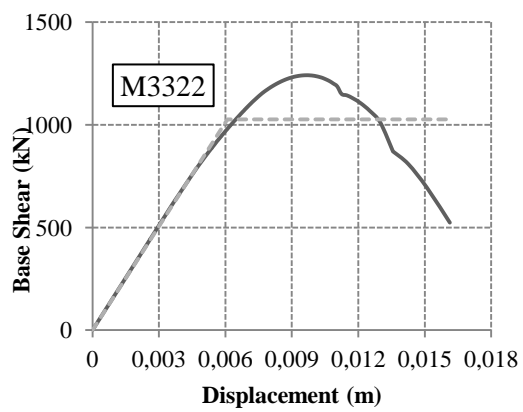
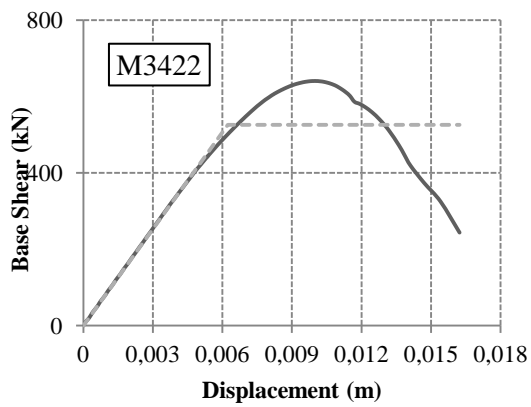
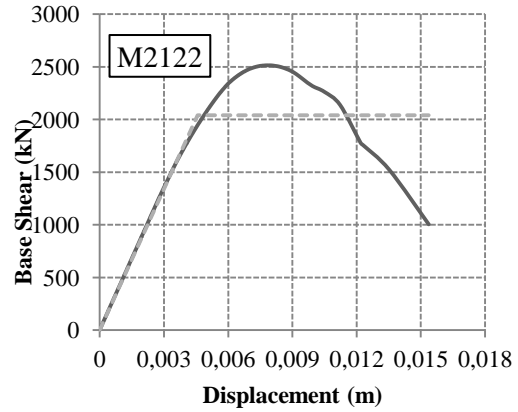
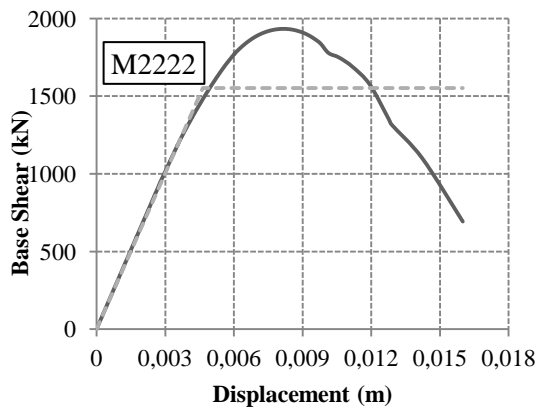
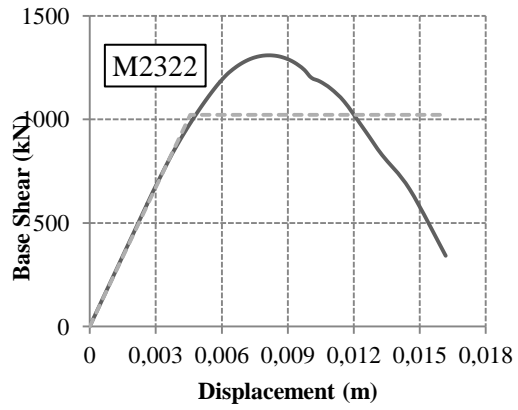
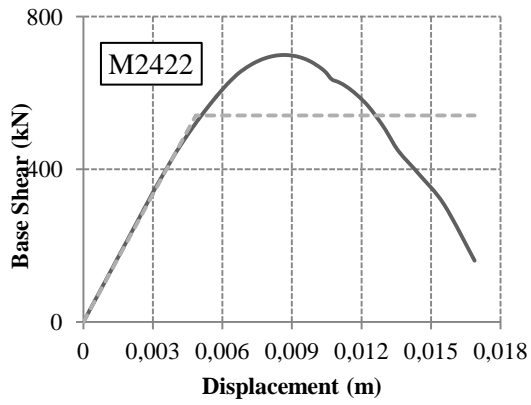


Figure B.5 Continued

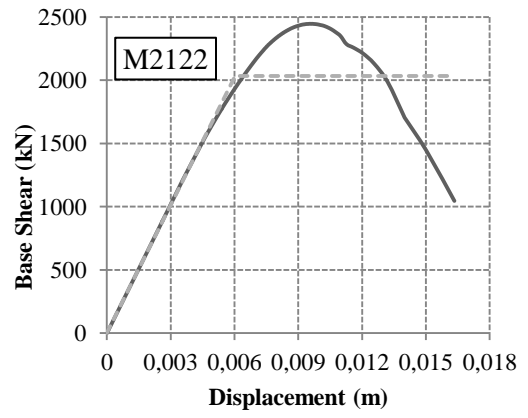
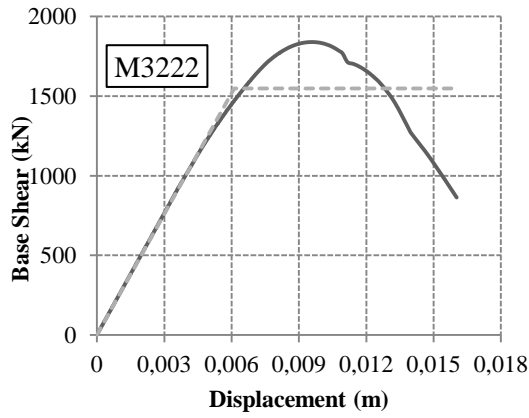


Figure B.5 Continued

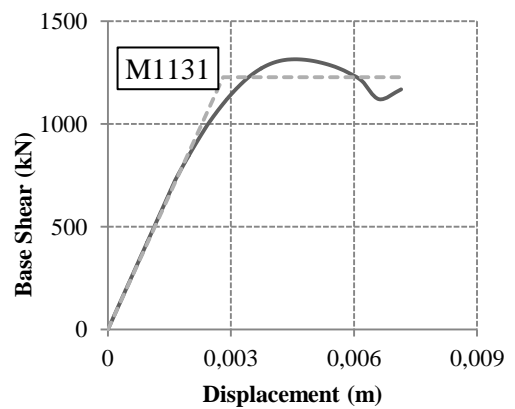
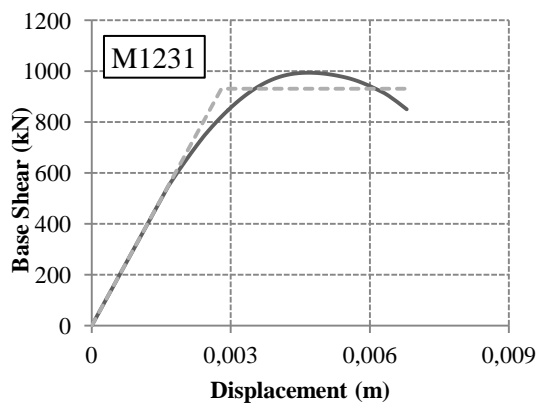
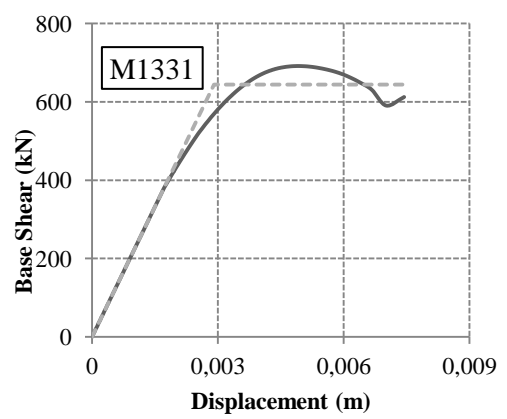
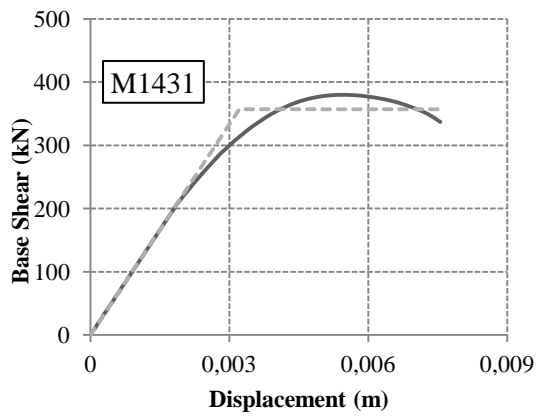


Figure B.6 Capacity Curves of subclass R2W3 of masonry building model

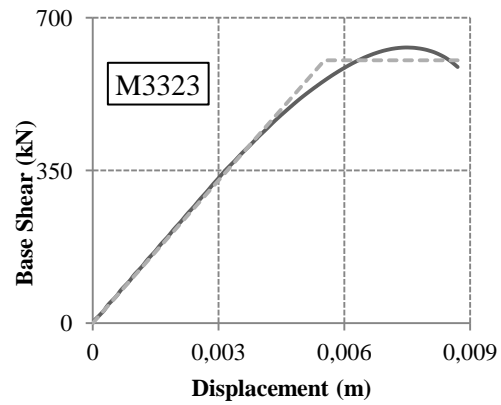
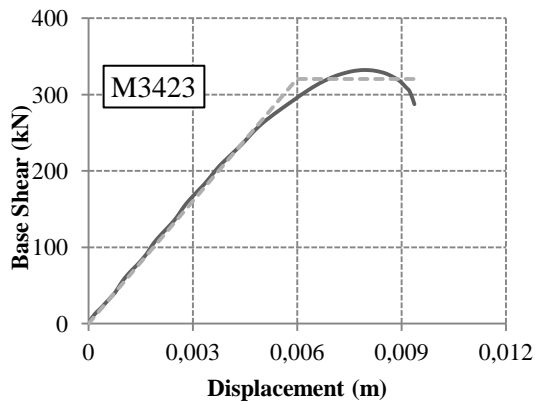
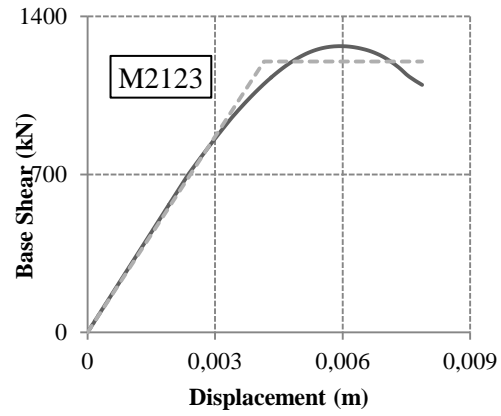
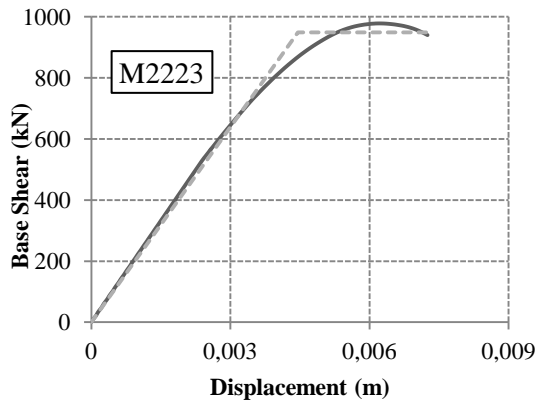
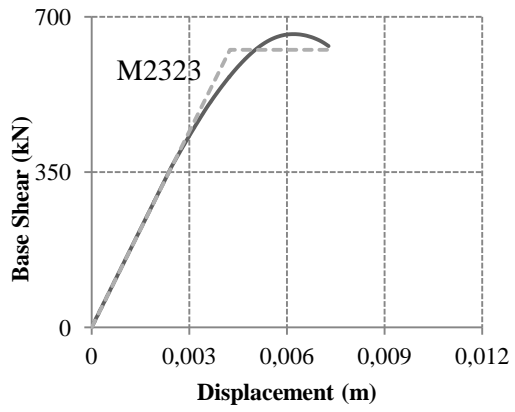
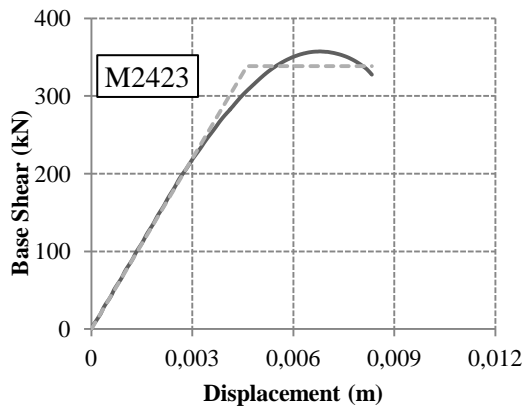


Figure B.6 Continued

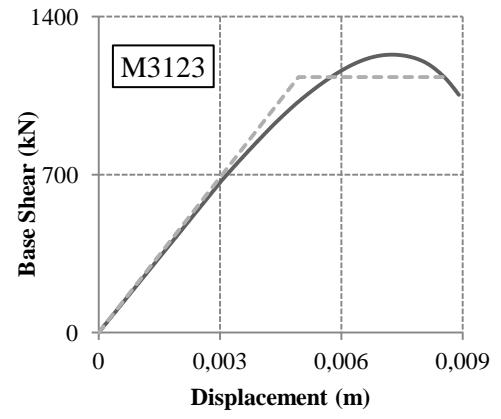
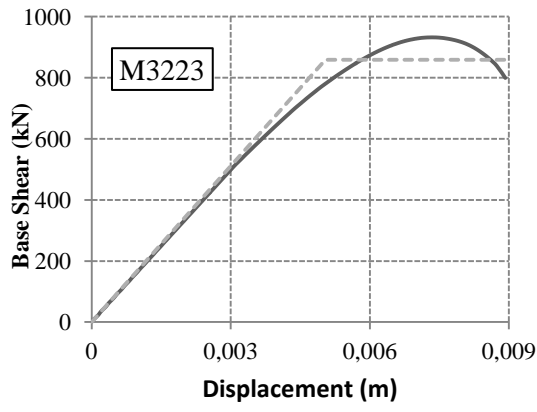


Figure B.6 Continued